

The Guardian of the Genome:
Regulation of the enhancer networks governing the p53-mediated stress response

By

Allison Nicole Catizone

A Dissertation

Submitted to the University at Albany, State University of New York

In partial fulfillment of
the Requirements for the Degree of
Doctor of Philosophy

College of Arts and Science

Department of Biological Sciences

2020

ProQuest Number: 27955483

All rights reserved

INFORMATION TO ALL USERS

The quality of this reproduction is dependent on the quality of the copy submitted.

In the unlikely event that the author did not send a complete manuscript and there are missing pages, these will be noted. Also, if material had to be removed, a note will indicate the deletion.



ProQuest 27955483

Published by ProQuest LLC (2020). Copyright of the Dissertation is held by the Author.

All Rights Reserved.

This work is protected against unauthorized copying under Title 17, United States Code
Microform Edition © ProQuest LLC.

ProQuest LLC
789 East Eisenhower Parkway
P.O. Box 1346
Ann Arbor, MI 48106 - 1346

ABSTRACT

After fertilization in vertebrates, cells work to build organs, tissues and begin to rapidly differentiate and proliferate. This process is the orchestration of finely tuned signals and perfectly timed gene expression patterns. The first step in gene expression, transcription, is governed by proteins known as transcription factors (TF). TFs are responsible for binding to DNA, altering chromatin structure, and driving activation of other genes based on the organism's needs. Once the process of development is complete, organisms shift their resources to maintaining homeostasis. Humans regularly encounter outside stressors such as UV radiation, pollution, allergens, and drugs. Cells also accumulate mutations as they travel through cell cycle. The doubling of cell volume and replication of DNA allows for potential errors. These insults and natural occurrences lead to a wide variety of molecular damage and the tumor suppressor protein, p53, is the central hub of the organism's core defenses against these insults.

Most famously, p53 is the activator of the apoptotic pathway, which prevents the proliferation and spread of mutated cells. p53 mediated stress pathways also include cell cycle arrest, DNA damage repair, senescence, unfolded protein response, and ER stress response. Certain cell types are known to be predisposed to different p53 pathway fates and the levels of p53 fluctuate differently based on the mode of activation. The gene targets downstream of p53 have been well studied, however, the variations in downstream gene expression across treatments and stress responses are still being elucidated. Utilizing both genotoxic (etoposide) and non-genotoxic (nutlin 3A), we examined the variations in chromatin accessibility, RNA polymerase docking, p53 location and enrichment, and gene expression. We found that 'core' tumor suppressor genes were activated in the same capacity and transcriptional regulation at p53 binding sites was similar across

the treatments. However, a specific set of inflammatory factors were activated only in the etoposide treatment, suggesting both a p53-dependent and p53-independent response. Thus, different stress responses may trigger both p53-dependent and stress dependent gene expression guiding cells down certain p53 pathway fates. In the future, we wish to perform these same studies with molecular insults such as UV radiation, amino acid deprivation and others in order to determine the differential gene expression patterns across stresses.

Being a transcription factor, p53 activates pathways such as cell cycle arrest and apoptosis through the binding of regulatory regions known as promoters and enhancers. While the regulation of p53 at promoters has been rigorously studied, much of p53's activity is facilitated through distal enhancer elements. In order to understand how p53 can regulate such a wide variety of cellular pathways, we chose to study the enhancer regions it binds. Enhancers are responsible for the temporal and spatial regulation of target genes, and have strong cell type-specificity. The role of enhancers in the control of p53's transcriptional activity is in debate. Recent work suggests that p53 works alone to initiate transcription at enhancer regions, which is a departure from the canonical model of enhancer activity involving multiple transcription factors. We utilized a massively parallel reporter assay to study 100s of p53 bound enhancers in parallel in order to determine the mechanisms regulating p53 activity at these elements. We found that p53 bound enhancers relied on more than just the core p53 binding site and required flanking sequences that contained other transcription factor binding sites. In the future, we plan to study the p53 enhancer networks more in depth *in vivo* to begin to understand how p53 bound enhancers work together in the presence of other transcription factors.

In recent years, we have learned that core p53 target genes are activated across all cell lineages. Conversely, there are hundreds of p53 target genes that are stress-responsive based on

cell type and cell state. Cell identity is governed and maintained by cell lineage specific proteins as well as unique chromatin topographies. We predicted that the variation in p53-dependent gene expression may be due to unique cell type-dependent factors and regulatory region accessibility that fluctuates between cell types. The p53 family of transcription factors contains the members p53, p63, and p73 that all bind a highly similar consensus sequence. p63 is a lineage determining factor for epithelial cells that maintains the chromatin topography and accessibility to important regulatory regions driving cell type specific genes. Both p53 and p63 are found bound at the same locations *in vivo*. The inherent differences between the response elements prevent p53 from binding some of the p63-mediated enhancers both *in vivo* and *in vitro*, however p63 has much more flexibility and is found at all active p53 enhancers in epithelial cells. We utilized the same massively parallel reporter assay to study both p63 and p53 dependent enhancers in parallel with different cell background: wildtype, p53-depleted, and p63-depleted mammary epithelial cells (MCF10a). Using this approach, we discovered that p63-dependent enhancers require flanking sequence for optimal activity and the presence of p63 protein, much like we observed with p53. We also found, in parallel studies, that p63 was not sufficient to drive enhancer activity alone. Finally, we discovered that p53 bound enhancers in p63 deficient epithelial cells worked at a lower capacity than they do in non-epithelial cells. Taken together, these data suggest that p63 is necessary for the epithelial-specific activity of p53, but that p63-bound enhancers still require additional cofactors and the appropriate cellular context for full activity. We believe these data provide a framework to understand how cell type specific lineage factors, like p63, play a role in p53 regulation and transcriptional activity. In the future, we plan to understand the regulation between p53 and p63, and other cell type specific factors. We will investigate this using differential gene expression studies across multiple epithelial cell lines to find genes that p53 and p63 both

regulate. We will also study the effect of different p63 isoform expression on p53 dependent transcriptional activity.

p53 mainly requires open and active *cis*-regulatory elements (CREs or enhancers) with modest exceptions. We believe this to be true for not only for cell type specific events but for core tumor suppressor pathways as well. To begin to peel back the layers of this complex transcriptional regulation, we sought out to study how the method of p53 activation and the binding partners at CREs control gene expression. Through the study of the p53 family of transcription factors and the identification of required cofactors at enhancers, we have begun to unravel the complexities of the various stress responses downstream of p53 and how it is finely tuned via differential enhancer networks. This work suggests that cell type, and not activation method, is the strongest predictor of wild-type p53 activity.

ACKNOWLEDGEMENTS

I am truly grateful for my advisor, Dr. Morgan Sammons. Even before the shelves were stocked in our brand-new lab, he accepted me as his first graduate student and all the challenges that came with it. I had much to learn to start in a new field of research. Dr. Sammons personally taught me all the molecular biology techniques I have now mastered and fostered an environment where we not only grew as scientists but as individuals. Our time enjoying our own lives was just as important as our time at the bench thanks to his focus on work life balance. Because of him, I can say the journey of this dissertation was not a stressful one, but rather interesting, productive, and successful. I, again, am grateful for the skills I have learned to apply in my future career as well as in my life.

I am extremely thankful for my lab mates. Our lab took a few years to grow from when I started out, however, it is filled with the most wonderful people, both graduate and undergraduate. Serene and Dana are kind and intelligent women who are becoming amazing scientists and I have full confidence they will continue the trends we have set forth in our lab. I am also grateful for the endless patience, advice, and small talk they had to offer. Laughter and loud conversations could always be heard passing our lab's door and that is because we truly enjoyed each other's company and success. Serene, thank you especially for your friendship, being lab mates and roommates made my PhD and life so much better.

I am appreciative of my committee members Dr. Thomas Begley, Dr. Prashanth Rangan, and Dr. Gabrielle Fuchs. Your guidance in my thesis work was invaluable to streamlining my thoughts and

ideas as well as my sometimes-puzzling data. Your words of wisdom and outside perspectives were grounding and essential.

I especially want to thank my family: My father who always told me to “keep on pedaling” even though he had no idea what I was working on, my mother for her continued support and confidence that I can accomplish anything I set my mind to, my brother Joe, my extended family for all their support and pride at holidays, and my family members that passed during the last 5 years that did not get to see me accomplish my goals. Your support and relentless confidence in my abilities (even when I did not feel so confident myself), made this PhD possible.

Lastly, I’d like to thank the animals of my life and the moments we shared over the past five years that kept me focused on my goals when everything seemed so hectic. For my horse Mac, sitting in your stall at night and telling you about my thesis work (i.e. how none of it seemed to be working) was the highlight of my weekends, thank you for listening, I miss you. For my horse Mya, your demand for love, attention and energy has always kept me on my toes and was a wonderful, refreshing distraction from work, thank you for humbling me time and time again. For my dog Belle, my little helper, you’ve watched me grade papers, practice presentations, and gotten me out on long walks to clear my head, you deserve your own degree, thank you for the peace you bring me.

TABLE OF CONTENTS

ABSTRACT.....	ii
ACKNOWLEDGEMENTS	vi
TABLE OF CONTENTS	viii
LIST OF TABLES AND FIGURES.....	xiv
CHAPTER 1: Introduction.....	1
The Guardian of the Genome.....	1
Natural activation of p53 in vivo	3
p53 activating agents and dynamics of activation	4
p53 protein structure	5
p53 binding to DNA.....	5
Inhibition or manipulation of the p53 pathway.....	6
General transcription.....	8
Chromatin as a regulator of transcription	10
Transcription factor maintenance of chromatin.....	10
Pioneer factors and p53 as a pioneer factor	11
p53 binding to gene regulatory elements: promoters.....	12
p53 binding to gene regulatory elements: enhancers.....	13
Enhancer models:.....	15
The p53 gene regulatory network	16

Apoptosis	17
Cell cycle arrest.....	17
Senescence	18
Cell type effects on p53 activity	19
p53's role in cell identity	21
p53's role in cell reprogramming.....	22
Conclusions.....	23
CHAPTER 2: Comparison of genotoxic versus nongenotoxic stabilization of p53 provides insight into parallel stress-responsive transcriptional networks.....	25
Introduction.....	25
Results.....	28
Comparison of p53 interaction with the genome after genotoxic and non-genotoxic activation.....	28
Chromatin context at p53 binding sites provides evidence for common gene regulation downstream of nutlin 3A and etoposide-mediated activation of p53	32
Transcriptional and promoter dynamics after nutlin 3A- and etoposide-induced p53 activation.....	35
Etoposide-specific genes are likely p53-independent, DNA damage-induced NF-kB transcriptional targets.....	40
Discussion.....	47

CHAPTER 3: Locally acting transcription factors regulate p53-dependent cis-regulatory element activity.....	52
Introduction.....	52
Results.....	55
Design and execution of a massively parallel reporter assay for determinants of p53-dependent CRE activity	55
p53-bound CREs require direct-binding of p53 for Nutlin-3A-induced activity	63
Variation in flanking sequence context alters p53-dependent CRE activity	65
An SP1/KLF family motif is required for p53-dependent activity of the CCNG1 CRE.....	75
Loss of the SP1/KLF motif leads to reduced CCNG1 transcription and reduced p53 binding	78
p53-dependent transcription of GDF15 requires regulatory factors at two separate distal CREs	83
Discussion	88
CHAPTER 4: p63 and p53 co-regulate transcriptional activity at enhancers.....	95
Introduction.....	95
Results.....	98
Execution of an MPRA for enhancer activity in MCF10a cells lines.....	98
p53-enhancers require direct-interaction of p53 and p63-bound require direct-interaction of p63.....	101

p63 is required, but not sufficient, to drive p63-mediated enhancer activity in a p63 non-native cell type	102
Discussion	105
CHAPTER 5: Discussion and Future Directions.....	108
CHAPTER 6: Detailed materials and methods of CHAPTERS 2, 3, and 4.....	116
Model System	116
Cell Culture:.....	116
Cell Treatments:.....	116
Molecular Biology	117
Quantitative real time PCR:	117
Western blotting:.....	117
Enzyme-linked immunosorbent assay (ELISA):	117
Antibodies:.....	118
Luciferase plasmid cloning and expression assays:.....	118
Sequencing	119
ATAC-seq:.....	119
ChIP-seq:.....	119
RNA-seq:	121
Massively Parallel Reporter Assay	122
Selection of candidate enhancers:	122

Massively Parallel Reporter Assay (MPRA) oligo design:	122
Two-step vector library cloning and verification:	123
MPRA virus production and transduction:	124
MPRA Amplicon enrichment and RNA-seq library preparation:	124
CRISPR-Cas9 Cell Lines.....	125
In vivo CRISPR/Cas9 mutagenesis and amplicon ChIP- sequencing:	125
Targeting KRAB to enhancers at genomic loci:	127
Generation of doxycycline inducible p63 isoform cell lines	127
Biochemistry	127
Protein expression and purification:	127
CCNG1 p53 electrophoretic mobility shift assay:	128
Data analysis	129
Massively Parallel Reporter Assay (MPRA) data analysis:	129
Transcription factor peak intersections:.....	130
Transcription factor motif analysis:	130
Data Availability	131
Catizone et. al 2019 and Chapter 2:	131
Catizone et. al 2020 and Chapters 3-4:	131
Reagent tables	132
Table 1: QPCR primers.....	132

Table 2: EMSA oligo sequences.....	132
Table 3: Plasmid Cloning primers	133
Table 4: CRISPR guide primers	134
Table 5: Barcoded Library primers.....	135
Table 6: Plasmid list.....	136
CHAPTER 7: Copyright details	137
CHAPTER 8: Contributions.....	138
CHAPTER 9: References	139

LIST OF TABLES AND FIGURES

Figure 1: Nutlin 3A activates p53 in the absence of DNA damage of S15 phosphorylation	28
Figure 2: p53 is more significantly enriched after Nutlin 3A vs Etoposide treatment compared to DMSO control.....	29
Figure 3: Overall enrichment between nutlin 3A and etoposide treatments are well correlated..	31
Figure 4: Peaks containing a canonical p53 motif are located farther from transcriptional start sites	32
Figure 5: Both nutlin 3A and etoposide treatments have the same overall enrichment of active regulatory region chromatin marks	33
Figure 6: ChIP-seq analysis suggest that both treatments have the same levels of chromatin marks, RNAPOLII occupancy, and accessibility	34
Figure 7: Nutlin 3A and etoposide treatments have common upregulated and downregulated genes	36
Figure 8: Transcriptional output of upregulated and downregulated genes is similar between both treatments.....	37
Figure 9: p53 occupancy is increased near TSS of upregulated genes while p53 enrichment is distal to TSS for downregulated genes	37
Figure 10: Chromatin marks present at TSS are consistent across treatment conditions	38
Figure 11: p53 may influence transcriptional pause release in addition to direct RNA polymerase II recruitment to promoters	39
Figure 12: Inflammatory pathway genes differentially regulated between nutlin 3A and etoposide treatments	40

Figure 13: p53 is most proximal to common targets between nutlin 3A and etoposide	41
Figure 14: Cells treated with BAY-11 show upregulation of p53 canonical targets with nutlin 3A and etoposide	42
Figure 15: Inflammatory genes respond only to etoposide treatment and are inhibited by BAY-11	43
Figure 16: Trends are consistent across different cell types; foreskin fibroblasts	43
Figure 17: Loss of p53 does not affect upregulation of inflammatory genes	44
Figure 18: RNA-seq analysis confirms etoposide specific genes are dependent on NF-KB.....	45
Figure 19: A barcoded massively parallel reporter assay was used to assess the affect sequence variation had on enhancer activity	55
Figure 20: p53 motif containing enhancers were grouped into bound and unbound by in vivo occupancy	56
Figure 21: p53 bound regions have high scoring response elements matching canonical sequences	56
Figure 23: P53 bound enhancers have signs of active regulatory regions	57
Figure 22: p53-bound regions are highly enriched for active chromatin marks compared to unbound regions.....	57
Figure 24: p53 bound regions produce more eRNA compared to unbound regions	58
Figure 25: Biological replicates for MPRA assay are highly correlated	60
Figure 26: p53 bound regions are more transcriptionally active in the MPRA compared to unbound regions.....	61
Figure 27: Ubiquitous enhancer activity is affected but randomization but not Nutlin 3A treatment or the loss of p53 protein expression	61

Figure 28: p53 bound enhancers show increased eRNA activity between after Nutlin 3A treatment	62
Figure 29: eRNA enrichment is only weakly correlated with p53 occupancy at bound enhancers	63
Figure 30: p53 bound enhancers are significantly less active when expressed in HCT116 p53-/- cells	63
Figure 31: Loss of the p53RE severely depletes transcriptional activity of p53 bound enhancers	64
Figure 32: Only loss of the p53RE disrupts transcriptional activity across the majority of the enhancers.....	65
Figure 33: Individual enhancer activity is affected by mutated flanking sequences in a context specific manner	66
Figure 34: Most flanking sequence variants with significant changes to activity show decreased transcriptional outputs.....	67
Figure 35: Flanking regions are highly enriched for transcription factor binding sites.....	69
Figure 36: DNA elements important for CRE function can be found in any position relative to the p53RE.....	70
Figure 37: Transcription factor binding sites are highly enriched flanking the p53RE.....	70
Figure 38: p53 bound regions contain transcription factor binding sites that cluster with transcription factor families	71
Figure 39: Enhancers lose approximately 2 transcription factor binding sites per variation but not INRs	72

Figure 40: Enhancers for two canonical p53 targets have functionally important flanking regions	73
Figure 41: Both the p53RE and the R2 position are evolutionary conserved across species	75
Figure 42: The R2 position's function is conserved across cell type and species and contributes to p53's optimal transcriptional activity	76
Figure 43: The R2 position's SP1/KLF motif has highly conserved G residues.....	77
Figure 44: Mutating a single conserved G reduces transcriptional activity of CCNG1's enhancer	77
Figure 45: Schematic depicting the CRISPR/Cas9 mutagenesis strategy to mutate R2 in vivo ..	78
Figure 46: Mutation of the R2 position in vivo significantly reduces CCNG1 mRNA levels	79
Figure 47: Loss of the SP1/KLF motif in vivo reduces p53 enrichment at the CCNG1 enhancer	80
Figure 48: Loss of R2 position in vitro modestly reduces p53 affinity for the CCNG1 enhancer	82
Figure 49: GDF15 has two putative p53 bound enhancers upstream of the gene body	83
Figure 50: Repression of the two putative p53 enhancers upstream of GDF15 deplete endogenous GDF15 mRNA.....	84
Figure 51: The stress factor ATF3 is strongly bound at the 3' GDF15 enhancer.....	85
Figure 52: GDF15's 3' enhancer is dependent on ATF3 but not the 5' enhancer.....	86
Figure 53: RNA-seq analysis confirms ATF3 protein expression is required for GDF15 mRNA production	87
Figure 54: Motif containing enhancers have varied p53 and p63 occupancy in vivo	98
Figure 55: p53RE motifs within the three clusters have differently scored binding sites	99
Figure 56: Cluster 2 enhancers bound only by p63 do not respond to Nutlin 3A treatment	99

Figure 57: Enhancer activity was significantly reduced compared to expression in wildtype cells	100
Figure 58: Loss of the p53RE disrupted enhancer activity in MCF10a cells	101
Figure 59: Loss of p63 but not p53 affects cluster 2 enhancers.....	102
Figure 60: Cluster 2 enhancers are only strongly active in native p63 expressing cells	103
Figure 61: Cluster 2 enhancers have reduced activity in absence of p63 protein.....	103
Figure 62: p63 expression is not sufficient to activate cluster 2 enhancers.....	104

CHAPTER 1: Introduction

The Guardian of the Genome

The tumor suppressor p53 is known as ‘the guardian of the genome’ for its critical role in the activation of tumor suppressor genes. p53 protects cells within the organism from DNA damage and other environmental insults (Meek, 2015)(Kastenhuber & Lowe, 2017). It does this a transcription factor through its control of a wide-ranging gene network. Ironically, upon its initial discovery, p53 was deemed an oncogene because of its abundance in cancer cells and its interactions with the SV40 DNA virus large T antigen protein (Kress et al., 1979)(Linzer & Levine, 1979)(Linzer & Levine, 1979). We now know that p53 is the acute response to cellular damage. While p53 is not critical for development (organisms lacking p53 are viable), they are more susceptible to tumor formation with age (McKinley & Cheeseman, 2017)(Powell et al., 2014). Cells that lack p53 grow uncontrollably and do not respond to many common drug therapeutics. Approximately 30% of cancers have a mutation to the p53 protein which are directly responsible for tumorigenesis (Kotler et al., 2018)(Khoo et al., 2014). p53 is one of the most studied proteins of all time, yielding over 99,000 publications available in the NCBI PubMed database as of 2020. p53 is rigorously studied for its roles in human cancers, however, its regulation over cellular damage is seen in multiple stress response pathways.

p53 and its apoptotic functions are conserved across metazoans. Invertebrates, like flies and worms, possess p53 like proteins mainly to protect the gametes through the activation of apoptosis or cell death (Herzog et al., 2012)(Fischer, 2019)(Sogame et al., 2003). Germ cells give rise to the next generation of the organism and preventing mutated cells from proliferating is prudent. p53’s role in genome protection expanded in vertebrates to include activity in somatic

cells and tissues. In vertebrates, it is also responsible for pausing the cell cycle, regulating DNA damage repair, and activating senescence (Meek, 2015)(J. Chen, 2016). Larger genomes of more complex organisms provide novel regulatory regions in which p53 is able to interact allowing for expanding functions and control.

p53 is the hub of a number of stress response pathways such as apoptosis, DNA damage repair, cell cycle arrest, and senescence. Although we have rigorously studied p53 since its discovery in 1979, its roles and regulation during homeostasis and disease have only spread and become more complex (Kress et al., 1979; Linzer & Levine, 1979). Starting as early as development, p53 is responsible for controlled cell death such as removing vestigial tissues like the webbing between the digits in human embryos (Jain & Barton, 2018). Throughout the organism's life, p53 plays roles in aging by activating senescence, reprogramming by promoting the expression of identity factors, stem cell maintenance and viral replication (Jeanine L Van Nostrand et al., 2017). An organism's cells also encounter a number of environmental and cellular insults in which p53 responds. Environmental stresses such as UV damage that causes DNA double stranded breaks triggers p53 to pause the cell cycle and allow for repairs to be made before proliferation continues. Naturally occurring errors and mutations in DNA can lead to p53 activation and force the cells to apoptose and be cleared from the organism (Hafner et al., 2019). p53 is the center factor that is able to specifically activate various signaling pathways through multiple inputs and cause a range of downstream effects that tend to be disease state and/or cell type specific. How p53 is regulated and what factors influence pathway choices and outputs remains an open and critical question in the field.

Natural activation of p53 in vivo

Increased levels of p53 immediately trigger gene expression of tumor suppressor targets which can be detrimental to the cell if left unchecked (J. L. Van Nostrand et al., 2014). However, p53 must have the ability to be rapidly induced upon stress. To accomplish this, the p53 protein is kept inactive at steady state levels through proteosome-dependent degradation mediated by an E3 ubiquitin ligase, MDM2 (Shlevkov & Morata, 2012)(Meikrantz & Schlegel, 1995). p53 protein is constantly being produced and degraded and upon DNA damage, a phosphorylation cascade occurs, releasing active p53 from MDM2-mediated ubiquitination (Vassilev, 2004). After liberation in the cell, p53 forms tetramers with identical subunits and regulates these acute stress responses through the binding of non-coding regulatory regions known as promoters and enhancers (Smeenk et al., 2008). p53 can be activated in DNA damage-dependent and – independent manners. p53-independent manners include: oncogene activation, ribosomal stress, loss of cell adhesions, and hypoxia (Horn & Vousden, 2007). Besides environmental stresses and molecular damage, other small molecule agents and drugs can be used to activate p53 in vitro and in vivo. Many chemotherapeutics (like etoposide, doxorubicin, cisplatin, etc.) induce DNA damage as a means to activate p53, thus hoping to elicit a p53-dependent cell death pathway as a means to control tumor growth. Recently developed small molecule inhibitors mimic the natural activation of p53 without damaging DNA (Burgess et al., 2016). The hope being that the activation of p53 will target and kill highly proliferative cells that exist in tumors without damaging healthy, non-tumorigenic cells.

p53 activating agents and dynamics of activation

Nutlin 3A is an MDM2 inhibitor that leads to stabilization of p53 protein in the absence of DNA damage. Nutlin 3A is highly specific for the p53:MDM2 interaction with transcriptional profiling showing minimal off-target effects (Burgess et al., 2016)(Catizone, Good, et al., 2019). Nutlin 3A, along with other nongenotoxic small-molecule p53 activators, has become a highly used laboratory tool for p53 stabilization without affecting parallel DNA damage pathways. Numerous FDA-approved chemotherapeutics, such as etoposide, doxorubicin, and cisplatin, are used to activate p53 in patients and in the laboratory.

The dynamics of p53 protein stabilization and abundance in the cell depend on the means of p53 activation. Exposure to gamma irradiation leads to fluctuating p53 protein levels over a 24-hour period, whereas UV treatment produces sustained p53 level over a longer period of time. In contrast, single doses of nutlin 3A lead to rapid p53 stabilization that is later reversed due to both nutlin 3A degradation and increased p53-dependent expression of MDM2 (Loewer et al., 2010)(Paek et al., 2016b)(Henseleit et al., 1997)(X. Chen et al., 2013). These p53 dynamics appear to control the ultimate outcomes of p53 activation, including the decision to commit to senescence or apoptosis. Although the dynamics of p53 protein levels are directly influenced by the method of p53 stabilization, whether this leads to differential p53:DNA binding or gene activation is less clear. Stabilization of p53 by genotoxic (such as the topoisomerase inhibitor etoposide) and non-genotoxic (Nutlin 3A) methods yield nearly identical DNA binding within highly similar local chromatin environments (Catizone, Good, et al., 2019). p53 engagement with the genome and transcriptional targets are cell type intrinsic and the study of these interactions is crucial for understanding the regulation of these critical stress pathways. The role of locally acting transcription factors and chromatin environment in p53 pathways are still under investigation.

p53 protein structure

The p53 protein is encoded by the *TP53* gene in humans. It contains 13 total exons on human chromosome 17p13.1 and has a specific DNA binding domain that shares 80% similarity among its family members p63 and p73 (Vieler & Sanyal, 2018)(Chillemi et al., 2017). 12 known p53 isoforms with varying domain structure are generated through transcription at multiple promoters and alternative splicing. Full length p53 (TAp53-alpha) consists of 2 transactivation domains (TADS) (I/II), a proline rich domain (PRD), a DNA binding domain (DBD), an oligomerization domain (OD), and a C terminal domain (CTD) (Chillemi et al., 2017). All of these domains are found in the canonical TAp53-alpha isoform, which will be referred to as p53. The DBD is responsible for binding specificity to the DNA and the TADs interact with transcriptional machinery (Chillemi et al., 2017). p53's TADs interact with a number of functional proteins such as TFIID, MDM2, TBP, and CBP/p300 which regulate both p53 and transcription. The OD allows for dimerization and tetramerization, which is required for DNA binding and transcriptional activation (Beckerman & Prives, 2010). The CTD aids with localization of p53 to the DNA and binding specificity to sub-optimal regions through extensive post-translational modification.

p53 binding to DNA

p53 binds a specific, canonical DNA sequence consisting of 20 nucleotides with the composition RRCWWGYYYRRRCWWGYYY (R: A or G; W: A or T; Y: C or T) (Sullivan et al., 2018). There are nearly 100,000 regions in the genome predicted to contain a canonical p53 response element (p53RE) (Szak et al., 2001). Despite this large number of motifs, only about 1500 of those sites are occupied *in vivo* (*Verfaillie et al., 2016*). Direct p53 binding sites are

characterized by high levels of H4K16ac, while indirect ChIP-seq- derived p53 binding events are found within highly accessible, promoter regions (Catizone, Uzunbas, et al., 2019; Karsli Uzunbas et al., 2019). A recent multi-omics approach suggests that high-affinity p53 binding sites are shared across cell types, whereas the observed cell type-specific binding events were lower affinity sites. p53 occupancy changes between cell types (Verfaillie et al., 2016; Younger et al., 2015). For example, in epithelial cells there are close to 12,000 p53 bound regions that differ from fibroblasts (Karsli Uzunbas et al., 2019). That is because p53 can control both core and cell type specific genes. Cell identities are governed by cell type specific factors as well as their specific chromatin topography (Karsli Uzunbas et al., 2019)(Saifudeen et al., 2002). It seems the more open regulatory locations with p53RE sequences, the more accessibility there is for p53 protein to bind and drive transcription at basal and stress conditions.

Inhibition or manipulation of the p53 pathway

The p53 pathway can be inactivated in a number of ways and through different mechanisms. The protein itself can be mutated or lost, however, loss of any number of downstream targets of p53 cripple the cellular stress response (Meek, 2015). Most mutations of p53 protein exist in the DNA binding domain because this directly inhibits p53's ability to specifically and successfully bind DNA (Freed-Pastor & Prives, 2012). Approximately 1200 unique p53 codon mutations have been identified in the DBD in cancer, however, other mutations do exist along the gene body. Codons for amino acids 175, 248, and 273 account for 20% of all somatic mutations of p53 protein most likely because they are within the DBD(Freed-Pastor & Prives, 2012). They are the amino acids that directly interact with the major groove of DNA regulatory regions and the p53RE. Other inhibitions of the pathway include deletion of the p53 gene (1 or both alleles), over-

activation of the inhibitors MDM2 or MDM4, mislocalization of p53 to the cytoplasm, and viral inactivation via viral p53-inhibitory proteins (Freed-Pastor & Prives, 2012). In general, many cancers progress due to the inactivation of full length p53. It has been shown that p53's isoforms have varying expression among different tissues both across different cell types and cancer types (Vieler & Sanyal, 2018)(Surget et al., 2013). Out of all cancer types only approximately 30% of cases have mutations to the p53 protein directly, usually residing in the DBD. This suggest that up to 70% of other cancers possess a wildtype p53 protein. As stated above, this could mean other factors or downstream targets have been mutated or loss. But there have been many reported cases of variations in p53 isoform expression that may be linked to tumorigenesis in an otherwise p53 wildtype background.

The DNA binding domain contains 80% of all missense mutations. Some other mutations exist in the TADs probably due to the fact that the TADs are responsible for recruiting important transcriptional machinery linked to the preinitiation complex. However, the overall number of mutations in this area are very low, suggesting that this is not the most efficient way to disrupt the p53 stress pathways (Boettcher et al., 2019). Mutations in the CTD can prevent important proteins from interacting with p53 guiding it to locations in the genome. Some modifications outside the DBD cause dysregulation, as an example, methylation of a lysine residue leads to dysregulation of wildtype p53 in testicular Tera carcinoma cells (Zhu et al., 2016). Cancer mutations are not only extremely varied across tissue types but across sub-types within the same tissues. It is possible that specific mutations to combinatorial factors or non-coding regulatory regions are responsible for the miss-regulation in the presence of wildtype p53. For example, loss of the CEBP site in the p21 enhancer prevents the senescence pathway in fibroblasts (Cohen et al., 2018). However, the study of regulatory region mutations and loss of p53 function has been only modestly investigated.

Cancers with the largest amount of mutations include ovarian, colorectal and lung cancer, while less mutations are seen in leukemia, sarcoma, and malignant melanoma (Freed-Pastor & Prives, 2012). There is a disconnect between why certain types of cancers (prominent in certain tissue types) have a predisposition for certain types of mutations. This might suggest why there are not more than ~30% of p53 protein mutations in cancer (Freed-Pastor & Prives, 2012). When p53 protein is mutated, one of the common causes of dysregulation of the p53 pathway is the dominant negative effect of mutant p53. As opposed to p53 deletions, mutated p53 tetramerizes with its wildtype counterpart and can prevent specific binding to DNA through the loss of important binding amino acids (Boettcher et al., 2019). This leads to the loss of expression of important downstream gene expression through the loss of transcriptional machinery recruitment. Because mutant p53 can also display gain of function mutations or develop novel functions, we can see the emergence of new gene expression patterns not seen in healthy tissues. These include gains of function in metastasis, cell proliferation, angiogenesis, and cell metabolism all inducing tumorigenesis. p53's function is disrupted specifically where it binds DNA (Vieler & Sanyal, 2018). However, any insult causing variation or loss of target gene expression will inhibit p53 pathway stress responses.

General transcription

Transcription is the recruitment of factors to regulatory regions such as promoters and enhancers. Promoters are the docking sites for the transcription machinery and are located next to the first exon of the gene body (B. L. Allen & Taatjes, 2015)(Soutourina, 2018). Enhancers control the timing of transcription as well as the amount of transcription that occurs. They are landing pads for DNA binding factors that can amplify or regulate the transcriptional signal that is facilitated

through the promoter (Hu & Tee, 2017). The central dogma of biology indicates first the DNA message is copied into RNA, and then translated into proteins. Those proteins then maintain homeostasis of the organism and respond to external signals eventually cycling back to transcription (Furlong & Levine, 2018). The process of transcription involves three distinct phases: Initiation, Elongation, and Termination. Initiation is the most highly regulated phase of transcription, with recruitment and release of RNA polymerase II being key control points. RNA polymerase II binds to regulatory regions of DNA (promoters), actively transcribes, and then releases the finished RNA product. Multiple co-factors cooperate to recruit RNA polymerase II including general transcription factors and sequence-specific transcription factors (B. L. Allen & Taatjes, 2015). In order for the proteins to interact at these regulatory regions the DNA must be made accessible to them.

Chromatin is the packaging and organization of DNA within the nucleus. Four core histone proteins form an octamer, and \approx 160bp of DNA wrap around those histones to form the basic organizational unit of chromatin, the nucleosome (Sainsbury et al., 2015). DNA coiled into these nucleosome structures is normally inaccessible to other binding proteins. The “unwinding” of DNA from nucleosomes and histones makes them accessible to other protein binding factors (B. L. Allen & Taatjes, 2015). Nucleosomes must be repositioned in order for transcription to occur in at least two scenarios. First, recruitment of RNA polymerase to gene promoters requires accessible DNA devoid of nucleosomes (Platt et al., 2016). Second, nucleosomes along the transcribing path of RNA polymerase must be evicted and replaced after RNA polymerase passes (Guertin & Lis, 2013). The temporal and spatial maintenance of chromatin is critical for the activation of important genes like in times of stress or in response to a stimulus.

Chromatin as a regulator of transcription

Nucleosomes shift and histones exchange positions based on post translation modifications on the histone proteins. These can be acetylations, methylations, and phosphorylations (Hu & Tee, 2017). These modifications can be added without affecting the DNA sequences and can alter gene expression through the opening and closing of the chromatin. “Active marks” or modifications as well as “repressive marks” can be seen all over the genome on histones in both basal and stress conditions (Hu & Tee, 2017). Active regions of DNA are often associated with methylations of Histone 3 (H3K4) and acetylations of Histone 3 (H3K27). Post translational modifications are added by “writer” proteins such as histone acetyltransferases, which mark the DNA to be “opened” or act as a mark of DNA that has been open or active (Spitz & Furlong, 2012)(Venkatesh & Workman, 2015). Chromatin remodeler proteins are recruited to these areas based on the modifications and open the DNA. This precise layering of signals drives chromatin accessibility which allows the next phase of proteins to occupy the area. These proteins include sequence specific transcription factors.

Transcription factor maintenance of chromatin

Transcription factors (TFs) are the driving force behind the temporal and spatial control of gene activation. They manipulate the DNA, block nucleosome repositioning, remodel chromatin, and recruit other cofactors (Spitz & Furlong, 2012). TFs tend to work in cohorts and their expression is governed by cell type and cell state as mentioned above. TFs can interact with themselves forming dimers and tetramers, as well as interacting with other members of their family (Spitz & Furlong, 2012)(Venkatesh & Workman, 2015). TF families are designated by their DNA binding domain and consensus binding sequence. One TF can have any number of roles and those

roles may be depicted or change based on the location where they are binding and the other TFs present (Reiter et al., 2017).

p53, as a transcription factor, is a transactivator with 2 TADs and is mainly responsible for recruiting transcriptional machinery (Levine, 1997). p53 is most commonly found at open and active areas of regulatory DNA suggesting that these regions are poised for rapid responses to outside stimuli and stress. We see this in other stimulant dependent factors such as glucocorticoid and estrogen receptors (Menendez et al., 2007)(McDowell et al., 2018). These transcription factors rely on a signal which has them travel to the nucleus and drive transcription at poised enhancers. However, there are cases where p53 is bound to inaccessible chromatin showing “pioneer factor” activity (Iwafuchi-Doi & Zaret, 2016). Pioneer factors are transcription factors that are able to open areas of DNA or drive transcription in the absence of other factors.

Pioneer factors and p53 as a pioneer factor

Pioneer factors are required for establishment of active transcriptional regulatory regions (Morris, 2016). These proteins can actively bind specific DNA-sequences wrapped around nucleosomes and drive nucleosome remodeling and repositioning. Pioneer factors can also take a more passive role and occupy regulatory regions to bookmark and drive transcription without as many factors present (Zaret & Carroll, 2011). Common pioneer factors are known as the fork head box (FOX) or zinc finger (GATA). Pioneer factors can recruit histone modification factors to regulatory regions which further facilitates transcription factor recruitment (Zaret & Carroll, 2011). Pioneer factors are normally signal or stimulus activated which targets them to important regulatory regions. p53 normally acts as a transactivator protein recruiting RNAPOLII and other preinitiation cofactors to already open chromatin (Sainsbury et al., 2015). p53 is able to bind closed

chromatin as long as its consensus sequence is appropriately positioned on the outside of the histone (Uzunbas et al., 2018)(Sammons et al., 2015). p53 only rarely, directly affects chromatin structure with modest pioneer factor activity and has been found at regulatory regions lacking H3K4 methylation. Both p63 and p73, members of the p53 family of transcription factors, have strong pioneer factor activity and cell lineage roles although the specific molecular mechanisms driving this activity is unknown. p53, in the majority, binds open regulatory regions known as promoters and enhancers. This suggests there is a potential enhancer mechanisms and string of cofactors that drive p53-mediated transcriptional activity and gene expression.

p53 binding to gene regulatory elements: promoters

p53 was first associated with binding to DNA specifically at promoters (Szak et al., 2001). Reports of p53 being bound within 300bp of the TSS of canonical genes like CDKN1A/p21 strengthened the argument that p53 mediated transcription through promoters (Szak et al., 2001). We know now that p53 binds enhancer elements in the majority, however, promoter binding is still crucial for the activation of critical downstream tumor suppressor targets. While all p53-dependent genes have p53 bound at one of their regulatory elements, promoters and enhancers do not need to both be occupied by the transcription factor. In fact, occupation by p53 at regulatory elements is varied across target genes. For example, CDKN1A/p21 has p53 bound at its promoter, as well as a number of its distal enhancer regions (M. A. Allen et al., 2014)(Joaquin M Espinosa & Emerson, 2001). The target gene GDF15 has p53 bound at its two distal enhancers, but not at its promoter (Catizone et al., 2020). And there are many well characterized examples of p53 target genes with only proximal promoter binding. It is still unclear how this variation plays a role in tumor suppression, gene activation, and the response to stress by p53.

p53 mainly works as a transactivator recruiting transcriptional machinery to open areas of regulatory DNA. p53 is known to recruit different components of the pre-initiation complex such as TFIIA/D, p300/CBP, and others (G. S. Chang et al., 2014). Histones flanking promoters are acetylated upon binding of p53. H3K9ac, H3K27ac, and H4K16ac are most prevalent, likely because p53 binds to and directly recruits the histone acetyltransferase complexes mediating these modifications (Wang et al., 2016). This p53-dependent acetylation is observed under both basal and stress-dependent conditions. There is a rich understanding of p53's role at promoters with respect to the interplay between histone modifications and RNA pol II activity, suggesting that p53 orchestrates the recruitment of a wide variety of factors to drive transcription (Li et al., 2009; Rahnamoun et al., 2017).

Enrichment of p53 at a single location is not the sole driver of stress-dependent gene expression. p53 binds to many more promoters than the total number of genes activated, suggesting additional regulatory steps are required for gene activation. We see this in a few examples of RNAPOLII being poised at certain p53-dependent promoters pre-stress stimulus as well as other initiation factors (Joaquín M. Espinosa et al., 2003). This suggests that open regulatory regions are “prepped” for potential stress stimulus response before the activation of p53 (Joaquin M Espinosa & Emerson, 2001). Cell type and type of stress play a role in which factors are recruited and variation in binding as well as downstream gene expression strength. This suggests that other components besides p53 play a role in the type of gene activation we see downstream.

p53 binding to gene regulatory elements: enhancers

As stated previously, we now know that p53 is highly enriched at active enhancer regions. Enhancers are able to work in both cis and trans, allowing them to influence gene expression up

to a mega-base away from the TSS/promoter (Hu & Tee, 2017). They function in large networks comprised of multiple regulatory elements such as silencers, insulators, promoters, and other cis-regulatory units (Heinz et al., 2015). Enhancers serve as landing pads for collections of transcription factors, which fluctuate through times of stress, disease, homeostasis, development, and cell type(Spitz & Furlong, 2012)(Heinz et al., 2015).

While general transcription factors, like the TFIID complex, are involved in p53-dependent promoters, the requirement for other sequence-specific factors at enhancers remain an open question. A recent study suggested that p53 was necessary and sufficient for enhancer activity (Verfaillie et al., 2016; Younger & Rinn, 2017). However, multiple p53-dependent enhancers have shown to require other transcription factors, similar to the enhanceosome and billboard models. One study identified CEBP β -binding site within an enhancer regulating p21 required for p53-dependent cell cycle arrest and senescence (Appella et al., 1998)(Cohen et al., 2018). Transcription factors such as those in the AP-1 family have been implicated in the activation of p53-dependent genes. The utilization of multiple transcription factors would indicate p53 has the flexibility to cooperate with various combinations of transcription factors to drive downstream gene expression.

Loss of p53 activity is strongly linked to increased cancer risk and decreased life expectancy, and misregulation of p53 is associated with numerous other human disorders. The mechanisms by which tumorigenesis progresses in the presence of wild type p53 activity have not been well characterized and approximately 60-70% of cancer cases have wildtype p53(Meek, 2015). Recent evidence suggests that mutations in sequences within enhancers can influence p53 binding, transcriptional activity, and tumor suppressor function. While the presence of a canonical p53 response element (p53RE) is well understood, the influence of the local sequence environment

and the role of other transcription factor motifs within an enhancer on p53 activity remains an open question.

Enhancer models:

An enhancer model depicts the mechanism in which protein factors interact within the regulatory region to drive transcriptional activation. Transcription factor cooperativity and combinatorial activity is determined by the identity of the factors, how they interact, and in what order they bind the region (Furlong & Levine, 2018)(Hu & Tee, 2017). Enhancers can work in both *cis* and *trans* meaning they can influence the promoter from large genomic distances away but also through production of small enhancer-derived transcripts (eRNA) (M. A. Allen et al., 2014). The main hypothesis suggests that enhancer:promoter contacts are facilitated through a looping mechanism in which the factors that bind the regulatory region regulate and manipulate the DNA so enhancers and promoters come into contact(Furlong & Levine, 2018; Hu & Tee, 2017). Recruitment of factors to both the enhancer and promoter are critical for the correct protein interactions to drive transcription.

Two main enhancer models exist, while many have been proposed, which include the “enhanceosome” model and the “billboard” model. The enhanceosome model maintains a rigid motif organization for specific sets of factors (Arnosti & Kulkarni, 2005). These proteins bind in a specific order allowing for a scaffold to form driving downstream gene expression. In this model, all factors are required and loss of any one factor halts transcription. The best example we have of this enhancer model is the interferon beta enhancer (Thanos & Maniatis, 1995). The billboard model is more fluid allowing for flexibility in binding with multiple cohorts of transcription factors (Arnosti & Kulkarni, 2005). Thus, allowing these enhancers to be influenced by different cell

conditions and transcription factor availabilities (Reiter et al., 2017). This flexibility seems to come from the collection of binding sites that are “sub-optimal” and protein-protein interactions that occur before binding. In this model, transcription factors can bind in any order on the enhancer. The enhanceosome model, evolutionarily speaking, provides the most reliable signal in terms of timing and strength of transcriptional activation (Thanos & Maniatis, 1995). However, a single mutation in sequence or loss of a single protein factor can halt all transcriptional capacity of the region. Therefore, what the billboard model lacks in rigidity, it gains in fluidity to various stress or disease conditions preserving gene activation. There have been some reports of a “single factor” model in which only one factor is required for chromatin accessibility, stimulating enhancer:promoter contacts, the recruitment of transcriptional machinery, and the driving force behind transcription (Verfaillie et al., 2016; Younger & Rinn, 2017). Two publications have evidence that p53 may work strictly in a ‘single factor’ model, however, whether p53 works in an enhanceosome, billboard, or ‘single factor’ enhancer model (or a combination of all three) is still an open question.

The p53 gene regulatory network

Transcription factor motifs are abundant in canonical p53 enhancers. Multiple p53 bound regulatory regions can be found upstream of canonical p53 targets such as *p21*, *PUMA*, *GDF15*, *CCNG1*, and many others (Brady et al., 2011). The DNA binding factors that interact with these regions may be the reason certain p53 pathways are chosen in a certain cell type or given a certain stress stimulus.

Apoptosis

Each p53 pathway has a unique gene expression dynamics. Apoptosis is a type of programmed cell death that maintains homeostasis, as well as functioning in development of tissues and structures, and in times of cellular stress (D'Errico et al., 2003). The logic behind apoptosis after cellular insult is to protect the whole organism or tissue by killing cells that are beyond repair or may be deleterious if left in the population (Meikrantz & Schlegel, 1995). Apoptosis is triggered through two pathways: the extrinsic and intrinsic pathways. Extrinsic pathway is initiated by the TNF signaling pathway activating the DISC (Death inducing signal complex) triggering a cascade of caspase cleavages and causing apoptosis (Pucci et al., 2000). In the extrinsic pathway, p53 target genes include the TNF-R family of death receptors as well as caspase 8 directly (Pucci et al., 2000)(Maximov & Maximov, 2008). The intrinsic pathway is associated with the mitochondria and the release of cytochrome C. Activation of APAF-1 generates the apoptosome induces the cleavage of caspase 9 and eventually caspase 3 causing cell death. Cleaved caspase 3 is a distinct marker used to identify cell death via the intrinsic pathway (Pucci et al., 2000). p53 directly activates proteins such as BIM and BBC3 (PUMA) which regulate Bcl-2 and Bcl-XL anti-apoptotic proteins, which are a part of the intrinsic pathway (Pucci et al., 2000). BAX is also a direct target of p53 which interacts with the mitochondria to propagate the release of cytochrome C (Maximov & Maximov, 2008). Apoptosis or programmed cell death is the just one of the p53-mediated stress pathways.

Cell cycle arrest

Cell cycle arrest is activated by p53 allowing for repair of the DNA damage or leading to permanent cell cycle arrest (senescence). After cell cycle arrest, if the damage cannot be repaired

the either the apoptotic or senescence pathways are initiated. The cell cycle is a set of perfectly timed events that drive cell proliferation. These phases are G1 (growth stage 1), S (DNA replication), G2 (growth stage 2 and doubling of cell volume), and M (cell division) (Rufini et al., 2013). There are specific check points for DNA damage during this cycle at G1/S and G2/M. Cell cycle is mediated by the fluctuations of various proteins known as cyclins and cyclins are regulated by CDKs (cyclin dependent kinases)(Pucci et al., 2000). p53 has been shown to influence both check points and is most notably responsible for the G1/S pause in which it activates the canonical p53 target gene, p21(Pucci et al., 2000). p21 is known as a CKI (cyclin kinase inhibitor) which prevents the protein retinoblastoma (Rb) from being phosphorylated halting cell cycle. In p21 deficient cells, cell cycle arrest cannot occur at the G1/S check point, however, increasing levels of p53 can still drive apoptosis(Pucci et al., 2000)(Haferkamp et al., 2009). p53 can turn on a number of downstream gene targets that independently regulate the various stress pathways. Loss of anyone factor only affects its specific p53-mediated pathway leaving the other stress responses intact.

Senescence

Senescence or permanent cell cycle arrest is another host defense activated by p53 after DNA damage. It guards against the spread of mutated or damaged cells without directly leading to apoptosis (Shen et al., 2009). Senescent cells cannot reenter the cell cycle and are eventually removed by the immune system. Replicative senescence is caused by the shortening of telomeres which is why many primary cells in culture reach a “limit” of replication and senesce (Chien et al., 2011)(Itahana et al., 2001). However, p53 induced senescence is driven by the presence of DNA damage, as an example, by oxidative stress. The overexpression of oncogenic factors can

trigger senescence such as RAS and RAF, as well as the over expression of tumor suppressor genes like p16 and p14 (and MDM2 regulator) (Haferkamp et al., 2009)(Itahana et al., 2001). Senescent cells arrest growth in the G1 phase of cell cycle and become resistant to apoptosis. Cell morphology also changes leading to enlarged cells and expression of increased levels of beta-galactosidase (Rufini et al., 2013). p53 levels go up with DNA damage-dependent senescence along with p21 expression. It is thought that this pauses the cells in G1/S phase and causes the irreversible cell cycle arrest.

Cell type effects on p53 activity

p53 dependent pathways include apoptosis, cell cycle arrest, DNA damage repair and senescence. Observations conclude that while all cells seem to be capable of the various downstream responses, cell types tend to be predisposed to p53 dependent cell fates. For example, it is known that fibroblasts tend to senesce while epithelial cells tend to undergo apoptosis when p53 is activated (Georgakopoulou et al., 2016). Fibroblasts tend to senesce while epithelial cells tend to apoptose suggesting there are cell type specific drivers that influence p53 pathway choice (Georgakopoulou et al., 2016). The current mechanism for why this occurs is not fully elucidated. One possibility is that different tissue lineages trend towards senescence due to their roles in tissue and organ integrity, where apoptosis would be catastrophic to structural or organismal integrity (Childs et al., 2014). Other cell types can therefore undergo apoptosis to clear out highly proliferative cells that are easily and quickly replaced. The control over p53 pathway fates could lie in the balance of gene expression (i.e. p21 towards senescence or PUMA towards apoptosis) as well as cell type specific gene dynamics.

Previous studies have stated that the likelihood for certain cells to undergo either apoptosis or cell cycle arrest may be due to the levels and timing of p53 activation (Paek et al., 2016). One group determined using single cell analysis from a p53 activated population of cells that p53 must reach a certain threshold of expression for apoptosis to occur and failure to reach that threshold led to cells going into cell cycle arrest. However, this study does not take this theory into other cell types or other potential models of cell fate choice (Loewer et al., 2010) (Hafner et al., 2019)(Joaquin M Espinosa & Emerson, 2001).

p53 is well known as a strong transactivator. Higher enrichment of p53 at more locations in the genome may be the cause of different stress pathway fates among cells. In fact, it is known that p53 total expression is varied across cell lineages, not taking into account cell size and volume. One study utilized a transcriptional activation mutant and found while it poorly activated a majority of the canonical down-stream targets, it was still able to suppress tumors in multiple tissue types. Most p53 cancer mutations are directed towards the DNA binding domain which prevents p53 from specifically binding promoters and enhancers and subsequently preventing down-stream gene expression. However, this study found that it's the binding and presence of p53 at these locations, not its transactivation that was necessarily required for tumor suppression function (Freed-Pastor & Prives, 2012). This may suggest that it's the binding of p53 to multiple regulatory units such as enhancers and its ability to work in combination with other local trans-activators that may be causing the underlying tumor suppressor properties of p53(Bowen et al., 2019)(McDade et al., 2014).

Both p63 and p53 bind similar consensus sequences and p63 is able to bind all place p53 occupies in vivo. This study found that between the two cell types used, fibroblasts and epithelial cells, p53 activated a range of either ‘core’ or ‘cell type specific’ targets (Karsli Uzunbas et al.,

2019). They came to the conclusion that p63 both regulated p53 activity and maintained the identity of the epithelial cells while p53 activated certain cell type specific gene expression. In this study p63 was found to maintain open chromatin locations for p53 to bind and activate and these open locations contained cis-regulatory units known as enhancers. A current hypothesis for regulation of p53 dependent transcription is that the local chromatin context, aka the open and available regulatory units, are what govern p53 acute responses (Uzunbas et al., 2018). So, the question remains on how cell type specific chromatin environments affect p53 responses and downstream pathways.

p53's role in cell identity

While loss of p53 in mice leads to phenotypically normal pups, those animals become increasingly susceptible to tumor formation as they age compared to wildtype animals. However, upon closer examination, others have found that the loss of p53 does in fact have negative phenotypic outcomes, especially in the epithelium. One group found that in renal epithelium, p53 is highly enriched as well as other factors called renal function genes (RFGs) (Saifudeen et al., 2002). These genes are only present in differentiating renal epithelium and are absent from both progenitors and terminally differentiated cells. p53 -/- pups showed incomplete differentiation of epithelial tissues in their kidneys and had low expression of the RFGs (Saifudeen et al., 2002). p53 specifically activated these critical differentiation genes through the binding of their promoters. The authors state that transcription factors used in differentiation may have cell type specific targets suggesting p53 may have cell type specific roles in the epithelium. Another group saw that loss of p53 protein forced epithelial cells into epithelial-mesenchymal transition (EMT) and increased the stem cell population of the mammary tissues (Saifudeen et al., 2002). p53 specifically

regulated a microRNA, miR200c, through the binding of its promoter. miR200c is thought to be responsible for protecting against EMT or loss of epithelial cell identity (Schubert & Brabletz, 2011). As a strong trans-activator, p53 has the capability of governing an acute response to important genes during the differentiation process.

The p53 paralog p63 has been recently implicated as a cell type specific epithelial identity factor (C.-J. Chang et al., 2011). It has many known roles in epithelial maintenance, differentiation, and proliferation (Koster et al., 2004). In fact, loss of p63 is usually lethal in epithelial cell culture and many cells do not tolerate reduction of p63 protein expression. In the mammary epithelial cell line MCF10A, reduction of p63 forces the cells to begin the EMT process and produce mesenchymal markers (Qu et al., 2018). The role of p53 in this process is currently unknown.

p53's role in cell reprogramming

Reprogramming of fibroblasts to various cell types has been rigorously examined for its potential use in therapeutics. The addition of the reprogramming factors Oct4, Sox2, c-myc, and Klf4 induce pluripotency in cells, however, this is relatively inefficient with only ~1% of the cell population converting to iPSCs (Takahashi & Yamanaka, 2016). Studies have shown that p53 governs terminal differentiation making it difficult for cells to change cell types. This was first shown in 2002, where the authors found that loss of p53 allowed for a higher percentage of fibroblasts converting to iPSCs, however, they accumulated high levels of DNA damage (Marión et al., 2009). Thus, suggesting that p53 was responsible for preventing damaged cells (like those with uncapped telomeres or double strand breaks) from reprogramming. Interestingly, they found the depletion of ATM (the activating kinase upstream of p53) had no effect on cell reprogramming suggesting p53's potential redundant stress pathway response to repress the transition to iPSCs.

Over a decade later, multiple studies revealed that depletion of p53 was sufficient to convert fibroblasts directly to all three neuronal lineages by growing them in the appropriate nutrient media, skipping the iPSC stage entirely (Zhou et al., 2014). p53 has been shown to have roles in neural precursor cell renewal and differentiation. Not only does reduction of p53 allow for cell fate change, it also induced a number of neurogenic transcription factors such as NeuroD2. They also showed that p53 bound many of the promoters of these neurogenic specific factors. This work suggests that outside of p53's roles inducing cell stress responses, p53 may play another role as a transcription factor binding cell type specific regulatory units to guard terminal differentiation (C.-J. Chang et al., 2011).

Conclusions

What we can begin to hypothesize is that the varying chromatin landscapes across cell types and the availability of different co-factors could influence p53 activity. We find that p53 has critical roles in not only guarding the genome against DNA damage but serving as a gate keeper for terminal differentiation. p53 acts through promoters and enhancers to regulate cell type specific gene expression protecting cells from de-differentiation or ‘reprogramming’ and the loss of p53 allows us to reprogram cells in higher efficiency. Although this shows to come at a price as these p53-/ reprogrammed cells tend to harbor DNA damage.

p53, and its paralogs, seem to maintain cell lineage and loss of these factors causes cells to undergo radical gene expression changes. Nevertheless, it seems in all its importance in guarding cell identity and fate, p53 is heavily controlled by the cell type it is in. This control is extended across the chromatin context and variation among cell lineages and the availability of open regulatory regions for p53 to bind. Thus, p53 can activate both ‘core’ and ‘cell type specific’ stress

programs through the availability of the regulatory regions. Finally, p53 offers a range of redundant programs that are most likely controlled by different downstream cofactors and combinatorial proteins ensuring the stress response pathways are turned on. It is the manipulation of these accessory factors that may be the cause of tumor progression in cancers containing a wildtype p53 protein. Thus, p53 has many roles outside its tumor suppressor function and is not only a guardian of the genome, but of cell fate as well.

CHAPTER 2: Comparison of genotoxic versus nongenotoxic stabilization of p53 provides insight into parallel stress-responsive transcriptional networks

This chapter was published as:

Catizone AN *et al.*, Cell Cycle (2019)

Introduction

The transcription factor p53 serves as a central hub in the transcriptional response to DNA damage (Zilfou & Lowe, 2009). p53 directly binds a consensus response element (RE) sequence within promoters and enhancers to activate a cell and organism-protective gene regulatory network (El-Deiry et al., 1992). This transcriptional response involves upregulation of numerous genes involved in cell cycle arrest, apoptosis, DNA repair, and metabolism (Daniel Menendez et al., 2009; Vousden & Lane, 2007). As loss of p53 activity is highly correlated with tumorigenesis (Zilfou & Lowe, 2009) there is strong and continued interest in deciphering the gene networks downstream of wild-type p53 activation.

The p53 protein is kept inactive at steady-state through proteosome-dependent degradation mediated by the E3 ubiquitin ligase MDM2 (Haupt et al., 1997). Upon the onset of DNA damage, the ATM and ATR kinases signal through CHK1 and CHK2 to phosphorylate p53, thus liberating active p53 from MDM2-mediated ubiquitination and turnover (Abraham, 2001). Nutlin 3A is an MDM2 antagonist that leads to rapid stabilization and activation of p53 protein in the absence of DNA damage and ATM/ATR signaling (Vassilev et al., 2004). Importantly, nutlin 3A is highly specific for the p53:MDM2 interaction with transcriptional profiling demonstrating minimal off-target gene expression changes after treatment (Allen et al., 2014). Chemical derivatives of nutlin 3A are still under investigation for the treatment of wild-type p53-containing cancers due to the

high specificity and seemingly non-genotoxic mechanism of action (Burgess et al., 2016). Nutlin 3A, along with other non-genotoxic small molecule p53 activators, has become a highly used laboratory tool for p53 stabilization without affecting potential parallel DNA damage pathways.

The dynamics of p53 protein stabilization and subsequent cellular-level phenotypes depend on the method used to activate p53, with significant differences observed within different DNA damage paradigms or nutlin 3A (Paek et al., 2016; Purvis et al., 2012). Exposure to gamma irradiation lead to oscillating p53 protein levels over a 24-hour period whereas UV treatment produces sustained p53 levels with an overall higher amplitude. In contrast, single doses of nutlin 3A lead to rapid p53 stabilization that is later reversed due to both nutlin 3A degradation and increased p53-dependent expression of MDM2. These p53 dynamics appear to control the ultimate outcomes of p53 activation, including the decision to commit to senescence or apoptosis (Paek et al., 2016; Purvis et al., 2012). Although the dynamics of p53 protein levels are directly influenced by the method of p53 stabilization, whether this leads to differential p53:DNA binding or gene activation is less clear(Hafner, Stewart-Ornstein, et al., 2017; D. Menendez et al., 2013; Verfaillie et al., 2016).

The first wave of genome-scale p53 ChIP-seq experiments suggested high spatial variability of p53 binding in response to various p53 activating conditions, even within the same cell type (Bentley et al., 2008; Botcheva et al., 2011; D. Menendez et al., 2013; Nikulenkov et al., 2012; Smeenk et al., 2008). Reanalysis of these datasets and multiple other p53 ChIP-seq datasets from a variety of transformed cell types and p53 stabilization methods suggested p53 DNA binding is much less variable (M. Fischer, 2017; Verfaillie et al., 2016). Approximately 1,000 p53 binding sites display high concordance across multiple labs, cell types, and experimental methods when consistent data processing methods are used (Verfaillie et al., 2016). Conversely, two recent

preprints demonstrate widespread cell type-specific p53 binding events that are driven by differences in chromatin accessibility (Hafner, Lahav, et al., 2017; Uzunbas et al., 2018). A recent multi-omics approach suggests that high affinity p53 binding sites are shared across cell types, whereas the observed cell type-specific binding events were lower affinity sites (Allen et al., 2014).

We therefore sought to better understand functional differences between genotoxic and non-genotoxic stabilization of p53 and the resulting transcriptomes. Here, we find that stabilization of p53 by genotoxic (etoposide) and non-genotoxic (nutlin 3A) methods yield nearly identical DNA binding within highly similar local chromatin environments. Direct p53 binding sites are characterized by high levels of H4K16ac, while indirect ChIP-seq-derived p53 binding events are found within highly accessible, promoter regions. Genotoxic activation of p53 using etoposide leads to significantly more activated gene targets than using nutlin 3A, with the majority of these genes classified as inflammatory response genes. Expression of these etoposide-activated genes is abrogated by treatment with NF- κ B pathway inhibitors, suggesting a DNA damage-dependent, but p53-independent, mechanism of action. These data provide increased evidence that p53 engagement with the genome and transcriptional targets are cell type-intrinsic and that careful analysis of crosstalk between DNA damage signaling pathways is prudent.

Results

Comparison of p53 interaction with the genome after genotoxic and non-genotoxic activation

We used low-passage (PD 25-30) primary human fibroblasts (IMR90) cultured under normoxic conditions (3% O₂) to assess whether p53-mediated gene expression and genome binding dynamics vary based on the method of p53 stabilization and activation. IMR90 are non-transformed fibroblast cells that undergo canonical hallmarks of senescence after sustained replicative growth, suggesting that the full p53 pathway is intact. Further, the epigenome and other genomic characteristics of IMR90 cells were analyzed by the ENCODE project, providing us additional context for studying p53 activity. Etoposide is a commonly used chemotherapeutic that inhibits topoisomerase II, leading to a failure to resolve dsDNA breaks and activation of p53 through an ATM-mediated signaling cascade (Maanen et al., 1988; Shieh et al., 1997). Phosphorylation of p53 at serine 15 (p53 S15ph) disrupts the interaction with the E3 ligase MDM2 and results in stabilization of the p53 protein (Sammons et al., 2015).

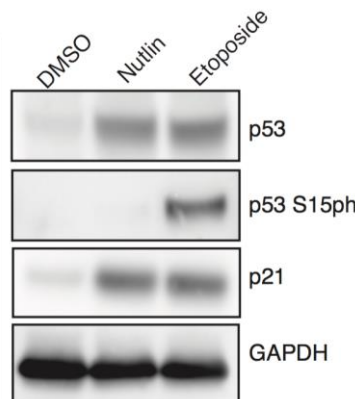


Figure 1: Nutlin 3A activates p53 in the absence of DNA damage of S15 phosphorylation

Western blot analysis of p53, p53 serine 15 phosphorylation, p21, and GAPDH in IMR90 fetal lung fibroblasts (cultured at 3% O₂ in DMEM plus 10% fetal bovine serum) 6 h after treatment with either DMSO (vehicle), nutlin 3A (5 μM final), or etoposide (100 μM final).

The small molecule nutlin-3A is an inhibitor of the p53:MDM2 interaction, and leads to stabilization and activation of p53 in the absence of DNA damage or p53-S15ph (Figure 1, (Vassilev et al., 2004). Treatment with either 100 μ M Etoposide or 5 μ M nutlin 3A lead to similar p53 and CDKN1A/p21 protein accumulation 6 hours post-treatment compared to a DMSO vehicle control (Figure 1), suggesting approximately equivalent effects on p53 stabilization and activity.

Etoposide treatment led to an increase in phosphorylation of serine 15 (Figure 1), which is downstream of DNA damage-dependent kinases and is required for endogenous stabilization of p53 after DNA damage (Zilfou & Lowe, 2009).

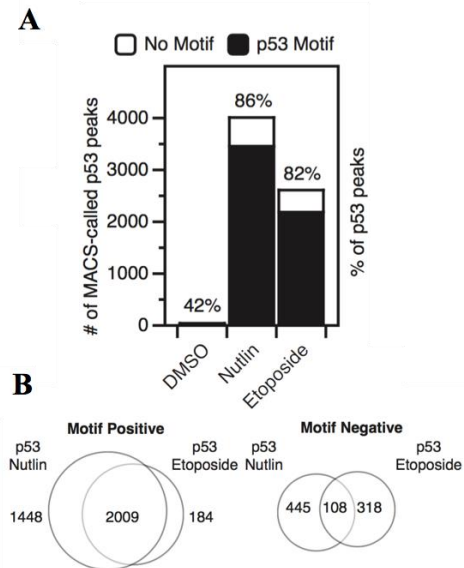


Figure 2: p53 is more significantly enriched after Nutlin 3A vs Etoposide treatment compared to DMSO control

(a) The number of MACS (v1.4)-derived p53 peaks ($q < 0.05$) with (black) or without (white) a canonical p53 motif (as determined by p53scan) under DMSO, nutlin 3A, or etoposide treatment conditions. (b) Intersection between nutlin 3A and etoposide p53 peaks containing a p53 motif (left) or lacking a p53 motif (right) as determined by BedTools intersectBed.

We then used chromatin immunoprecipitation coupled to highly parallel sequencing (ChIP-seq) to determine the genome-wide binding sites of p53 after 6 hours of treatment with 100 μ M etoposide and compared this treatment to previously published datasets for DMSO and nutlin (heinz). Importantly, all p53 ChIP-seq experiments were performed using identical conditions

(Heinz et al., 2010a). Treatment with either nutlin or etoposide dramatically increased the number of observed input-normalized p53 peaks compared to DMSO vehicle controls (Figure 2A), with more statistically enriched peaks (FDR > 0.01) observed after treatment with nutlin 3A than with etoposide. The large majority of p53 binding events in both conditions contain a full canonical p53 response element motif (86% and 82% for nutlin 3A and etoposide, respectively) as determined by p53scan (smeenk), and *de novo* motif finding using HOMER (quinlan) yielded highly similar DNA elements underlying nutlin 3A and etoposide induced p53 binding sites.

In order to identify putative functional differences between two p53 activating conditions, we analyzed whether nutlin 3A and etoposide-induced p53 binding events occurred within similar genomic loci. We parsed peaks by the presence of a canonical p53 response element motif (motif positive) and those lacking such a motif (motif negative) using p53scan (Smeenk et al., 2008) and then performed peak overlap analysis using bedTools (Jain et al., 2015). Over 90% of etoposide p53 motif+ peaks intersect with nutlin 3A motif+ peaks (Figure 2B), while we observe nearly 1,500 nutlin 3A-specific p53 binding events. Conversely, only 25% of etoposide p53 peaks lacking a canonical p53 motif overlap motif- peaks found after nutlin 3A treatment (Figure 2B). These peak-based results are similar to previous reports of p53 binding after stabilization using various p53 activation paradigms (Lowe et al., 2014)(Nikulenkov et al., 2012).

We next examined the ChIP enrichment of motif-positive common, nutlin 3A-specific, and etoposide-specific p53 binding events to determine more quantitative differences between the groups. Despite the seemingly large number of observed nutlin 3A-specific p53 enriched peaks relative to etoposide (Figure 2B), the enrichment of p53 signal within each peak region is well

correlated between nutlin and etoposide treatments (Figure 3A). The same is true when looking at enrichment of nutlin-induced p53 binding events at etoposide-specific locations (Figure 3B). Overall, enrichment at nutlin 3A and etoposide p53 binding events with p53 motifs are well correlated (Pearson $\rho=0.9451$), while enrichment of peaks lacking p53 motifs are uncorrelated (Pearson $\rho=0.0134$). These data suggest that virtually all inducible p53 binding events are observed independent of p53 activation method when considering enrichment instead of strict peak calling methods. This is in contrast to previous reports using peak calling methodologies (Nguyen et al., 2018; Nikulenkov et al., 2012), but similar to meta-analyses of those (and other) data showing high similarity across p53 conditions when considering ChIP enrichment (Verfaillie et al., 2016). Our data demonstrate that p53 engagement with the genome is highly similar between non-genotoxic (nutlin 3A) and genotoxic (etoposide) stabilization methods. Further, these results suggest that p53 ChIP-seq peaks lacking canonical p53 motifs are variable and do not correlate

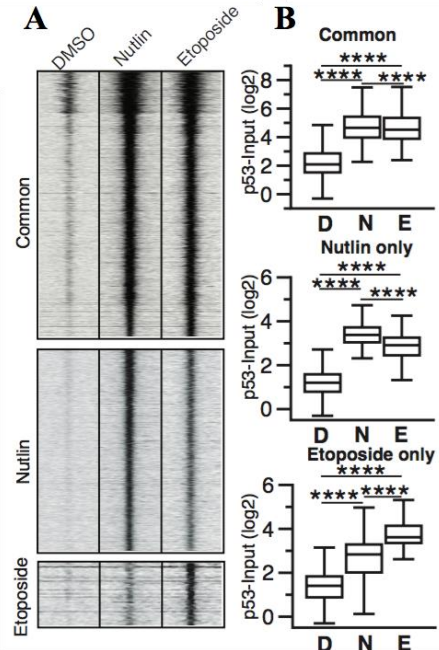


Figure 3: Overall enrichment between nutlin 3A and etoposide treatments are well correlated

(a) Input-subtracted p53 ChIP-seq tag enrichment at common, nutlin 3A-specific, or etoposide-specific p53 motif-containing peaks (± 1000 bp from p53 motif center). (b) Box plot quantification showing input-subtracted p53 enrichment (\log_2 , ± 1000 bp) at common (top), nutlin 3A-specific (middle), or etoposide-specific (bottom) p53 motif-containing peaks ($****p < 0.0001$, Wilcoxon sign-rank test)

between stabilization conditions, suggesting they represent experimental or technical artifacts observed in ChIP-seq experiments.

Chromatin context at p53 binding sites provides evidence for common gene regulation downstream of nutlin 3A and etoposide-mediated activation of p53

p53 ChIP-seq peaks containing a canonical p53 motif (motif +) are located significantly further from transcriptional start sites (TSS) than peaks lacking a canonical motif (motif -), with the modal group of motif (-) peaks located within 5kb of a TSS (Figure 4). Transcriptional start sites and highly expressed genes can cause significant artifacts and false-positives in ChIP-seq experiments (Baldwin & Osheroff, 2005; Teytelman et al., 2013). We therefore sought to better understand both groups of p53 ChIP-seq peaks by extending our analysis to include chromatin context at p53 binding sites.

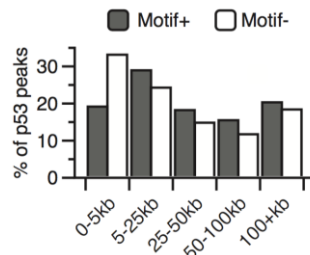


Figure 4: Peaks containing a canonical p53 motif are located farther from transcriptional start sites
Distance of nutlin 3A and etoposide common p53 peaks containing (grey) or not containing (white) a canonical p53 motif from the nearest transcriptional start site (TSS).

Specific chromatin structure and modifications are associated with transcriptional regulatory regions, such as the enrichment of trimethylation at lysine 4 of histone H3 (H3K4me3) at promoters/TSS (Barski et al., 2007). H3K4me3 is strongly enriched at TSS and nearly absent from enhancers and is often used as a proxy of actively transcribed genes. p53 binding occurs

predominantly within cis-regulatory regions, like enhancers and promoters, in primary skin fibroblasts (Heinz et al., 2010a; Younger & Rinn, 2017). Thus, we compared p53 binding locations with regions of enriched enhancer and promoter-associated chromatin modifications.

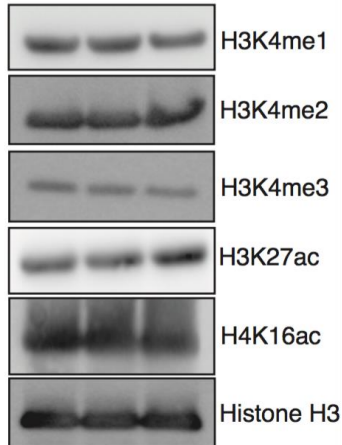


Figure 5: Both nutlin 3A and etoposide treatments have the same overall enrichment of active regulatory region chromatin marks

Western blot analysis of histone modifications used for ChIP-seq analysis from IMR90 fetal lung fibroblasts (cultured at 3% O₂ in DMEM plus 10% fetal bovine serum) 6 h after treatment with either DMSO (vehicle-left lane), nutlin 3A (5 μM final-middle lane), or etoposide (100 μM final-right lane).

Global histone modification levels for transcriptionally-associated H3K4me1/2/3, H3K27ac, and H4K16ac were highly similar across treatment conditions as determined by western blotting (Figure 5). We then performed ChIP-seq for these modifications (and total histone H3) under etoposide-treated conditions to determine how DNA damage-associated chromatin dynamics compare to previous observations after DMSO and nutlin-3A treatment (Heinz et al., 2010a).

Nutlin 3A and etoposide-induced p53 binding events occur within similar local chromatin environments (Figure 6A). We observe an increase in the number of motif + p53 peaks characterized by *de novo* histone acetylation (both H3K27ac and H4K16ac), increased RNApol II occupancy, and slightly more accessible chromatin (ATAC-seq) after treatment with both nutlin

3A and etoposide (Figure 6A) (Buenrostro et al., 2013). The local chromatin environment at p53 binding sites are similar between treatments (Figure 6A), which further supports our previous observations that chromatin structure and modifications are primarily independent of p53 stabilization (Heinz et al., 2010).

We next asked whether there were any distinguishing features of p53 ChIP-seq peaks containing or lacking canonical p53 motifs (El-Deiry et al., 1992). Motif+ peaks displayed higher input-subtracted p53 ChIP enrichment in both nutlin and etoposide conditions compared to p53 motif- peaks (Figure 6B, p53). This is consistent with previous reports that the p53 motif is the

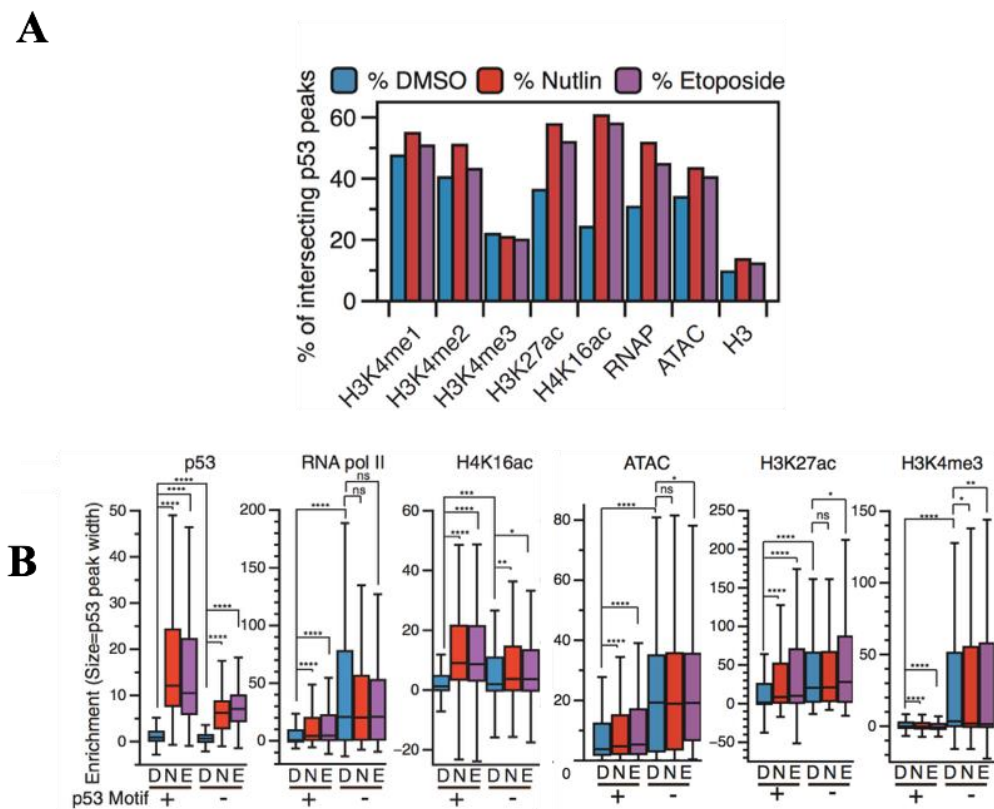


Figure 6: ChIP-seq analysis suggest that both treatments have the same levels of chromatin marks, RNAPolII occupancy, and accessibility

(a)Intersection between nutlin 3A and etoposide p53 common peaks and histone modification, RNA polymerase II, or open chromatin (ATAC-seq) peaks as determined by BedTools intersectBed. (b) Box plot quantification of input-subtracted p53, RNA pol II, H4K16ac, open chromatin/ATAC, H3K27ac, and H3K4me3 across DMSO, nutlin 3A (N), and etoposide (E). Treatment conditions for motif containing (+) and motif lacking (-) p53 peaks (* $p < 0.05$, ** $p < 0.01$, *** $p < 0.001$, **** $p < 0.0001$, Wilcoxon sign-rank test).

primary determinant for binding affinity (El-Deiry et al., 1992). Motif- peaks show significantly higher enrichment of RNA polymerase II, H3K4me3, H3K27ac, and ATAC-seq tags than motif+ peaks (Figure 6B). As motif- peaks are also more closely localized to TSS (Figure 4), these data are consistent with technical ChIP-seq artifacts due to actively transcribed and accessible chromatin regions.

p53 activation-dependent enrichment of RNA pol II, H4K16ac, and H3K27ac relative to DMSO is observed only at motif+ peaks (Figure 6B), consistent with multiple reports that p53 genome binding leads to the recruitment of RNA polymerase II and transcriptional co-activators like histone acetyltransferase. The H4K16ac-catalyzing enzymes hMOF and TIP60 and H3K27ac-catalyzing enzymes p300/CBP directly interact with and can be recruited to specific genomic loci by p53 (Chang et al., 2014; El-Deiry et al., 1992; Heinz et al., 2010b). Taken together, our analysis of local chromatin dynamics reveals strong similarity between p53 binding events downstream of disparate p53 stabilization methods. Further, these data demonstrate that p53 ChIP-seq peaks lacking the canonical p53 RE localize primarily within accessible chromatin near promoters and are less likely to be observed across p53 activating conditions.

Transcriptional and promoter dynamics after nutlin 3A- and etoposide-induced p53 activation

Stabilization of p53 via nutlin 3A is highly specific, with very few predicted off-target effects (Allen et al., 2014). Etoposide, on the other hand, leads to p53 stabilization through failure to repair topoisomerase-induced double-stranded DNA breaks (Maanen et al., 1988). DNA damage itself can activate a number of parallel DNA-damage responsive transcriptional pathways (Chien et al., 2011). Our data suggest that p53 binding induced by both nutlin 3A and etoposide

treatment display similar spatial localization within chromatin, but whether these two treatment conditions produce similar transcriptional responses is not yet known. We therefore investigated whether differential mechanisms of p53 stabilization leads to altered transcriptional activation profiles. PolyA+ RNA from fibroblasts treated with DMSO, 5 μ M nutlin 3A, or 100 μ M etoposide for 6 hours was deep sequenced and transcriptome differences between experimental conditions were assessed. Of note, the DMSO and nutlin 3A dataset was previously characterized using

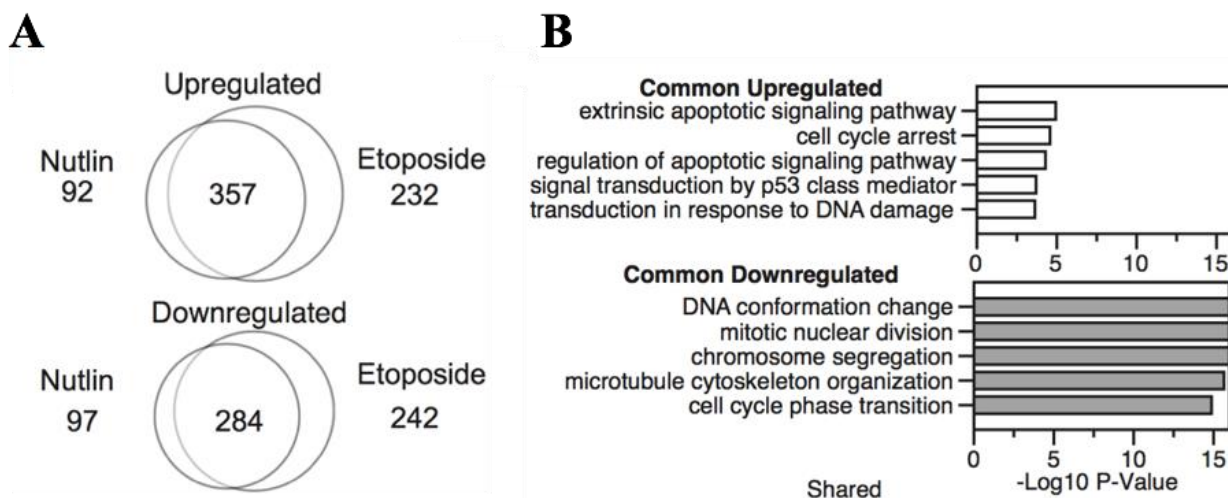


Figure 7: Nutlin 3A and etoposide treatments have common upregulated and downregulated genes

(a) Intersection between twofold upregulated (top) or downregulated (bottom) genes after 6 h of nutlin 3A (5 μ M final) or etoposide (100 μ M final). (b) Gene ontology analysis of common upregulated (top) or downregulated (bottom) between nutlin 3A and etoposide treatment of IMR90 fetal lung fibroblasts.

identical conditions (Heinz et al., 2010b). Using a threshold of 2-fold change between DMSO and the treatment condition, we observe 357 genes upregulated in response to p53 activation downstream of both nutlin and etoposide, whereas 284 genes show reduced expression (Figure 7A). As expected, commonly upregulated genes include canonical p53 targets involved in cell cycle arrest and apoptosis (Figure 7B, top) (Daniel Menendez et al., 2009).

Downregulated genes are strongly enriched in GO categories for cell cycle maintenance and cell division (Figure 7B, bottom), consistent with a direct role for p53 in transcriptional

activation of CDKN1A/p21 and an indirect repression of cell cycle genes through the p21/DREAM complex (Martin Fischer et al., 2014, 2016). These data are consistent with indirect transcriptional

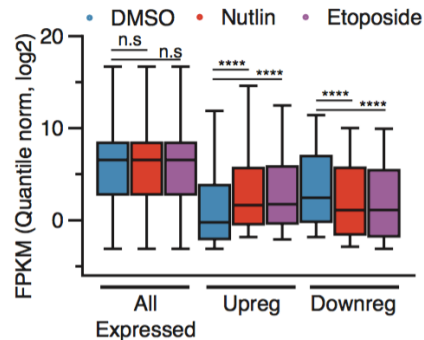


Figure 8: Transcriptional output of upregulated and downregulated genes is similar between both treatments
Box plot analysis of quantile normalized FPKM values for all expressed genes ($\text{FPKM} > 0.1$), twofold upregulated genes, and twofold downregulated genes across DMSO, nutlin 3A, and etoposide treatment conditions (n.s $p > 0.05$, **** $p < 0.0001$).

repression by p53 through p21-mediated mechanisms, as p53 binds more closely to the promoters of activated targets compared to repressed targets (Figure 4). Ultimately, we cannot rule out additional indirect or direct p53-dependent repression mechanisms such as an promoter/enhancer interference model (M. Li et al., 2012), although the large number of p53 binding sites at enhancers make testing these alternative models critically important.

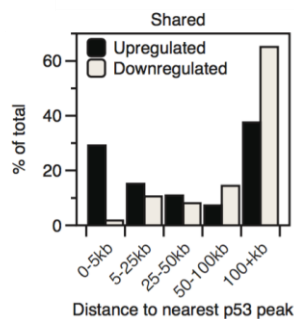


Figure 9: p53 occupancy is increased near TSS of upregulated genes while p53 enrichment is distal to TSS for downregulated genes
Distance of upregulated (black) or downregulated (gray) genes to the nearest p53 binding site.

Overall, treatment of IMR90 fetal lung fibroblasts with either nutlin 3A or etoposide yield almost identical transcript expression distributions (Figure 8). Nearly 30% of all common upregulated genes have a p53 binding site within 5kB of its TSS (Figure 9), supporting previous observations that proximal p53 binding is required for gene activation (Allen et al., 2014; Andrysiak et al., 2017). Of note, over 70% of all commonly upregulated genes are over 5kb from the nearest p53 peak suggesting significant contributions from distal regulatory regions like enhancers. Genes that are commonly downregulated have a skewed distribution, with the modal group of genes displaying p53 binding over 100kb from the nearest gene (Figure 9). These results are consistent with the hypothesis that p53 acts solely as a direct transcriptional activator and that downregulated genes are controlled by p53-dependent indirect transcriptional pathways (fischer steiner).

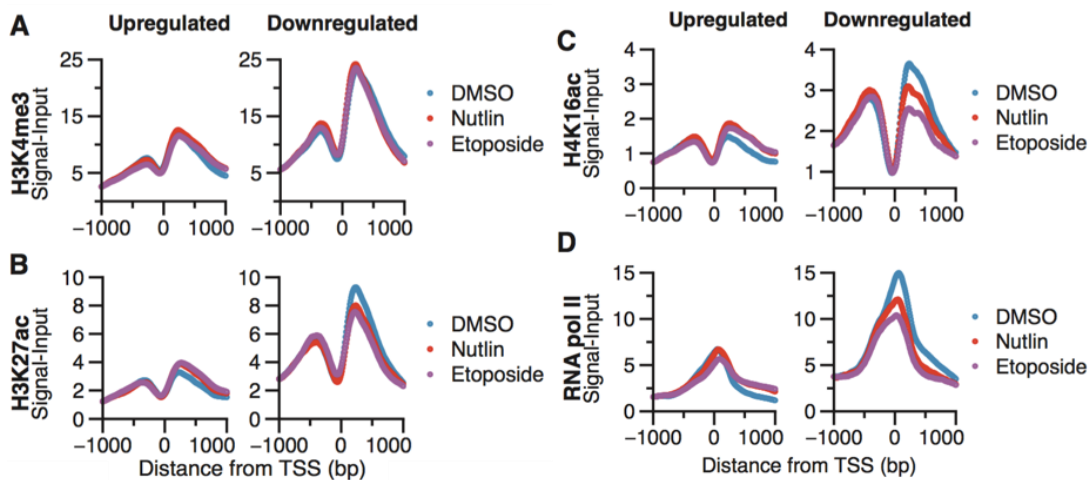


Figure 10: Chromatin marks present at TSS are consistent across treatment conditions

Metaplot analysis at the TSS (± 1000 bp) of twofold upregulated (left) or downregulated (right) genes in response to DMSO, nutlin 3A, or etoposide treatment for (a) H3K4me3, (b) H3K27ac, (c) H4K16ac, and (d) RNA polymerase II.

Measurement of histone post-translational modifications at transcriptional start sites (TSS) and other regulatory regions has been used extensively to infer transcriptional activity and dynamics (Barski et al., 2007; The FANTOM Consortium et al., 2014). Therefore, we assessed

changes in chromatin modification status at TSS of p53-responsive genes to discern differences in p53 activating conditions. These analyses also allow the dissection of potential chromatin and transcriptional regulatory mechanisms at p53-activated genes. H3K4me3 and RNA polymerase II, canonical transcriptional start site-associated factors, are enriched at p53 upregulated targets before activation by nutlin 3A or etoposide (Figure 10A and Figure 10D). H4K16ac and H3K27ac

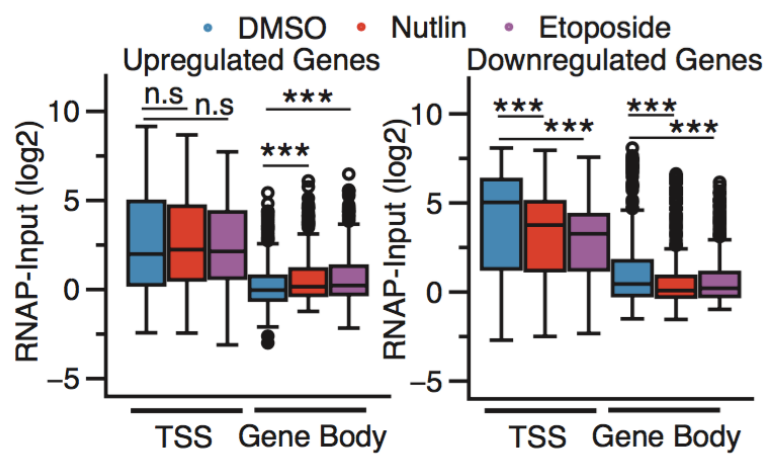


Figure 11: p53 may influence transcriptional pause release in addition to direct RNA polymerase II recruitment to promoters

Box plot analysis of RNA polymerase II occupancy over the TSS or gene body of upregulated (left) or downregulated (right) genes. TSS was defined as ± 250 bp from the TSS, while gene body was defined as $+251$ bp to the transcriptional termination site (TTS) of the gene. Significance was defined by using the Mann-Whitney U test with *** denoting $p < 0.001$.

levels increase at p53-activated target gene TSS after treatment with either nutlin 3A or etoposide (Figure 10B-C. left). Both of these histone acetylation events are lost at the TSS of genes indirectly downregulated after p53 activation (Figure 10B-C, right) Downregulated genes have significantly higher transcriptionally associated chromatin modifications and RNA polymerase II occupancy compared to p53-activated target genes (Figure 10A-D), consistent with the overall higher level of steady state RNA observed for these genes by RNA-seq analysis (Figure 8).

Pausing analysis (Figure 10D and Figure 11) of p53-activated genes shows increasing RNA pol II occupancy over the gene body of p53 target genes (Figure 11, left gene body), but not at the

TSS (Figure 11, left). This suggests that p53 may influence transcriptional pause release in addition to direct RNA polymerase II recruitment to promoters as has been previously suggested (Gaertner & Zeitlinger, 2014; Liu et al., 2015). Conversely, downregulated genes display loss of RNA pol II occupancy at both the TSS and along the gene body (Figure 11, right) consistent with broad loss of transcriptional activity at these genes in response to p53 activation.

*Etoposide-specific genes are likely p53-independent, DNA damage-induced NF-*k*B transcriptional targets*

The majority of p53 binding events (Figure 3) and induced transcripts (Figure 7B) are shared between etoposide and nutlin 3A treatment and share similar modes of regulation (Figure 6B, Figure 10A-D). We next sought to characterize transcriptional differences between our genotoxic and non-genotoxic p53 activating conditions. Less than 100 genes are downregulated or upregulated specifically upon nutlin 3A relative to DMSO treatment (Figure 7B). These genes fall within three lowly enriched GO categories (Figure 12A), consistent with previous observations of

A

Upregulated in Nutlin Only

Category	Number	Description	Log-P Value
Reactome Gene Sets	R-HSA-111933	Calmodulin induced events	-4.18
GO Biological Processes	GO:0051926	negative regulation of calcium ion transport	-3.33
GO Biological Processes	GO:0046434	organophosphate catabolic process	-2.30

B

Upregulated in Etoposide Only

Category	Number	Description	Log-P Value
KEGG Pathway	hsa04668	TNF signalling pathway	-7.05
GO Biological Processes	GO:0048660	regulation of smooth muscle cell proliferation	-6.86
GO Biological Processes	GO:0008015	blood circulation	-5.95
Reactome Gene Sets	R-HSA-500792	GPCR ligand binding	-5.75
GO Biological Processes	GO:0051707	response to other organism	-5.74
GO Biological Processes	GO:0001817	regulation of cytokine production	-5.57
GO Biological Processes	GO:0060326	cell chemotaxis	-5.32
GO Biological Processes	GO:0045986	negative regulation of smooth muscle contraction	-5.12
GO Biological Processes	GO:0050873	brown fat cell differentiation	-4.42
GO Biological Processes	GO:0030217	T cell differentiation	-4.40

Figure 12: Inflammatory pathway genes differentially regulated between nutlin 3A and etoposide treatments
(a) Gene ontology analysis of twofold upregulated genes in nutlin 3A treatment conditions relative to DMSO vehicle control. **(b)** Gene ontology analysis of twofold upregulated genes in etoposide treatment conditions relative to DMSO vehicle control. The top 10 gene ontology terms are depicted.

the high specificity of nutlin 3A for inhibition of MDM2 and subsequent stabilization of p53. Conversely, etoposide treatment induced 232 transcripts 2-fold relative to DMSO treatment that were not found after treatment with nutlin 3A (Figure 7B). Gene enrichment analysis revealed that these etoposide-specific induced transcripts are related to TNF and inflammatory-dependent signaling (Figure 12B) (Tripathi et al., 2015). DNA damage is a known activator of both p53 and the NF-kB-dependent inflammatory signaling network (chien scuoppo). p53 is implicated in crosstalk with NF-kB in the activation of critical inflammatory genes in immune and epithelial cell types, but not yet in fibroblasts (Iannetti et al., 2014; M. Li et al., 2012; Lowe et al., 2014; Webster & Perkins, 1999).

We therefore investigated whether p53 is directly involved in inflammatory signaling crosstalk in fibroblasts downstream of etoposide treatment. Our nutlin 3A-induced transcriptome does not show a direct p53-dependent activation of inflammatory target genes (Figure 12A). As p53 binding events occur more proximally to p53-dependent genes than p53-independent genes (Figure 9 and (Andrysiak et al., 2017)), we analyzed the distance of etoposide and nutlin 3A-specific genes to p53 binding sites. The median distance between p53 binding events and common p53

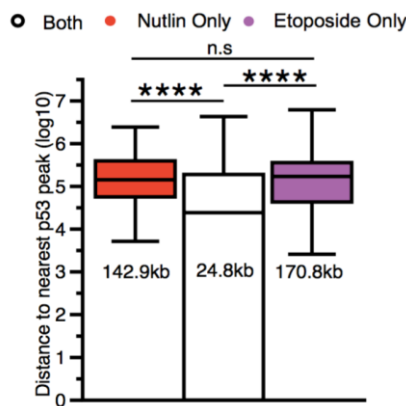


Figure 13: p53 is most proximal to common targets between nutlin 3A and etoposide

Distance of nutlin-specific, etoposide-specific, or commonly upregulated genes to the nearest p53 motif-containing p53 peak (**p< 0.0001, Mann–Whitney U test).

target genes is 24.8 kb (Figure 13). This distance increases to over 170 kb and 140 kb for etoposide or nutlin 3A-specific genes, respectively, and is, significantly further than the median distance for *bona fide* p53 targets (Figure 13).

Multiple reports demonstrate a direct connection between DNA damage-induced inflammatory signaling and the NF- κ B pathway (Chien et al., 2011; Lowe et al., 2014). Etoposide-specific induced genes are enriched with inflammatory/TNF signaling targets which are under the control of the NF- κ B pathway. We therefore tested the possibility that etoposide-specific activated genes are NF- κ B-dependent and p53-independent. The p65 subunit of the NF- κ B complex is repressed by the activity of I κ B and is depressed by phosphorylation by I κ K (Hayden & Ghosh, 2008; Webster & Perkins, 1999). Bay 11-7082 is a small molecule inhibitor of the I κ kinase family and suppresses NF- κ B pathway signaling by maintaining the inactive state of p65 (Pierce et al., 1997). We performed RT-qPCR for three canonical p53 targets and three etoposide-specific inflammatory targets after treatment with I κ K inhibitors and activation of p53 by nutlin 3A or etoposide (Figure 14). The p53 canonical targets CDKN1A, BBC3, and MDM2 are activated in

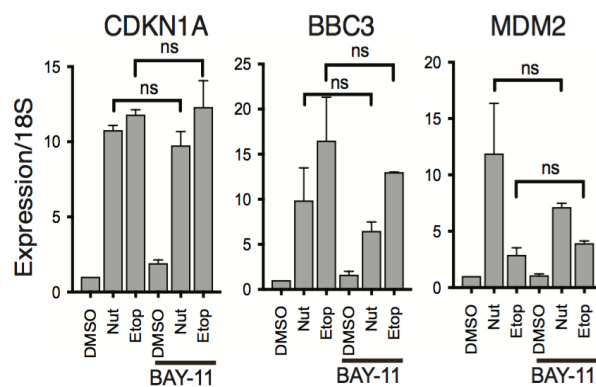


Figure 14: Cells treated with BAY-11 show upregulation of p53 canonical targets with nutlin 3A and etoposide

RT-qPCR analysis of canonical p53 target genes CDKN1A/p21, BBC3/puma, and MDM2 in IMR90 fetal lung fibroblasts in response to treatment with DMSO, nutlin 3A, or etoposide (6 h total). Samples were co-treated with Bay 11-7082 (5 μ M) or with additional DMSO. Statistical comparisons were computed using a ratio paired *t*-test.

response to both nutlin 3A and etoposide treatment and are unaffected by co-treatment with Bay 11-1043 (Figure 14, ratio paired t test).

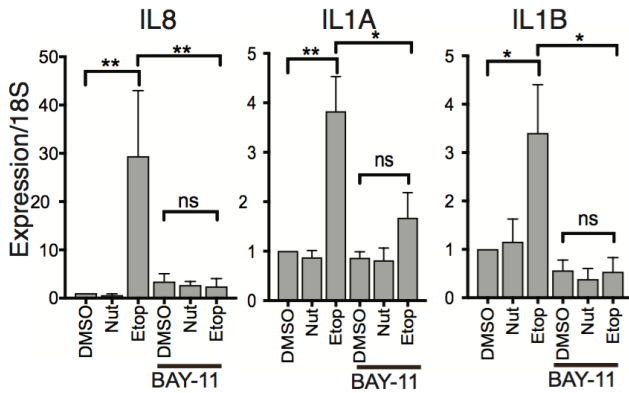


Figure 15: Inflammatory genes respond only to etoposide treatment and are inhibited by BAY-11

RT-qPCR analysis of etoposide-specific genes CXCL8/IL8, IL1A, and IL1B in IMR90 fetal lung fibroblasts in response to treatment with DMSO, nutlin 3A, or etoposide (6 h total). Samples were co-treated with Bay 11-7082 (5 μ M) or with additional DMSO. Statistical comparisons were computed using a ratio paired *t*-test.

In contrast, IL8, IL1A, and IL1B are all activated specifically after etoposide treatment (Figure 15, * $p < 0.01$, ** $p < 0.001$, ratio paired *t* test), similar to our initial RNA-seq observations. Further, co-treatment with Bay 11-7082 abrogates etoposide-induced expression of these genes (Figure 15, * $p < 0.01$, ** $p < 0.001$, ratio paired *t* test) suggesting these genes are downstream of DNA damage-induced NF- κ B signaling.

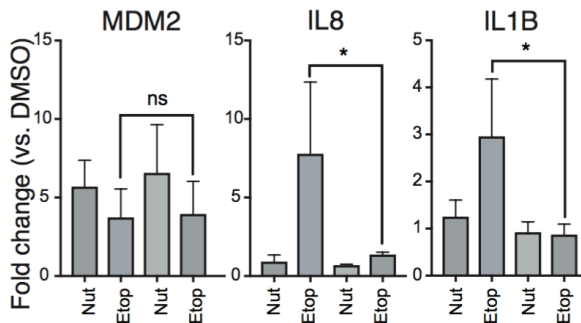


Figure 16: Trends are consistent across different cell types; foreskin fibroblasts

RT-qPCR analysis of p53 target gene MDM2 and etoposide-specific genes IL8 and IL1B in foreskin fibroblasts in response to treatment with DMSO, nutlin 3A, or etoposide (6 h total). Samples were co-treated with Bay 11-7082 (5 μ M) or with additional DMSO. Statistical comparisons were computed using a ratio paired *t*-test.
* $p < 0.05$, ** $p < 0.01$.

These observations are consistent in a second fibroblast line (normal foreskin fibroblasts, < 10 population doublings) grown at 20% O₂ levels. Expression of MDM2 is unaffected by treatment with Bay 11-7082 in either nutlin 3A or etoposide-treated conditions (Figure 16). IL8 and IL1B mRNA expression are not induced by treatment with nutlin 3A (fold change < 2) and are induced by etoposide (Figure 16, fold change >2).

Similar to our results in IMR90 fetal lung fibroblasts, etoposide-mediated IL8 and IL1B mRNA induction is prevented in the presence of Bay 11-7082 (Figure 16), suggesting that NF-kB signaling is required for induction.

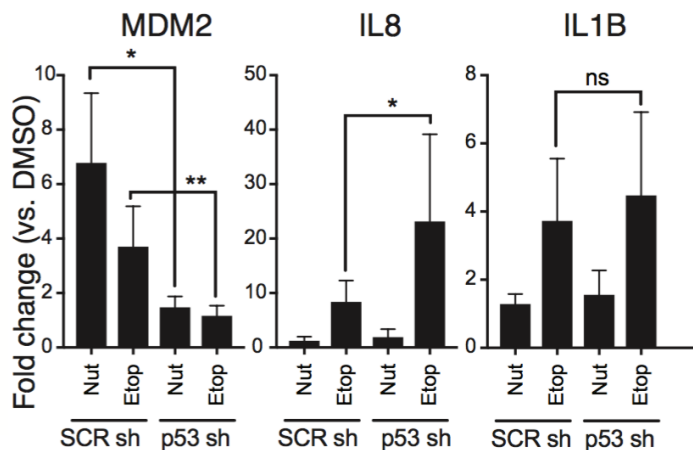


Figure 17: Loss of p53 does not affect upregulation of inflammatory genes

RT-qPCR analysis of p53 target gene MDM2 and etoposide-specific genes IL8 and IL1B in non-targeting shRNA or p53 targeting shRNA-expressing foreskin fibroblasts in response to treatment with DMSO, nutlin 3A, or etoposide (6 h total). Statistical comparisons were computed using a ratio paired *t*-test. **p* < 0.05, ***p* < 0.01.

NF-kB signaling appears to be required for induction of inflammatory targets after etoposide treatment of primary fibroblasts, and the lack of induction of the inflammatory gene targets after nutlin 3A treatment suggests they are p53-independent. To further test this, we examined etoposide-mediated induction of inflammatory gene targets in control (non-targeting) or p53-targeting shRNA-expressing foreskin fibroblasts. As expected, induction of the canonical p53 target MDM2 is severely diminished in p53 knockdown cells relative to control shRNA in both

nutlin 3A ($p < 0.05$) and etoposide treated conditions ($p < 0.01$) (Figure 17). Etoposide-mediated IL1B induction is unaffected by loss of p53 (Figure 17), while IL8 induction is actually higher in the absence of p53 (Figure 17, $p < 0.05$). Overall, these data suggest that p53 is not required for DNA damage/etoposide-mediated induction of inflammatory response genes in fibroblasts, and that NF- κ B signaling is responsible for the observed expression changes.

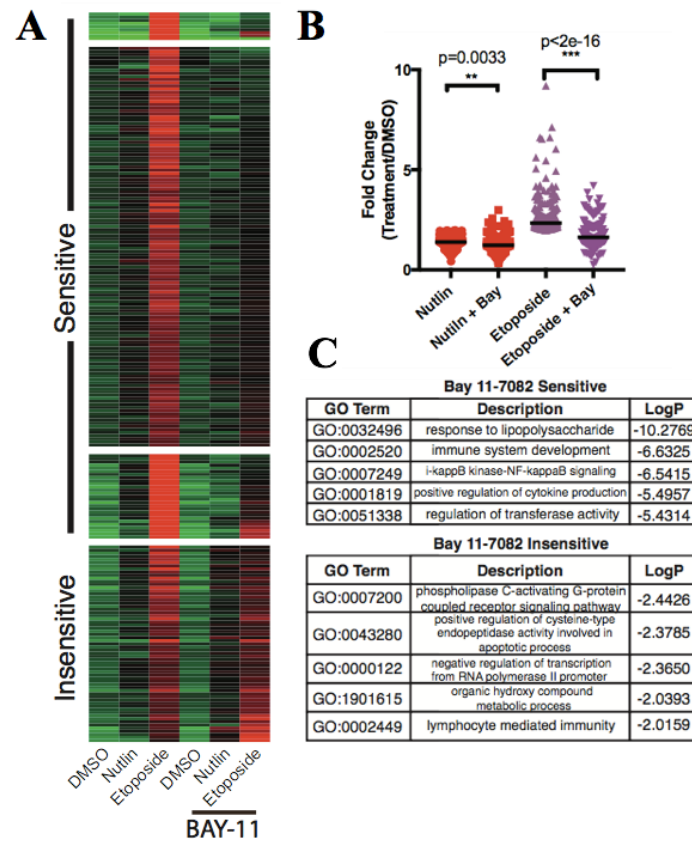


Figure 18: RNA-seq analysis confirms etoposide specific genes are dependent on NF- κ B

(a) Heatmap from RNA-seq of IMR90 fetal lung fibroblasts in response to treatment with DMSO, nutlin 3A, or etoposide (6 h total), with co-treatment with Bay 11-7082 (5 μ M) or additional DMSO. (b) Data were partitioned into four clusters using a k -means clustering approach. Fold change (treatment/DMSO) of etoposide-induced genes from IMR90 fetal lung fibroblasts with statistics representing results of a paired Mann–Whitney U test. (c) Gene ontology analysis of Bay 11-7082 sensitive (top) and Bay 11-7082 insensitive (bottom) etoposide-specific genes in IMR90 fetal lung fibroblasts. The top five categories for each group are depicted.

We extended this analysis by surveying the polyA+ transcriptome after treatment with p53 activators and NF- κ B signaling pathway inhibition with Bay-11-7082. We used k -means clustering

to identify four strong gene clusters of RNA targets with increased abundance after etoposide treatment (Figure 18A). Three of these clusters contained genes that are specifically upregulated by etoposide treatment, but show reduced activation when co-treated with Bay 11-7082 (Figure 18C, Sensitive). Another cluster contained genes whose etoposide-induced expression was insensitive to treatment with Bay 11-7082 (Figure 18C, Insensitive). Broadly, treatment with Bay-11-7082 reduces expression of etoposide-specific targets after nutlin 3A treatment (Figure 18B, nutlin vs. nutlin/bay, $p=0.0033$, Mann Whitney U), suggesting some of these genes are basally regulated by NF-kB signaling. Bay-11-7082 treatment strongly reduces expression of the etoposide-specific gene set relative to no treatment (Figure 18B. $p<2e^{-16}$, Mann Whitney U). Gene Ontology analysis of the Bay-sensitive gene network confirmed these genes are associated with NF-kB pathway and inflammatory signaling (Figure 18C), consistent with our hypothesis that these genes are likely NF-kB targets. Genes found in the Bay 11-7082-insensitive cluster were less enriched in total GO terms, but are related to apoptosis and immune signaling, suggesting that other transcriptional or post-transcriptional mechanisms regulate mRNA abundance downstream of DNA damage. These genes are therefore putative DNA damage-dependent, but likely NF-kB independent, target genes.

Discussion

Using comparative genomic approaches, we have demonstrated a conserved transcriptional and chromatin response to both genotoxic and non-genotoxic p53 stabilization methods in primary fibroblast cell lines. Binding of p53 to chromatin is highly similar across experimental conditions, with the majority of differences attributed to peak calling approaches. This observation is remarkably similar to a recent report of conserved p53 binding across cell types and experimental p53 activation methods using a meta-analysis approach (Verfaillie et al., 2016). One key aspect of this work is the use of a uniform methodology for genome alignment, peak calling, and statistical thresholding across laboratory and experimental conditions. We used a similar approach by first using macs2 to call significant peaks and then creating a combined peak list between experiments (Bentley et al., 2008; Liu et al., 2015; Tripathi et al., 2015). Then, we counted tag enrichment within the combined peak regions for both nutlin 3A and etoposide conditions, which yielded strikingly similar enrichment profiles. Condition-specific peaks (called by macs2) had higher tag counts within the peak region than did the other condition, but the overall profile between nutlin 3A and etoposide-induced p53 binding were well correlated. Taken together, these data provide additional evidence that p53 engagement with the genome is highly consistent within the same cell type when activated by disparate methods. It is important to note that our analysis was only performed after p53 activation with the MDM2 inhibitor nutlin 3A or topoisomerase II inhibitor, etoposide. Multiple other direct genotoxic activators, such as additional topoisomerase inhibitors, g-irradiation, DNA chemical crosslinking, and UVB-induced pyrimidine dimerization, have been tested for their ability to activate p53-dependent transcriptional signaling, but the genome-wide profile of p53 binding has not yet been established for all of these compounds or DNA-damage mechanisms. Further, the binding and activity of p53 downstream of additional p53-activating

conditions, like ribosomal stress, reactive oxygen species, nutrient deprivation, or activated oncogenes, are less well understood, opening up critical avenues for in-depth investigation.

DNA damage signaling leads to a number of post-translational modifications (PTM) to p53 (Barlev et al., 2001; M. Li et al., 2012), especially within the N-terminus (Kruse & Gu, 2008). These modifications include multiple phosphorylation events in the first transactivation domain of p53, which may help to block the interaction between p53 and MDM2, leading to p53 stabilization. The N-terminus of p53 contains two independent trans-activation domains (TADs), both of which can be extensively modified (Candau et al., 1997; Kruse & Gu, 2008; Raj & Attardi, 2017). Our data suggest that p53 DNA binding and p53-dependent gene activation are consistent between p53 stabilization methods even though our data suggest that at least serine 15 is differentially phosphorylated between nutlin 3A and etoposide-treated conditions. Post-translational modifications to p53 have been directly implicated in differential gene activation and cell fate (Sykes et al., 2006; Tang et al., 2006; The FANTOM Consortium et al., 2014), but their temporal and spatial distribution in the genome is virtually unknown. ChIP-seq of mouse p53 serine 18 phosphorylation closely mirrored results seen with pan-p53 antibodies (Candau et al., 1997). Mutation of p53 lysine 120 to arginine (K120R) alters p53 genome binding consistent with the predicted role of K120 acetylation in DNA contact (Monteith et al., 2016; Sykes et al., 2006; Tang et al., 2006), but whether the genome-wide shift in binding is due to loss of acetylation or altered DNA contacts with arginine has yet to be determined. Ultimately, whether differential p53 stabilization methods yield different patterns of p53 modifications, and whether these directly alter p53 DNA binding, are still open questions. Our data indicate that serine 15 phosphorylation does not drive p53 binding or transcriptional differences in fetal lung fibroblasts, although we note the

single six hour-post treatment time point used in our experiments. Additional time points should be examined to determine whether the method of stabilization alters direct p53 activities.

Recent work suggests that individual p53-dependent transcriptional pathways are dispensable for tumor suppression (Andrysik et al., 2017), consistent with previous reports that canonical p53-dependent pathways like cell cycle arrest and apoptosis are also not required (T. Li et al., 2012). Our comparative analysis revealed that DNA damage paradigms, in this case with chemotherapeutic small molecule etoposide, activate a parallel transcriptional response most likely controlled by the NF-kB transcription factor and not directly by p53. Interestingly, p53 directly activates IL6 and CXCL8/IL8 in primary macrophages (Chien et al., 2011) and IL1A and IL1B in primary mammary epithelial cells (Uzunbas et al., 2018). p53 specifically binds to epithelial-specific enhancers upstream of both IL1A and IL1B in mammary epithelial cells (McDade et al., 2014; Uzunbas et al., 2018) but does not bind to these regions in lung fibroblasts (this work) or dermal fibroblasts (Uzunbas et al., 2018). Here, we find no evidence that p53 directly activates these immune regulatory genes in primary fetal lung fibroblasts, including no change in transcript levels, RNA polymerase occupancy, or p53 binding. Multiple biological and technical differences between experimental conditions may explain the discrepancies between these datasets. Our primary fibroblasts were cultured under 3% O₂ conditions which yields lower levels of reactive oxygen species (ROS) and reduced telomere attrition compared to standard 20% O₂ conditions used in other experimental systems (Parrinello et al., 2003). ROS are well-known activators of DNA damage (Cadet & Wagner, 2013) and are involved in significant crosstalk with inflammatory and NF-kB signaling (Blaser et al., 2016; Webster & Perkins, 1999). Higher relative levels of ROS may prime p53 towards activation of inflammatory genes in collaboration with NF-kB (Lowe

et al., 2014), although we performed a number of validation experiments at 20% O₂ and failed to observe p53-dependent inflammatory gene activation. Alternatively, activation of p53 in cells with high ROS levels could co-activate NF-κB signaling and lead to expression of an inflammatory gene cascade. The underlying mechanisms of cross-talk between p53 and NF-κB, along with other stress-dependent transcriptional networks, represent an important and active area of investigation for both the immunology and cancer biology fields.

A second putative mechanism driving the observed differences in inflammatory gene expression relates to differential p53 activity across cell types. Thus far, inflammatory target gene expression downstream of p53 activation has been studied across varied types of primary and cancer derived cell lines. Every cell type is characterized by a unique collection of active and accessible regulatory elements (The FANTOM Consortium et al., 2014), and p53 binds primarily to active promoters and enhancers (Allen et al., 2014)(Heinz et al., 2010b; Uzunbas et al., 2018). The recent comprehensive meta-analyses of the majority of published human p53 ChIP-seq datasets (Verfaillie et al., 2016) suggests high similarity of p53 binding across cell types. One caveat is that the majority of the analyzed data were from either mesenchymal fibroblast cell lines or transformed cell lines. A conserved core group of p53 binding sites across three cancer cell lines was also recently observed (Rinaldi et al., 2016), but of note, each cell type had a unique spectrum of binding events. Two recent works suggest that cell type-dependent chromatin accessibility leads to varied p53 binding, which could explain differential p53-induced inflammatory target genes (Hafner, Lahav, et al., 2017; Uzunbas et al., 2018). An analysis of 12 transformed human cell lines demonstrates specific p53 binding to cell type-specific accessible chromatin (Hafner, Lahav, et al., 2017), including specific p53 binding to the IL1A locus in the metastatic melanoma LOXIMVI

cell line. In primary mammary epithelial cells, p53 binds to two separate active enhancers between IL1A and IL1B and leads to a p53-dependent activation of those genes (Uzunbas et al., 2018). The chromatin modification and accessibility-based markers suggest these enhancers are inactive in skin or lung fibroblast and that p53 is unable to bind to these regions (Uzunbas et al., 2018)(Heinz et al., 2010b). Our data demonstrate that these genes are not activated by p53 in primary human lung and dermal fibroblasts in response to nutilin 3A or etoposide treatment (Heinz et al., 2010b; Uzunbas et al., 2018). Cell type-specific chromatin accessibility and enhancer activity provides a powerful and intriguing mechanism for differential regulation of p53 target genes.

In summary, our work provides a comprehensive comparison of p53 binding, chromatin state, and transcriptional activity in primary lung fibroblasts exposed to either genotoxic or non-genotoxic activators of p53. We propose that p53 activity and chromatin/RNA polymerase II dynamics are highly correlated within the same cell type regardless of the method of p53 stabilization, and that crosstalk between other DNA damage-activated transcription factors contribute to observed transcriptional differences and cellular phenotypes.

CHAPTER 3: Locally acting transcription factors regulate p53-dependent *cis*-regulatory element activity

This chapter was published as:

Catizone AN et al., Nucleic Acids Research (2020)

Introduction

The master tumor suppressor p53 is a transcription factor with key roles in preserving genome fidelity and cellular homeostasis. In support of these activities, p53 regulates a core transcriptional program involved in cellular processes like cell cycle arrest, apoptosis, DNA repair, and senescence (Allen et al., 2014; Andrysiak et al., 2017; M Fischer, 2017). Loss of p53 activity is strongly linked to increased cancer risk and decreased life expectancy, and misregulation of p53 is associated with numerous other human disorders. Recent analyses suggest that p53 is mutated in greater than 30% of cancer cases and the majority of p53 variants are unable to bind DNA and enact a tumor suppressive gene expression program (Donehower et al., 2019). The mechanisms by which tumorigenesis progresses in the presence of wild type p53 activity have not been well characterized. Recent evidence suggests that sequence variation within *cis*-regulatory elements (CREs) can influence p53 binding, transcriptional activity, and tumor suppressor function (Menendez et al., 2019; Shao et al., 2019; Zeron-Medina et al., 2013). The critical nature of the core p53 response element (p53RE) on p53 binding and CRE activity is well understood (El-Deiry et al., 1992; Verfaillie et al., 2016; Younger & Rinn, 2017), but the influence of local sequence variation and the role of additional transcription factor motifs within a CRE on p53 activity remains an open and vital question.

Cis-regulatory elements, such as promoters and enhancers, govern gene expression through temporal, spatial, and quantitative control of transcription (Shlyueva et al., 2014; Spitz & Furlong, 2012). While multiple models for CRE function have been proposed, the majority involve cooperative binding of transcription factors and cofactors acting locally to fine-tune gene expression (Schoenfelder & Fraser, 2019; Shlyueva et al., 2014; Spitz & Furlong, 2012). The presence and availability of transcription factors, repressors, and other cofactors vary across cell states such as development, stress, disease, and cell type (Herz et al., 2014; Long et al., 2016; Rickels & Shilatifard, 2018; Smith & Shilatifard, 2014). This variability provides a mechanism for differential CRE activity and downstream gene expression. Loss of transcription factor binding, through variation in DNA sequence or through changes in *trans*-factor availability, can strongly influence CRE activity and gene expression (Kulkarni & Arnosti, 2003; Shlyueva et al., 2014; Spitz & Furlong, 2012), with direct implications in numerous developmental and disease states (Long et al., 2016; Rickels & Shilatifard, 2018).

While general transcription factors, like the TFIID complex (Chen et al., 1993; Seto et al., 1992), are involved in p53-dependent trans-activation at promoters, the requirement for other sequence-specific trans-factors at distally-acting CREs is unknown. A novel model was recently proposed whereby binding of a single transcription factor, in this case p53, was necessary and sufficient for CRE activity (Verfaillie et al., 2016). This model was supported by another study suggesting that a canonical p53 response element (p53RE) is the only sequence-based determinant of p53-dependent CRE activity (Younger & Rinn, 2017). However, multiple p53-dependent CREs have been reported to require other locally-acting transcription factors, in line with established CRE mechanisms like the enhanceosome and billboard models (Kulkarni & Arnosti, 2003; Thanos

& Maniatis, 1995). For example, CRISPR/Cas9-based screening identified a CEBPbeta-binding site within a CRE regulating *CDKN1A*/p21 required for p53-dependent senescence (Korkmaz et al., 2016). Transcription factors such as those in the AP-1 family and SP1 have also been implicated in the activation of p53-dependent gene targets (Koutsodontis et al., 2001; Li et al., 2014; Nikulenkov et al., 2012).

In order to directly address whether additional cofactors are required for p53-dependent transcriptional activity, we examined the effect of local sequence variation on putative p53 CREs using a massively parallel reporter assay (MPRA). Our results suggest that sequences flanking p53REs and transcription factors other than p53 are required for p53-dependent transcriptional activation. Consistent with previous reports, the p53RE is a strong determinant of p53-inducible activity. Loss of p53 occupancy through sequence manipulation or depletion of the protein strongly reduces CRE activity. We also identified sequences outside of the p53RE that positively or negatively regulate transcription. This includes a conserved SP1/KLF family binding site required for optimal transcription of the p53-dependent gene *CCNG1* (cyclin G1). We also identified two distinct CREs with different local transcription factor requirements that are both necessary for p53-dependent transcriptional activation of *GDF15*, a gene recently identified as a key mediator of inflammation and metabolic function (Luan et al., 2019; Patel et al., 2019, p. 15). Thus, p53-bound CREs do not depend on just one family of transcription factors for activity and can utilize multiple and different factors to regulate transcription. Thus, these data indicate p53's flexibility to collaborate with different combinations of locally available transcription factors to regulate CRE activity and downstream gene activation involved in key organism-level traits like tumor suppression.

Results

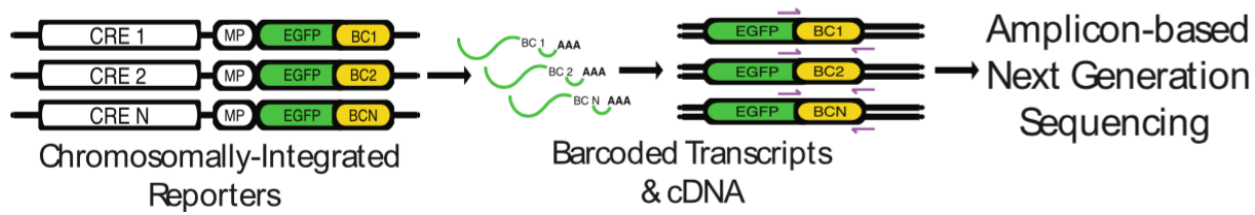


Figure 19: A barcoded massively parallel reporter assay was used to assess the affect sequence variation had on enhancer activity

Schematic and workflow for a massively parallel reporter assay (MPRA) to study the effect of flanking sequence context on p53 transcriptional activity.

Design and execution of a massively parallel reporter assay for determinants of p53-dependent CRE activity

We designed a barcoded and chromosomally integrated reporter system to assess the function of DNA sequences flanking the p53RE in p53-dependent CREs (Figure 19). The lentivirus-based system expresses eGFP under the control of a minimal promoter and a putative p53-dependent CRE sequence (Inoue et al., 2017). Each putative CRE was included in the library with five unique, 12 nucleotide barcodes encoded in the 3'UTR of eGFP to allow a molecular readout of transcriptional activity (Figure 19). We selected 296 putative p53 binding locations based on the presence of a canonical p53 family binding motif (p53RE), distance from the nearest transcriptional start site (< 100kb), and localization within a DNase hypersensitive site (DHS). The 20bp p53 family motif was centered in a 100bp fragment with 40bp of flanking genomic context on each side. We also included 196 p53-independent and constitutively active CREs as determined by FANTOM Consortium CAGE data as positive controls of CRE activity (The FANTOM Consortium et al., 2014). These sequences were cloned into the lentiviral plasmid

backbone pLS-MP as described in the Methods and similar to previously described MPRA designs (Inoue et al., 2017).

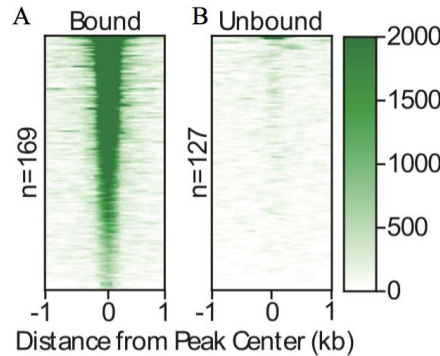


Figure 20: p53 motif containing enhancers were grouped into bound and unbound by in vivo occupancy
Heatmaps of p53 ChIP-seq enrichment from Nutlin-3A-treated HCT116 colon carcinoma cell lines for (A) p53-bound or (B) p53-unbound regions found in the MPRA pool.

We then examined the activity of our putative CREs using the model human colon carcinoma cell line HCT116 which is well-suited for studying p53-dependent transcriptional activity. Our 296 potential p53-dependent CREs clustered into two groups based on p53 occupancy using ChIP-seq data from HCT116 cells (Andrysiak et al., 2017). 169 out of 296 regions were scored as p53 binding sites (peaks) by MACS2 (Bound, Figure 20, *Model-based Analysis of ChIP-seq*, (Zhang et al., 2008)), whereas 127 regions lacked measurable p53 binding (Unbound, Figure 20). The average position weight matrix of the p53RE for each of the clusters is highly similar

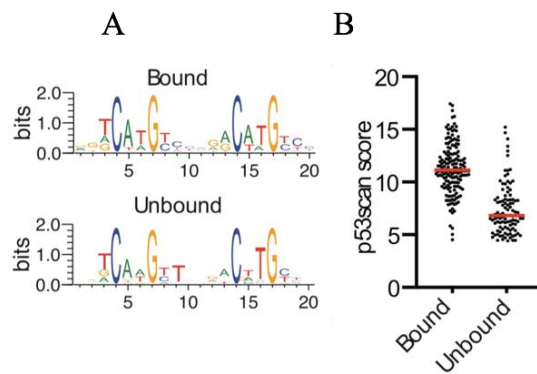


Figure 21: p53 bound regions have high scoring response elements matching canonical sequences
(A) DNA sequence weight motifs for p53-bound (top) or unbound (bottom) regions from the MPRA pool. (B) Jitter plot of scores from p53scan depicting the adherence to a canonical p53 family motif sequence for the p53-bound and p53-unbound regions.

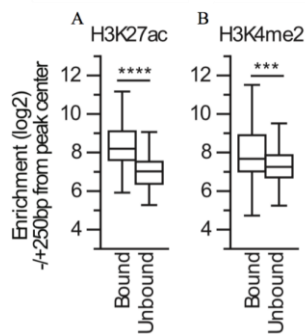


Figure 22: p53-bound regions are highly enriched for active chromatin marks compared to unbound regions
Enrichment of (A) H3K27ac or (B) H3K4me2 in Nutlin-3A-treated HCT116 cells at p53-bound or unbound regions. Statistics represent an unpaired, two-tailed *t*-test (**P < 0.001, ****P < 0.0001).

(Figure 21A), however, the consensus motif in p53-bound regions more closely resembles the optimal p53 consensus motif than do p53-unbound CREs (Figure 21B).

CREs bound by p53 show higher enrichment of canonical enhancer-associated histone modifications H3K27ac (Figure 22A), H3K4me1 (Figure 23A), and H3K4me2 (Figure 22B) than do those regions lacking p53 occupancy in HCT116 cells.

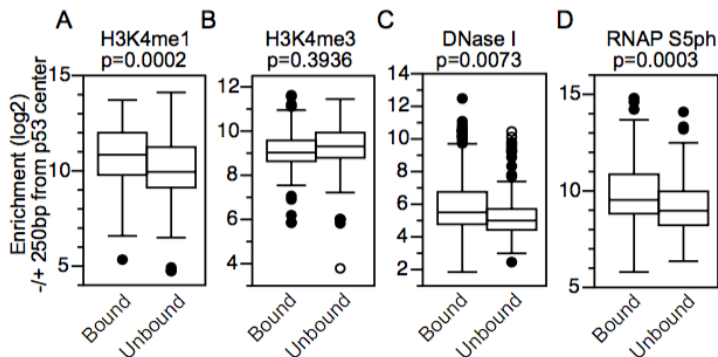


Figure 23: P53 bound enhancers have signs of active regulatory regions
(A) Enrichment of H3K4me1 in HCT116 cells at p53-bound or unbound CREs. Statistics represent an unpaired, two-tailed T test. (B) Enrichment of H3K4me3 in HCT116 cells at p53-bound or unbound CREs. Statistics represent an unpaired, two-tailed T-test (C) DNase I hypersensitivity enrichment in HCT116 cells at p53-bound or unbound CREs. Statistics represent an unpaired, two-tailed T-test. (D) RNA polymerase II (serine 5 phosphorylation) occupancy in HCT116 cells at p53-bound or unbound CREs. Statistics represent an unpaired, two-tailed T-test.

The promoter-associated histone modification H3K4me3 is similarly enriched across both p53 bound and unbound CREs (Figure 23B). p53-bound CREs are also found in regions with higher

DNAse-accessibility (Figure 23C) and are more enriched for the transcription initiation-associated RNA polymerase II C-terminal domain modification serine 5 phosphorylation (Figure 23D).

Consistent with the increased occupancy of transcriptionally associated features, enhancer RNA (eRNA) transcription is more prevalent at p53-bound CREs relative to those lacking p53 binding (Figure 24) (Allen et al., 2014; Andrysiak et al., 2017). These data suggest that CREs that are destined for binding by p53 have higher DNA accessibility, are more enriched for chromatin modifications associated with transcription, and produce more eRNA under basal/DMSO-treated conditions than those not bound by p53.

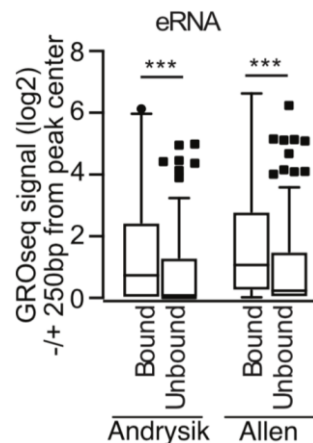


Figure 24: p53 bound regions produce more eRNA compared to unbound regions

eRNA enrichment measured by GRO-seq in p53-bound versus p53-unbound regions (± 250 bp from p53 response element/p53RE). Statistics represent an unpaired Mann–Whitney *U* test (***($P < 0.001$)).

We then performed triplicate biological measurements of p53-dependent CRE activity in HCT116 using our MPRA approach. MPRA-transduced cells were treated for 6 hours with either DMSO or the MDM2 inhibitor Nutlin-3A and expressed RNA barcodes were deep sequenced as described in Methods. Nutlin-3A leads to stabilization and activation of p53 at a similar level to

what is seen with DNA damaging agents like etoposide (Figure 30A) (Vassilev et al., 2004). Importantly, enhancer activity measurements across biological replicates, treatment conditions, and cell lines were highly correlated (Figure 25).

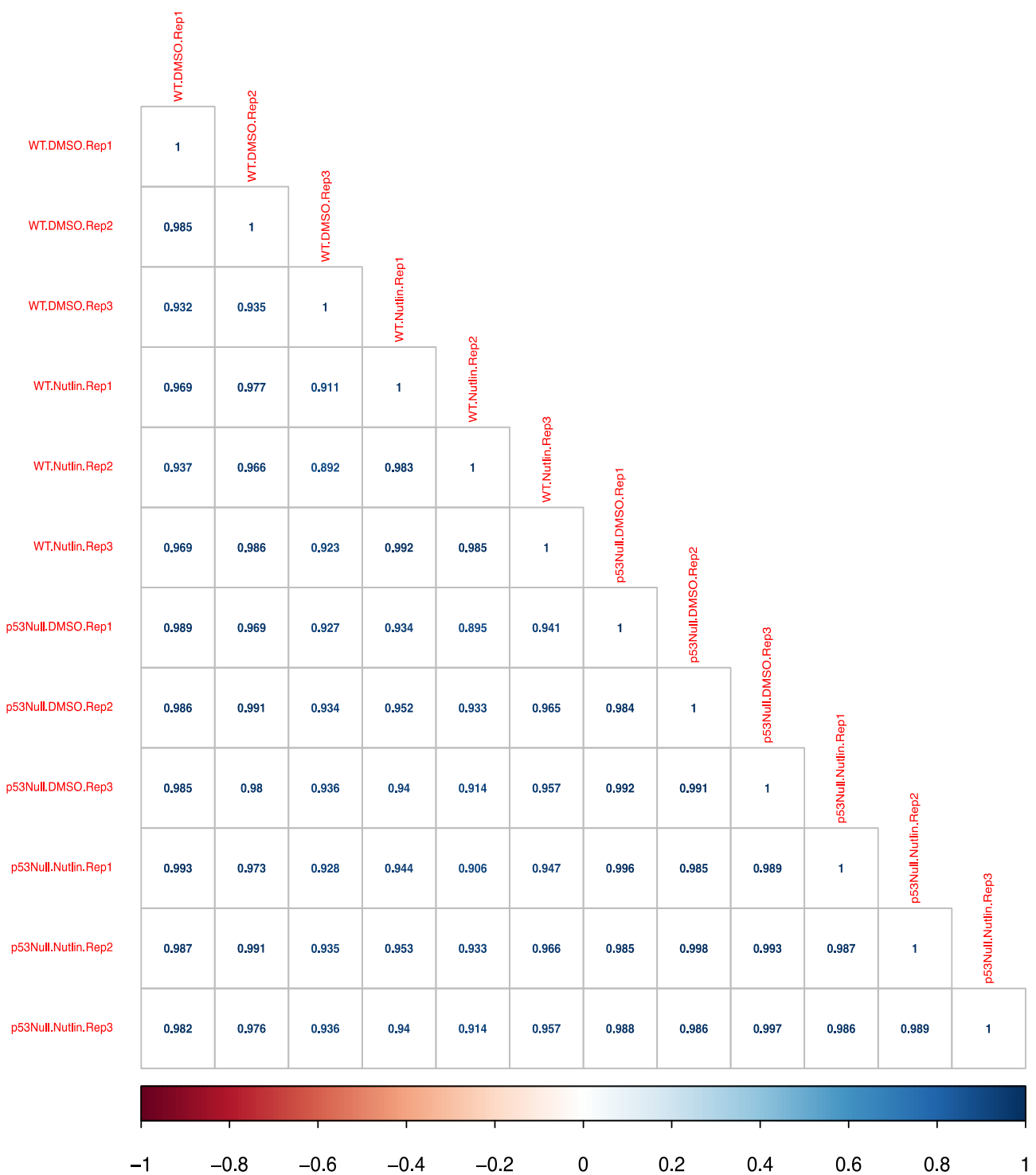


Figure 25: Biological replicates for MPRA assay are highly correlated

Pearson correlation values (R^2) for enhancer barcode counts from three biological replicates across HCT116 p53^{+/+} and HCT116 p53^{-/-} cells treated with either DMSO or 5μM of Nutlin-3A for 6 hours. Rep1 = biological replicate #1, Rep2 = biological replicate #2, Rep3 = biological replicate #3

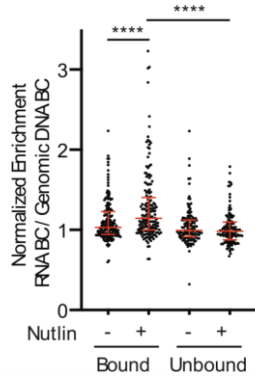


Figure 26: p53 bound regions are more transcriptionally active in the MPRA compared to unbound regions
 Normalized transcriptional activity of p53-bound or unbound regions from the MPRA assay after 6 h of either DMSO or 5 uM Nutlin-3A treatment. Data are depicted as enrichment of the 3'UTR-encoded barcode linked to each putative regulatory region normalized to the enrichment of that same sequence integrated into the genome and represent the averages from three biological replicates of each condition (**** $P < 0.0001$ by one-way ANOVA).

As expected from our analysis of p53 occupancy, p53-bound CREs showed a bulk Nutlin-3A-dependent increase in activity compared to treatment with DMSO (Figure 26, **** $p < 0.0001$, one way ANOVA). Unbound CRE activity was not affected by Nutlin-3A treatment relative to DMSO and was substantially lower than p53-bound CREs (Figure 26, **** $p < 0.0001$, one way

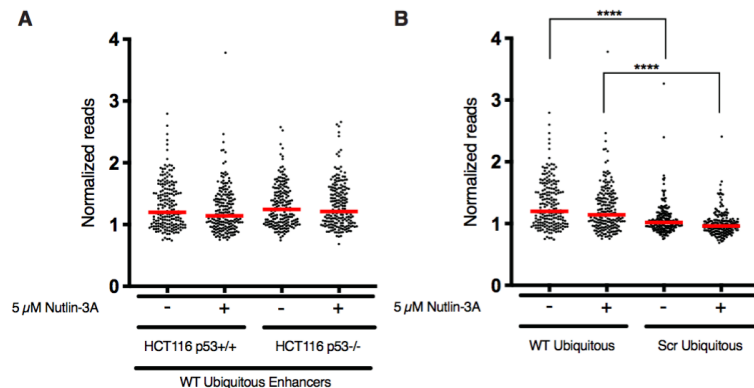


Figure 27: Ubiquitous enhancer activity is affected but randomization but not Nutlin 3A treatment or the loss of p53 protein expression

(A) Jitter plot of normalized CRE activity (RNA barcode/genomic DNA barcode) for 196 ubiquitously expressed CREs from the FANTOM Consortium in HCT116 p53+/+ and p53-/- cells treated with either DMSO or 5μM Nutlin-3A for 6 hours. Red line represents the median expression values. All conditions were statistically similar using a one-way ANOVA. (B) Jitter plot of normalized CRE activity (RNA barcode/genomic DNA barcode) for 196 ubiquitously expressed CREs or 196 randomized sequences from the FANTOM Consortium in HCT116 p53+/+ treated with either DMSO or 5μM Nutlin-3A for 6 hours (**** $p < 0.0001$ by one-way ANOVA). Red line represents the median expression values.

ANOVA). Activity of the ubiquitous CRE controls were unaffected by the induction of p53 by Nutlin-3A (Figure 27A).

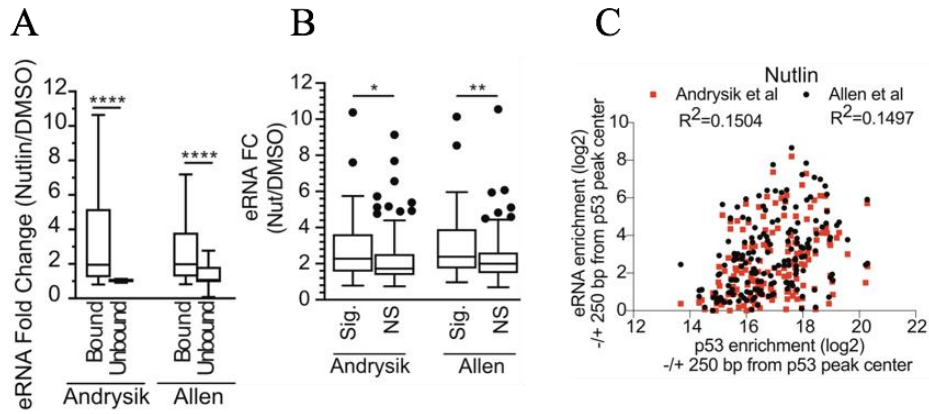


Figure 28: p53 bound enhancers show increased eRNA activity between after Nutlin 3A treatment

(A) eRNA fold-change (Nutlin-3A versus DMSO conditions) as measured by GRO-seq at p53-bound versus p53-unbound regions. Statistics represent an unpaired Mann–Whitney *U* test (**** $P < 0.0001$). (B) eRNA enrichment fold-change (Nutlin-3A versus DMSO conditions) as measured by GRO-seq Nutlin/DMSO at p53-bound regions that significantly increased (Sig.) in MPRA transcriptional activity upon Nutlin treatment versus p53-bound regions that did not significantly increase (NS) in MPRA transcriptional activity (* $P < 0.05$, ** $P < 0.01$ by unpaired Mann–Whitney *U* test. (C) Spearman correlation analysis of eRNA enrichment (\log_2) at p53-bound CREs relative to enrichment of p53 (\log_2) in a region ± 250 bp from the p53RE between eRNA enrichment and p53-enrichment at MPRA regions.

eRNA transcription was more highly upregulated at p53-bound CREs upon Nutlin-3A treatment than at unbound CREs (Figure 28A), consistent with the observed Nutlin-3A-dependent increase in p53-bound CRE activity (Figure 26). CREs with significantly increased MPRA activity upon Nutlin-3A-treatment had more robust eRNA induction (DMSO vs. Nutlin-3A) than CREs with lower activity (Figure 28B). However, p53 enrichment is only weakly correlated with total eRNA abundance at a given CRE suggesting that p53 occupancy alone is not an indicator of eRNA transcription (Figure 28C for Nutlin-3A-treated conditions, Figure 29 for DMSO-treated conditions), as has been previously reported (Allen et al., 2014; Azofeifa et al., 2018; Sammons et al., 2015). These data demonstrate that known markers of transcriptional activity, including histone modifications and eRNA transcription (Azofeifa et al., 2018), distinguish p53-bound versus p53-unbound CREs, but that additional features contribute to the activity of p53-bound CREs.

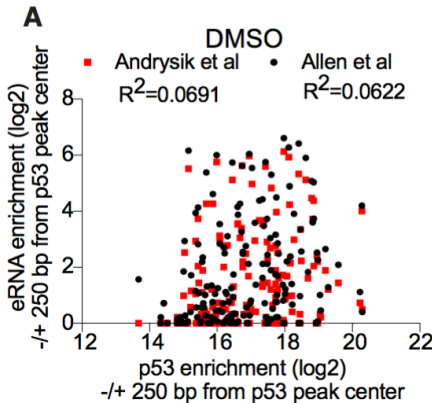


Figure 29: eRNA enrichment is only weakly correlated with p53 occupancy at bound enhancers

Spearman correlation analysis of eRNA enrichment (log2) at p53-bound CREs under DMSO-treated conditions relative to enrichment of p53 (log2) in a region +/- 250bp from the p53RE between eRNA enrichment and p53-enrichment at MPRA regions.

p53-bound CREs require direct-binding of p53 for Nutlin-3A-induced activity

In order to determine if Nutlin-3A-induced activity of p53-bound CREs is p53-dependent, we assessed transcriptional activity in matched HCT116 TP53^{+/+} and TP53^{-/-} cell lines (Figure 30A). Nutlin-3A-induced activity of p53-bound CREs was diminished in HCT116 TP53^{-/-} cells suggesting these enhancers are dependent on wild-type p53 (Figure 30B).

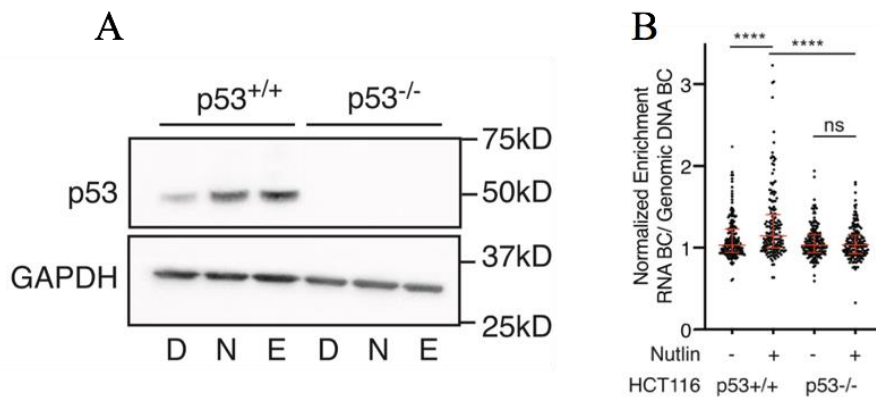


Figure 30: p53 bound enhancers are significantly less active when expressed in HCT116 p53^{-/-} cells

(A) Immunoblotting for p53 (top) or GAPDH (bottom) expression in HCT116 p53^{+/+} or p53^{-/-} colon carcinoma cells after 6 hours of treatment with DMSO (D), 5 uM Nutlin-3A (N) or 100 uM etoposide (E). (B) Normalized transcriptional activity of the wild-type p53-bound regions in either HCT116 p53^{+/+} or p53^{-/-} cells after a 6-h treatment of either DMSO or 5 uM Nutlin-3A. Data are depicted as enrichment of the 3'UTR-encoded barcode linked to each putative regulatory region normalized to the enrichment of that same sequence integrated into the genome and represent the averages from three biological replicates of each condition (****P < 0.0001 using an ordinary one-way ANOVA).

As expected, ubiquitously expressed CRE controls were unaffected by the loss of p53 expression (Figure 27A). To test whether CRE activity is direct or indirectly dependent on p53, we compared wild-type CRE sequences to those with either the 20bp p53RE (Mid) or the entire CRE sequence (Scr) randomized (Figure 31A). As a control for randomization, we fully scrambled the 196 ubiquitous CRE control sequences while preserving GC content, leading to a loss of activity ($p<0.0001$, one ANOVA, Figure 27B).

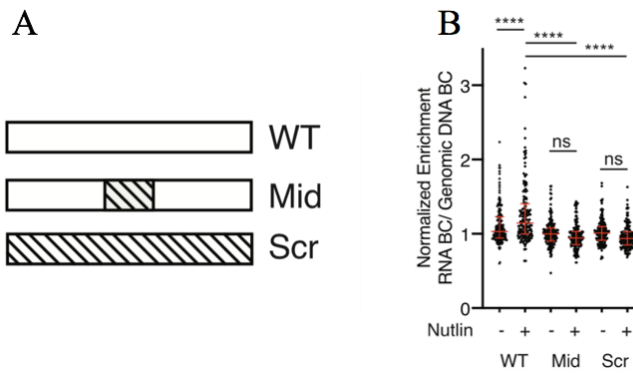


Figure 31: Loss of the p53RE severely depletes transcriptional activity of p53 bound enhancers

(A) Sequences within the wild-type p53-bound regions from the MPRA (WT) were shuffled (while preserving GC content) to alter either the 20 bp p53 binding site (Mid) or the entire 100 bp MPRA sequence. (B) Normalized transcriptional activity of p53-bound sequences for the wild-type (WT), p53-binding site scramble (Mid), or the full scramble (Scr) regions in HCT116 p53+/+ cells after a 6-h treatment of either DMSO or 5 uM Nutlin-3A. Data are depicted as enrichment of the 3'UTR-encoded barcode linked to each putative regulatory region normalized to the enrichment of that same sequence integrated into the genome and represent the averages from three biological replicates of each condition (***($P < 0.0001$) by one-way ANOVA).

Scrambling either the p53RE or the entire CRE sequence abrogates Nutlin-3A-dependent enhancer activity (Figure 31B, *** $p<0.0001$, one way ANOVA). In aggregate, wild-type CREs are more highly active than Mid or Scr CREs, suggesting that p53 strongly influences overall CRE activity (Figure 31B). Taken together, these data suggest that Nutlin-3A-induced activity of CREs requires direct binding of p53, in agreement with previous observations (Verfaillie et al., 2016; Younger & Rinn, 2017).

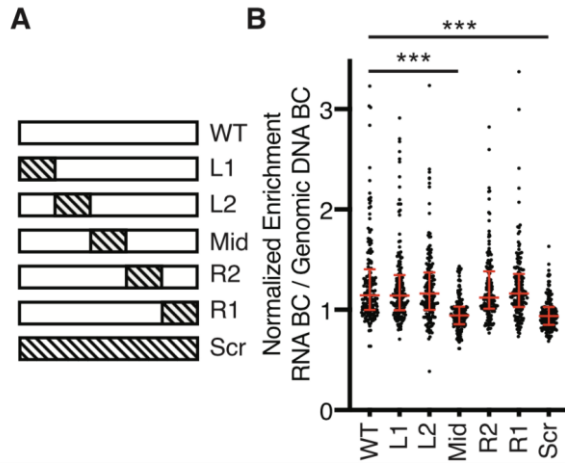


Figure 32: Only loss of the p53RE disrupts transcriptional activity across the majority of the enhancers

(A) Schematic depicting scrambling of 20 bp sequences within 100 bp p53-bound MPRA regions. Sequence scrambling was performed to preserve total GC content within the 20 bp scrambled region relative to the wild-type sequence. (B) Normalized transcriptional activity of the MPRA sequences depicted in (A) in HCT116 p53^{+/+} cells after a 6-h treatment with 5 uM Nutlin-3A. Data are depicted as enrichment of the 3'UTR-encoded barcode linked to each putative regulatory region normalized to the enrichment of that same sequence integrated into the genome and represent the averages from three biological replicates of each condition. (***($P < 0.001$) using an ordinary one-way ANOVA).

Variation in flanking sequence context alters p53-dependent CRE activity

Previous work suggests that p53-dependent CREs uniquely work in a single-factor mechanism in which only the presence of p53 is required for activation of transcription (Verfaillie et al., 2016). Thus, this model implies that other transcription factors are required for CRE activity. Similarly, analysis of DNA sequences flanking functional p53REs revealed no consistent enrichment or requirement for other transcription factor binding motifs or sequences outside of the p53RE (Verfaillie et al., 2016; Younger & Rinn, 2017). Because this model represents a potential novel mechanism for enhancer function and diverges from canonical CRE models, we sought to directly test whether p53-dependent CRE activity requires sequences or transcription factor motifs outside of the p53RE. We systematically scrambled non-overlapping 20bp regions of each CRE

starting at the 5' end (Figure 32A). As previously discussed, we also included controls where the p53RE and the entire CRE sequence were randomized (Figure 32A).

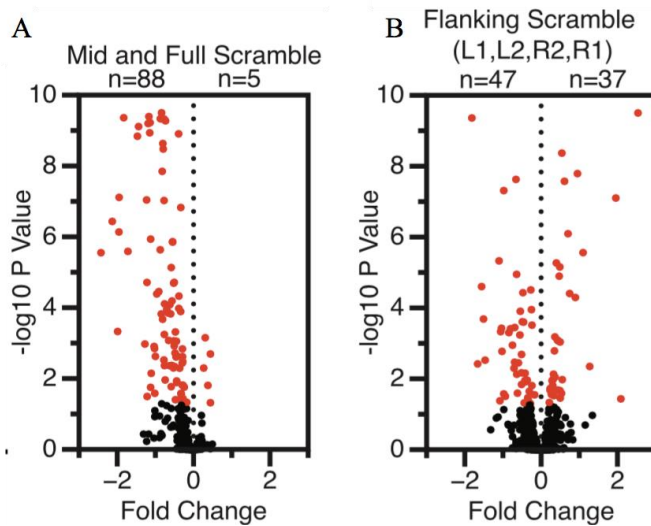


Figure 33: Individual enhancer activity is affected by mutated flanking sequences in a context specific manner

(A) Volcano plot of wild-type MPRA sequence activity compared to Mid or Full scramble. Data are plotted as Fold Change (WT over scramble) versus $-\log_{10}P$ -value (from a one-way ANOVA with Tukey post-hoc test). (B) Volcano plot of wild-type MPRA sequence activity compared to flanking scramble (L1, L2, R2 or R1). Data are plotted as Fold Change (WT over scramble) versus $-\log_{10}P$ -value (from a one-way ANOVA with Tukey post-hoc test).

We then asked whether individual CRE variants had significantly different transcriptional activity than their wild-type counterpart in Nutlin-3A-treated, wild-type HCT116 cells. Both the Mid and Scr variant CREs displayed significantly reduced activity relative to wild-type CREs (Figure 32B, $p < 0.001$, one way ANOVA), consistent with a loss of p53 binding and p53-dependent transactivation. Overall, 93 Mid or Scr CRE variants had statistically significant differential activity relative to the wild-type CRE, with 88 (95%) displaying reduced activity when sequences were randomized (Figure 33A, one-way ANOVA with Tukey HSD, $p < 0.05$). Only 1.5% of Mid or Scr variants (5/338) had statistically increased activity relative to the wild-type sequence (Figure 33A), with 2/5 of those more active variants representing scrambled CRE sequences that generated a novel canonical p53 binding site. The remaining three variants possessed unique combinations

of TF motifs with increased activity relative to the wild-type, p53RE-containing sequences. These data suggest that, overall, disruption of the p53RE is sufficient to decrease CRE activity.

Scrambling DNA sequence flanking a p53RE does not affect transcriptional activity in aggregate (Figure 32B, $p > 0.05$, one way ANOVA). However, individual CREs have significantly altered transcriptional outputs when context-specific regions are scrambled (Figure 33B, one-way ANOVA with Tukey HSD, $p < 0.05$). Variants with decreased p53-dependent CRE activity have wild-type counterparts with higher expression values than compared to those variants with increased activity (Figure 34, $p < 0.0001$, Mann-Whitney U).

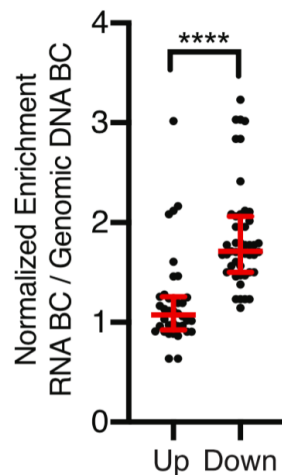


Figure 34: Most flanking sequence variants with significant changes to activity show decreased transcriptional outputs

Jitter plot depicting CRE activity values for wild-type p53-bound CREs (in the Nutlin-3A-treated condition) for those variants with increased (up) or decreased (down) activity relative to wild-type. P -value represents the result of an unpaired Mann-Whitney U test ($****P < 0.0001$).

We then wanted to determine whether the position of the scrambled sequence relative to the p53RE influenced the change in CRE activity by examining the proportion of significantly upregulated and downregulated CREs at each position. The Mid position, containing a p53RE, was more strongly associated with decreased CRE activity upon scrambling relative to any other

position (Figure 36, Fisher's Exact Test), consistent with a loss of p53-mediated activation. The R1 position (20-40bp 3' of the p53 RE) had a larger number of variants with displaying significantly different activity than wild-type than any of the other flanking region variants (Fisher's Exact Test, $p < 0.05$ for L1, L2, and R2), although the underlying mechanism for this observation is unclear. These data suggest that DNA elements important for CRE function can be found in any position relative to the p53RE and that local context and DNA sequence content may play key roles in p53-bound CRE activity.

Previous analyses of local sequence context at p53-bound CREs suggested a lack of enrichment of transcription factor motifs, besides the p53 RE, that might influence CRE activity (Younger & Rinn, 2017). Our MPRA approach demonstrates that sequences flanking p53RE can contribute to CRE activity (Figure 33B), but the context and content of DNA sequences influencing p53-bound CRE activity is unclear. Therefore, to determine whether the scrambling of flanking sequences might disrupt specific DNA-encoded information, like transcription factor motifs, we undertook a series of motif enrichment analyses on wild-type and scrambled sequences.

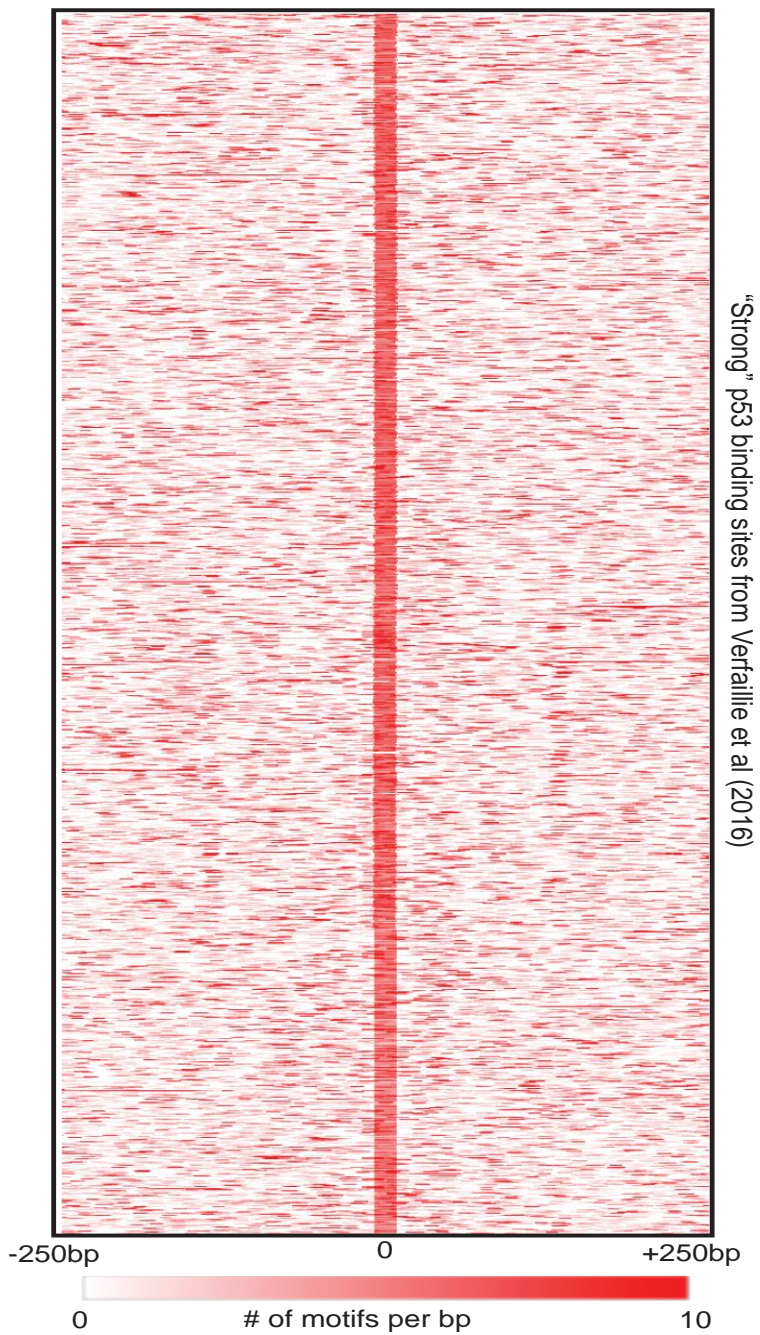


Figure 35: Flanking regions are highly enriched for transcription factor binding sites

Heatmap of transcription factor motif enrichment across 500bp of the "Strong" p53 binding locations from Verfaille et al. 2016. Data represent a per base pair score for the presence of JASPAR-derived transcription factor motifs ($p < 0.0001$, corresponding to a JASPAR score of 400 or greater). Regions are centered on the putative p53 family response element.

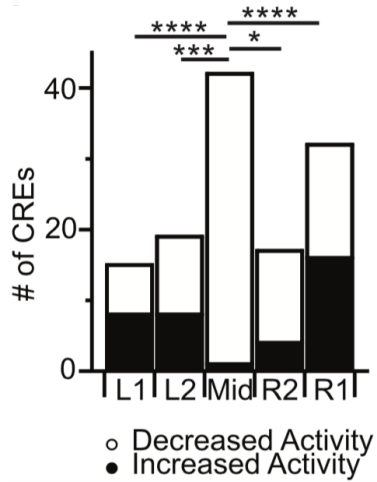


Figure 36: DNA elements important for CRE function can be found in any position relative to the p53RE
Number of CRE variants per position that significantly increase or decrease in MPRA transcriptional activity compared to WT sequences (* $P < 0.05$, ** $P < 0.001$, *** $P < 0.0001$ by Fisher Exact Test).

First, we examined the genome-wide enrichment of known transcription factor motifs across p53-bound CREs using HOMER (Heinz). Expectedly, p53 family motifs were highly enriched in the MPRA regions relative to size and GC-content matched genomic regions (Supplemental Table 6 from Catizone et. al. 2020). We also observed statistically significant

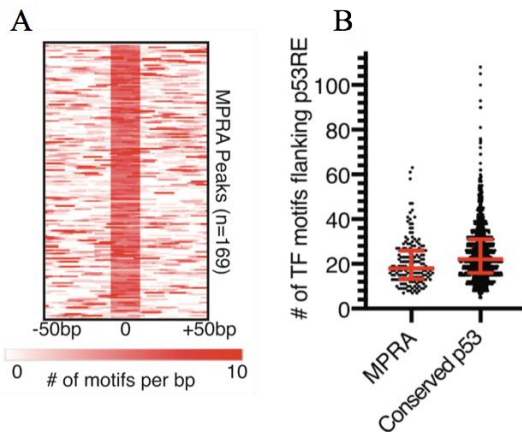


Figure 37: Transcription factor binding sites are highly enriched flanking the p53RE
(A) Heatmap of transcription factor motif enrichment across 100 bp of the 169 p53-bound MPRA regions in the current study. Data represent a per base pair score for the presence of JASPAR-derived transcription factor motifs ($P < 0.0001$, corresponding to a JASPAR score of 400 or greater). Regions are centered on the putative p53 family response element. Median values and the interquartile range are depicted in red. **(B)** Jitter plot representing the number of JASPAR-derived transcription factor motifs flanking the p53RE of the p53-bound CRE ($P < 0.0001$, corresponding to a JASPAR score of 400 or greater). Regions are centered on the putative p53 family response element (p53RE) and are extended -250 bp and $+250$ bp upstream.

(Bonferroni q value < 0.05) enrichment of other known transcription factor motifs, including those in the AP-1, GATA, and ETS families (Supplemental Table 6 from Catizone et. al. 2020).

The observed enrichment of transcription factor motifs near p53RE is similar in a group of 1,149 consensus p53 binding sites (Verfaillie et al., 2016). Of note, a wider range of transcription factor families are represented in this consensus set of p53 binding sites, likely due to the increase in number and length of surveyed regions included in the analysis (-/+ 250bp from p53RE) (Supplemental Table 7 from Catizone et. al. 2020, Figure 35, Figure 37B). In order to account for potential bias in a single motif enrichment strategy, we also used gimmeMotifs (van Heeringen & Veenstra, 2011) and the JASPAR vertebrate transcription factor database (Khan et al., 2018) to identify the position of transcription factor motifs relative to the p53RE. p53-bound CREs are

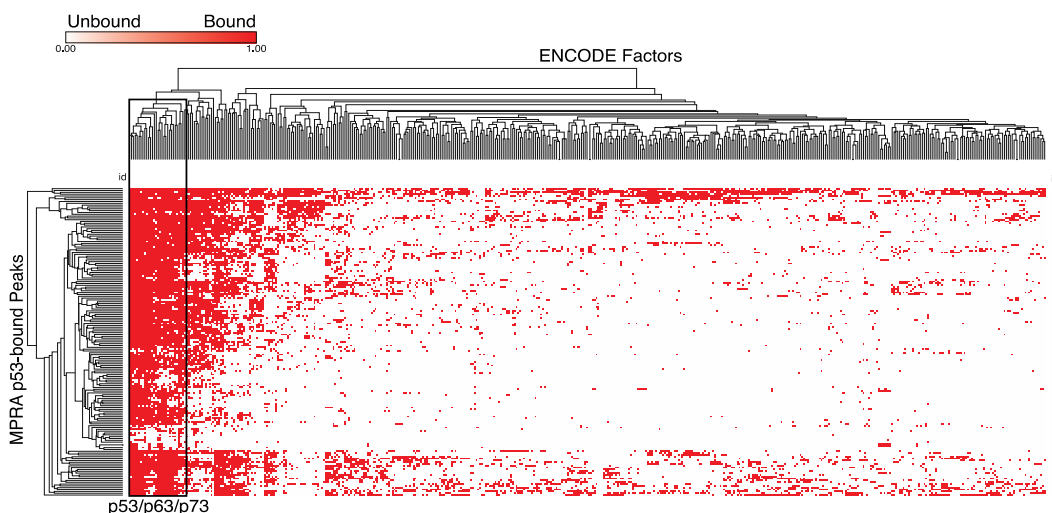


Figure 38: p53 bound regions contain transcription factor binding sites that cluster with transcription factor families

Hierarchical clustering of CISTROME-derived transcription factor binding with the 168 p53-bound MPRA regions from the current study. p53-bound MPRA regions are found on the Y-axis, while transcription factors bound to greater than 10 regions are found on the X axis. Only the peak summit for the CISTROME transcription factors were considered when intersecting with the p53-bound MPRA regions. Data were clustered by row and column using complete linkage and Pearson minus one correlation in the Morpheus software suite. The boxed region of the cladogram represents p53/p63/p73 datasets from the CISTROME database and shows strong enrichment of these factors with the MPRA regions from this study.

enriched for flanking transcription factor motifs (Figure 37A-B) with a median of 18 distinct motifs found per p53-bound CRE (Figure 37B). Examination of transcription factor chromatin immunoprecipitation (ChIP) data from the Cistrome Browser (Mei et al., 2017) suggests that numerous transcription factors are likely to occupy our group of p53-bound CREs (Figure 38). Thus, our data suggests that regions proximal to p53REs are enriched for transcription factor binding motifs that may be involved in p53-dependent CRE activity.

We then focused exclusively on CRE variants that displayed reduced activity relative to the wild-type CRE sequence to better understand how flanking sequence context might affect p53-dependent CRE activity. Our rationale was to identify potential transcription factors or functional DNA elements that facilitate p53-dependent transcriptional activity. The 47 p53-bound CREs with reduced activity (Figure 33B) had a median loss of 2 JASPAR-defined TF motifs relative to the wild-type sequence (Figure 39A). TF motif enrichment demonstrates that the AP-1 family motif is enriched in WT sequences and depleted from scrambled CREs (Supplemental Table 8 from

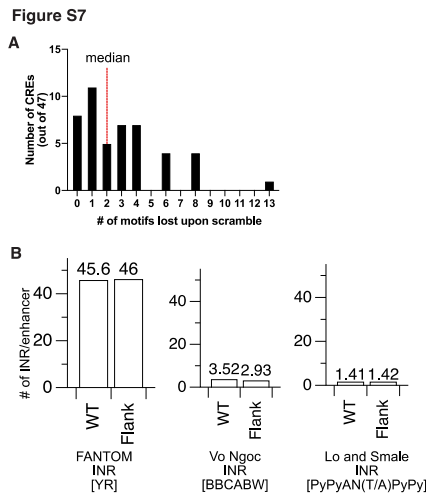


Figure 39: Enhancers lose approximately 2 transcription factor binding sites per variation but not INRs

(A) Number of JASPAR-defined transcription factor motifs at p53-bound CREs that significantly decrease in activity upon scrambling of a flanking region (corresponding to Figure 3D). (B) Number of INR elements per wild-type p53-bound CRE or variants that significantly decrease in activity relative to the wild-type. Three different definitions of an INR (initiator element) were used (FANTOM Consortium, Vo Ngoc et al, and Lo and Smale)

Catizone et. al. 2020), being lost from 17% of CREs with reduced activity. AP-1 family factors have wide-ranging roles in transcription regulation, including mediating chromatin accessibility at CREs (Biddie et al., 2011; Phanstiel et al., 2017; Vierbuchen et al., 2017). Overall, motifs for 95

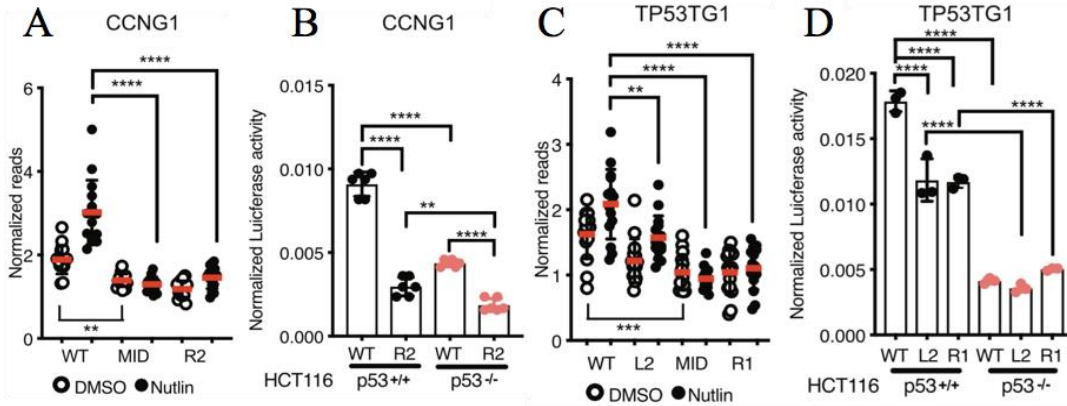


Figure 40: Enhancers for two canonical p53 targets have functionally important flanking regions

(A) Normalized transcriptional activity of the WT, Mid or R2 version of Region 36/CCNG1 from the MPRA in HCT116 p53^{+/+} cells after 6 h of either DMSO or 5uM Nutlin-3A treatment. (****P < 0.0001 using an ordinary one-way ANOVA). (B) Normalized Luciferase activity of either wild-type or R2-scrambled Region 36/CCNG1 sequence cloned upstream of a minimal promoter and driving expression of firefly luciferase in either HCT116 p53^{+/+} or p53^{-/-} colon carcinoma cells. Firefly luciferase values were normalized to those of Renilla luciferase driven by a CMV promoter and co-transfected with the candidate Firefly plasmid (**P < 0.01, ****P < 0.0001 using an ordinary one-way ANOVA) (C) Normalized transcriptional activity of the WT, L2, Mid or R1 version of the TP53TG1 CRE from the MPRA in HCT116 p53^{+/+} cells after 6 h of either DMSO or 5 uM Nutlin-3A treatment (**P < 0.01, ****P < 0.0001 using an ordinary one-way ANOVA). (D) Normalized Luciferase activity of either wild-type, L2, or R1-scrambled TP53TG1 CRE sequence cloned upstream of a minimal promoter and driving expression of firefly luciferase in either HCT116 p53^{+/+} or p53^{-/-} colon carcinoma cells. Firefly luciferase values were normalized to those of Renilla luciferase driven by a CMV promoter and co-transfected with the candidate Firefly plasmid (****P < 0.0001 by one-way ANOVA).

different TFs are lost within the 47 scrambled REs with reduced activity, including AP-1, GATA, SP1, and ETS family members (Supplemental Table 9 from Catizone et. al. 2020). Loss of activity is not correlated with loss of canonical transcription initiation sequences, like the INR element (Figure 39B)(Carninci et al., 2006; Frith et al., 2006; Lo & Smale, 1996; Vo Ngoc et al., 2017). These data, taken together, suggest that loss of a broad set of transcription factor motifs flanking p53RE can influence p53-dependent CRE activity.

We then moved to validate our observation that altering TF motifs flanking p53RE could reduce p53-dependent CRE activity. We first examined a CRE localized within the first intron of

the *CCNG1* gene that is induced upon Nutlin-3A treatment in a p53-dependent manner (Figure 40A). This activity is abrogated when either the p53RE or the 3' adjacent 20bp region are scrambled (position R2, Figure 40A). We observe similar results for a putative CRE localized within the second intron of *TP53TG1* where scrambling either the 5' adjacent 20bp or 40bp downstream of the p53RE (Figure 40C) leads to diminished p53-dependent CRE activity. We then sought to validate these MPRA results by utilizing a standard Luciferase reporter-based assay of CRE activity. In contrast to the 100bp sequence tested in the MPRA, we assessed the activity of a larger sequence encompassing an entire region of DNase hypersensitivity (DHS) as determined by ENCODE. DHS are putative regulatory regions often possessing transcriptional activity (Thurman et al., 2012). Both the *CCNG1* and *TP53TG1* wild-type CREs are dependent on p53 for full activity (Figure 40B, D, p53^{+/+}), consistent with the MPRA data. We confirmed that flanking region variants with loss of activity in the MPRA displayed a similar reduction of activity in traditional luciferase enhancer assays (Figure 40B, D), suggesting our MPRA results are not an artifact of the restricted sequence size (100bp) or differences in assay conditions. Under DMSO treated conditions, *CCNG1* and *TP53TG1* CRE activity is reduced in either p53-depleted cells (Figure 40B, D) or in the p53RE mutant (Mid) relative to the wild-type sequence (Figure 40B, D). These results are likely indicative of either basal p53 activity and genomic occupancy in unstimulated cells (Younger & Rinn, 2017) or that a population of cells is experiencing intrinsic stress, such as DNA damage during S phase (Loewer et al., 2010). For the *CCNG1* enhancer, loss of activity in the R2 variant is further reduced in the absence of p53 (Figure 40B, p<0.01, one-way ANOVA), suggesting potential combinatorial activity of p53 and the wild-type R2 sequence within the *CCNG1* CRE. This combinatorial activity was not observed for *TP53TG1*, as the wild-type CRE and the L2 and R1 variants have similar activity in cells lacking p53 (Figure 40D). These data

suggest that p53-dependent CREs require different sequences and motifs, and potentially TFs, flanking the p53RE for optimal activity.

An SP1/KLF family motif is required for p53-dependent activity of the CCNG1 CRE

We continued investigating the role of flanking DNA sequences on p53-dependent CRE activity by further examining the *CCNG1* CRE. Both the DNA sequence within the R2 position and the p53RE are highly conserved across vertebrates suggesting that this region may have a conserved functional regulatory role (Figure 41A). The p53-dependence of the *CCNG1* CRE is similar across human cell types, as the R2 variant leads to a similar reduction in enhancer activity relative to the wild-type sequence when assayed in the non-transformed human cell line MCF10A (Figure 41B). We then assessed the activity of the wild-type and R2 variant *CCNG1* CREs in *Trp53^{+/+}* and *Trp53^{-/-}* mouse embryonic fibroblasts (MEFs). The R2 variant has reduced activity compared to the wild-type *CCNG1* CRE in both wild-type and p53-deficient MEFs consistent with our observations in human cell lines (Figure 42 A, C, D).

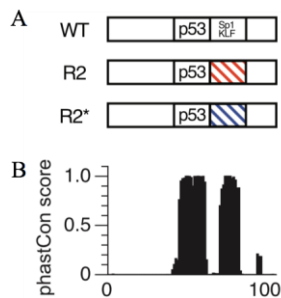


Figure 41: Both the p53RE and the R2 position are evolutionary conserved across species

(A) Schematic of the 100 bp Region 36/CCNG1 enhancer. R2 position is annotated with the predicted motif 'SP1/KLF' 20 bp 3' adjacent to the p53RE and (B) per-basepair vertebrate phastCon score.

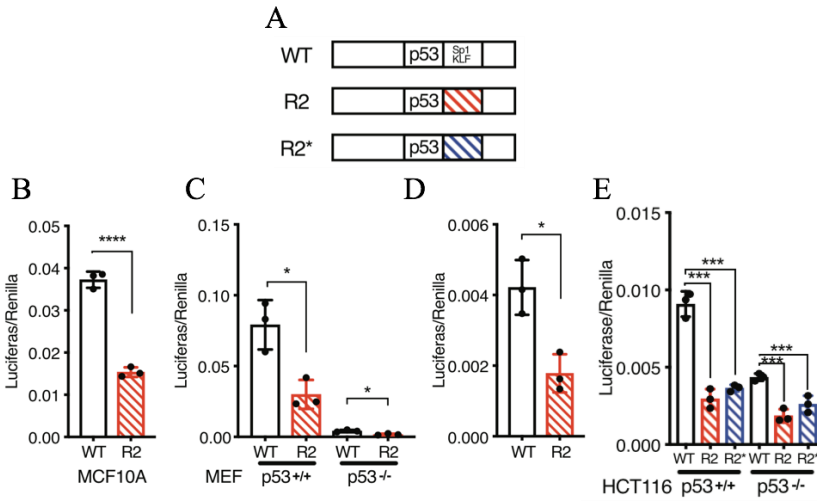


Figure 42: The R2 position's function is conserved across cell type and species and contributes to p53's optimal transcriptional activity

(A) Schematic of the 100 bp Region 36/CCNG1 enhancer. R2 position is annotated with the predicted motif 'SP1/KLF' 20 bp 3' adjacent to the p53RE (B) Normalized Luciferase activity (test sequence Firefly versus constitutive Renilla) for WT Region36/CCNG and the R2 version in the MCF10A mammary epithelial cell line (****P < 0.0001 paired t-test). (C) Normalized Luciferase activity (test sequence Firefly versus constitutive Renilla) for WT Region36/CCNG and the R2 version in either p53^{+/+} or p53^{-/-} mouse embryonic fibroblasts (*P < 0.05, paired t-test). (D) Rescaled view of p53^{-/-} reporter assay data from (C) depicting normalized Luciferase data for the wild-type or R2 version of the CCNG1 enhancer in p53^{-/-} mouse embryonic fibroblasts (*P < 0.05, paired t-test). (E) Normalized luciferase activity for either the wild-type, R2 or R2* version of the CCNG1 enhancer in HCT116 p53^{+/+} or p53^{-/-} cells. (**P < 0.001 by one-way ANOVA).

In order to determine if the decrease in *CCNG1* CRE activity via R2 scrambling is due to a loss of the wild-type sequence or a gain of function from the scrambled sequence, we created a second R2 variant (R2*) that preserves GC content but is further randomized from the wild-type sequence (Figure 42A). Both R2 and R2* variants lead to loss of *CCNG1* CRE activity relative to wild-type and are further reduced in the absence of p53 (Figure 42E). These results suggest that 20bp flanking the p53RE within *CCNG1* are required for p53-dependent CRE activity. The 20 bp immediately downstream of the p53RE within *CCNG1* enhancer contains several known transcription factor motifs based on analysis from JASPAR (Khan et al., 2018), suggesting that the loss of activity may be due to a loss of TF binding. The highest-scoring transcription factor motif from JASPAR are for members of the SP1/KLF family, and this G-rich motif is highly conserved across vertebrates (Figure 43A, B).

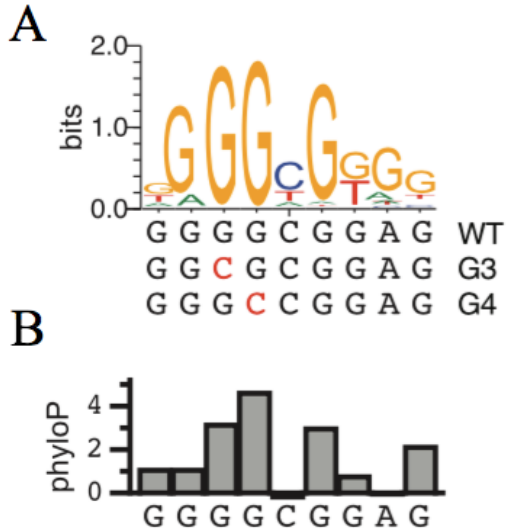


Figure 43: The R2 position's SPI/KLF motif has highly conserved G residues

(A) The canonical Sp1/KLF family motif sequence in the CCNG1 enhancer as a transcription factor logo compared to the wild-type, G3, or G4 variants. This motif is located within the R2 site of the CCNG1 CRE, between 0 and 20 bp from the p53 response element. (B) phyloP vertebrate conservation of the Sp1/KLF family motif within the wild-type CCNG1 enhancer sequence showing high conservation at the G3 and G4 positions.

We therefore made single base-pair mutations in the most conserved G3 and G4 residues of the SP1/KLF motif (Figure 43A,B) and asked whether loss of these residues was sufficient to reduce CRE activity (Jolma et al., 2013). Consistent with scrambling the entire 20bp R2 region,

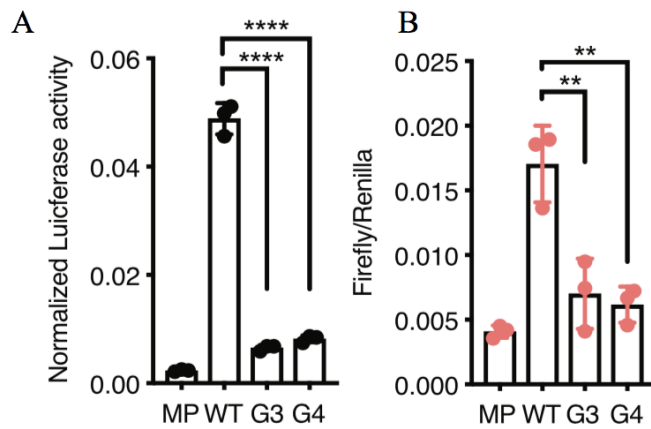


Figure 44: Mutating a single conserved G reduces transcriptional activity of CCNG1's enhancer

Normalized enhancer activity for the minimal promoter only (MP), WT, G2 or G3 CCNG1 variants in (A) HCT116 p53+/+ or (B) HCT116 p53-/- cells (** $P < 0.01$, **** $P < 0.0001$, by one-way ANOVA).

mutation of either the G3 or G4 position within the SP1/KLF motif severely diminishes transcriptional output in both wild-type and p53-deficient cell lines (Figure 44A, B). The additional reduction in CRE activity in p53-deficient cells seen in SP1/KLF motif variants suggests this region is functionally important independent of p53. Taken together, these data suggest that *CCNG1* CRE activity requires both p53 and a regulatory motif belonging to the SP1/KLF family.

*Loss of the SP1/KLF motif leads to reduced *CCNG1* transcription and reduced p53 binding*

Thus far, our data indicate that the p53-dependent *CCNG1* CRE also requires key DNA sequences flanking the p53RE and that these DNA sequences likely represents a binding motif for the SP1/KLF family. Therefore, we assessed the role of the p53RE and the R2 position sequence in their native genomic contexts using CRISPR/Cas9-mediated mutagenesis (Figure 45). Guide RNA sequences were targeted to either the p53RE, the R2 position, or the L2 position, which is 5' adjacent to the p53RE, generating a population of indel mutations (Figure 45, Supplemental Table

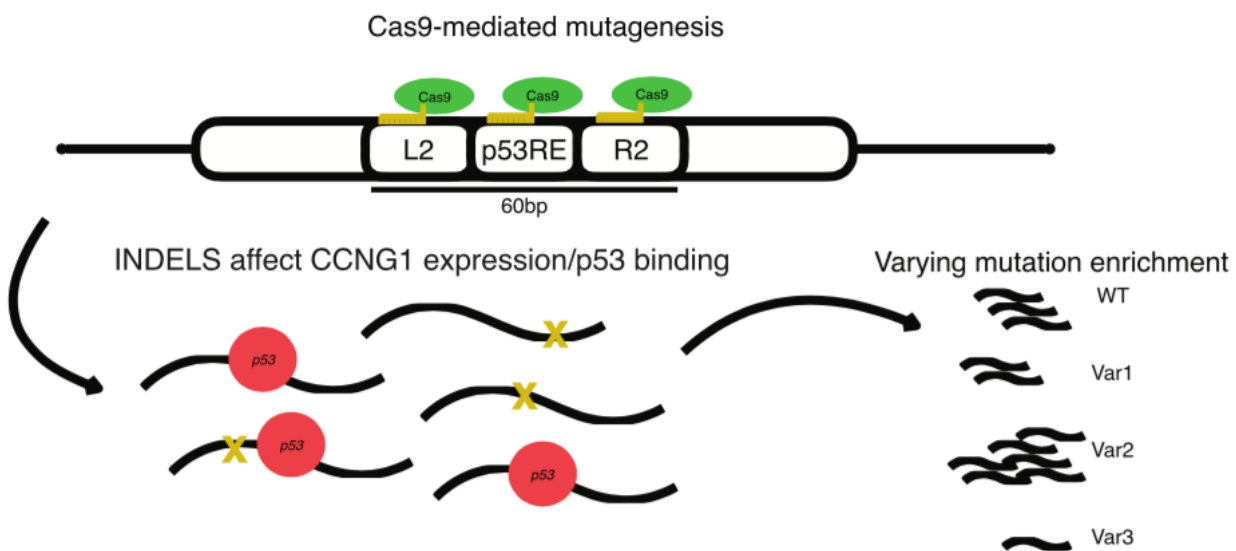


Figure 45: Schematic depicting the CRISPR/Cas9 mutagenesis strategy to mutate R2 in vivo

Schematic depicting strategy to introduce insertion-deletion (indels) mutations into the native *CCNG1* locus in HCT116 cell lines. Pools of indel-containing cells were then used for measurement of *CCNG1* mRNA expression and for analysis of p53 binding by ChIP-sequencing.

4 from Catizone et. al. 2020). Targeting of the p53RE substantially reduced endogenous *CCNG1* mRNA abundance relative to non-targeted Cas9 cells (Figure 46, $p < 0.0001$).

Consistent with *in vitro* observations of *CCNG1* enhancer activity, mutations within the R2 position reduce *CCNG1* mRNA levels, albeit not as severely as mutations in the p53RE (Figure 46, $p < 0.0001$). As a control for sequence variants proximal to the p53RE, we generated indel mutations in the L2 position which is found in the 20bp immediately preceding the p53RE. Targeting the L2 position did not reduce endogenous *CCNG1* mRNA levels suggesting that proximal DNA mutations are not sufficient to decrease transcriptional output (Figure 46). Additionally, the L2 control suggests that the act of targeting Cas9 to the *CCNG1* intron does not affect *CCNG1* transcription on its own. These data further suggest that the p53RE and sequences immediately downstream of the p53RE are required for endogenous expression of the *CCNG1* mRNA.

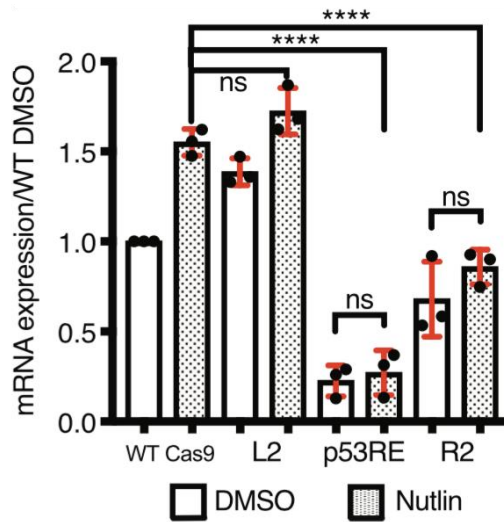


Figure 46: Mutation of the R2 position *in vivo* significantly reduces *CCNG1* mRNA levels

qRT-PCR data of *CCNG1* mRNA expression in control (WT Cas9), L2, p53RE or R2-targeted Cas9 experiments after 6 h of DMSO or 5uM Nutlin-3A treatment in HCT116 p53 $^{+/+}$ cell lines ($****P < 0.0001$, by one-way ANOVA).

We generated a pool of indel mutations at three locations within the *CCNG1* CRE, with mutations near the p53RE and the R2 position leading to a reduction in endogenous *CCNG1* mRNA expression (Figure 45 and Figure 46). We therefore coupled chromatin immunoprecipitation of p53 to amplicon sequencing to simultaneously determine indel mutations and their potential effect on p53 occupancy at the *CCNG1* CRE. As a control, we performed p53 ChIP under DMSO and Nutlin-3A-treated conditions on HCT116 p53^{+/+} cells expressing wild-type Cas9 without a gRNA to target it to DNA. We then amplified a 150bp region in the *CCNG1* CRE from the p53-immunoprecipitated and input samples and sequenced them using Illumina approaches. We observed a 2.98-fold enrichment of the amplified sequence in the Nutlin-3A-induced samples relative to DMSO (Figure 47A, dotted lines), suggesting our amplicon ChIP approach was valid.

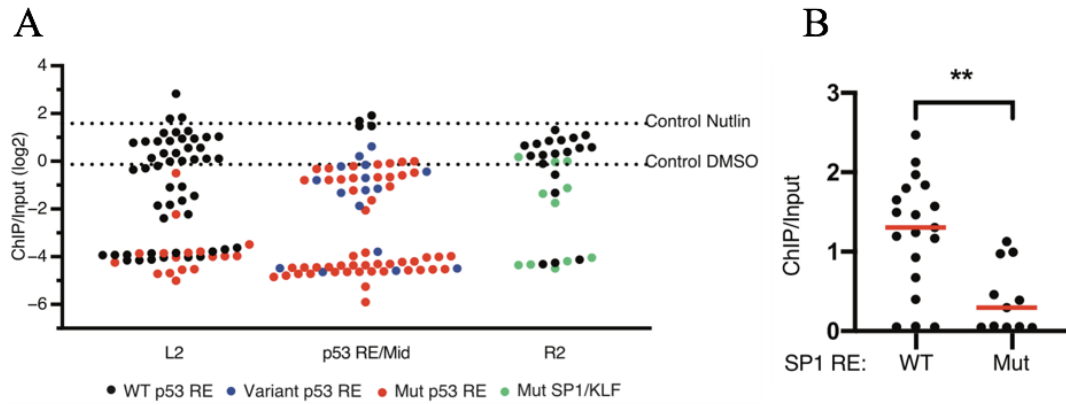


Figure 47: Loss of the SP1/KLF motif in vivo reduces p53 enrichment at the *CCNG1* enhancer

(A) Jitter plot of p53 ChIP-enrichment for each Cas9-induced mutation at the native *CCNG1* enhancer. Black dots represent genetic variants that retain a wild-type p53 response element motif, while red dots are genetic variants with a mutated p53 response-element. Green dots represent sequences with a mutated or missing ‘SP1/KLF’ motif. Dashed line represents p53 ChIP/Input enrichment (\log_2) for the control cell line after 6 h of Nutlin-3A treatment. (B) Comparison of p53 ChIP enrichment from variants with either a canonical or mutated Sp1/KLF family motif from the R2-targeted Cas9 experiment (red line is the median, ** $P < 0.01$, unpaired t -test).

We next performed ChIP experiments from DMSO and Nutlin-3A-treated cell lines with Cas9 targeted to the p53RE, L2, or R2 positions. 66 unique DNA variants were identified within our pool when targeting Cas9 to the p53RE within the *CCNG1* CRE (Supplemental Table 4 from Catizone et. al 2020, Figure 47A). As expected, the wild-type *CCNG1* CRE sequence and 3 variants with an intact p53RE were enriched near the levels seen in the Cas9 control (Figure 47A, p53RE, black dots). Enrichment of p53 is below or at DMSO levels when a p53RE is present but varies from the wild-type version (Figure 47A, blue dots). As expected, *CCNG1* variants lacking a p53RE show a strong reduction in p53 binding. Variants proximal to the p53RE generally reduced p53 binding to the level of DMSO treatment (no enrichment), but many variants were depleted to the level seen when the p53RE was mutated (Figure 47A). These data are consistent with data showing that Cas9-induced mutations proximal to GATA1 binding sites alter GATA1 occupancy (Behera et al., 2018). None of the R2 mutations identified contained variants within the p53RE; however, when the conserved SP1/KLF motif was mutated or lost, p53 occupancy was reduced relative to the presence of an intact motif (Figure 47A(green dots)-47B, $p<0.01$). Our ChIP-based approach

suggested that sequence variation flanking a p53RE can alter *in vivo* p53 binding in a context-dependent manner.

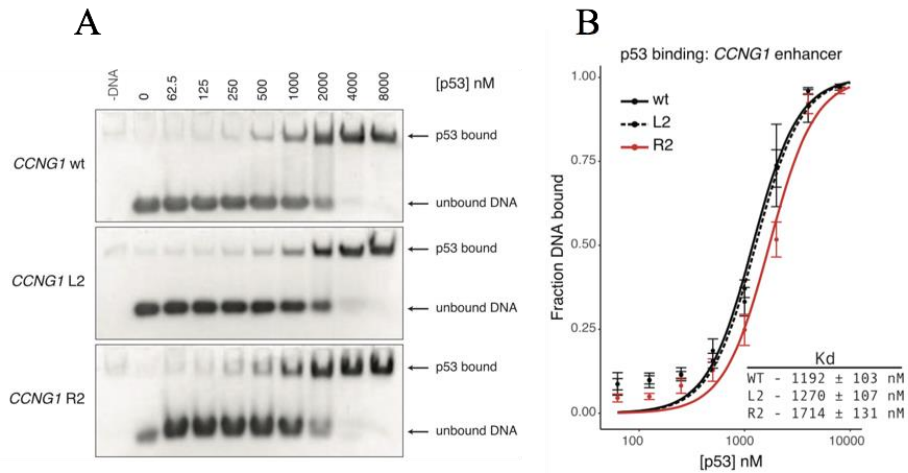


Figure 48: Loss of R2 position in vitro modestly reduces p53 affinity for the CCNG1 enhancer

(A) Electrophoretic Mobility Shift Assay (EMSA) for recombinant p53 bound to the wild type, L2 or R2 variant of the CCNG1 *cis*-regulatory element DNA sequence. Images are representative of four independent biological replicates. (B) Quantification of EMSA experiment in (E) performed as described in Materials and Methods. Fitted curves were fitted using a two-site binding model (Hill equation; Hill coefficient = 2) using a non-linear regression.

We also performed electrophoretic mobility shift assays (EMSA) to better understand the effect of flanking sequence variation on p53 binding to p53RE. Increasing concentrations of recombinant p53 were combined with 60bp double-stranded DNA fragments representing the wild-type *CCNG1* p53RE and either the L2 or R2 variants from the original MPRA experiment (Figure 48A). The R2 variant had a modest, but statistically significant, increase in K_d relative to either the wild-type or L2 variants (Figure 48B). The reduction in p53 binding observed in the R2 variant by EMSA is consistent with our results from the *in vivo* variant ChIP experiment as well as the reduced p53-dependent transcription of endogenous *CCNG1*. Surprisingly, although a number of L2 variants had reduced p53 binding *in vivo*, we observed similar p53 binding affinities for both the wild-type and L2 sequences by EMSA (Figure 48B). The fully randomized L2 variant does not affect p53-dependent CRE activity or affect p53 binding *in vitro*, suggesting that loss of

p53 binding observed *in vivo* for specific L2 variants may be context-specific. These data, along with our examination of endogenous *CCNG1* mRNA expression, indicate that the specific sequences proximal to the p53RE in the *CCNG1* enhancer, which includes an SP1/KLF family motif, leads to increased p53 occupancy and higher *CCNG1* mRNA expression.

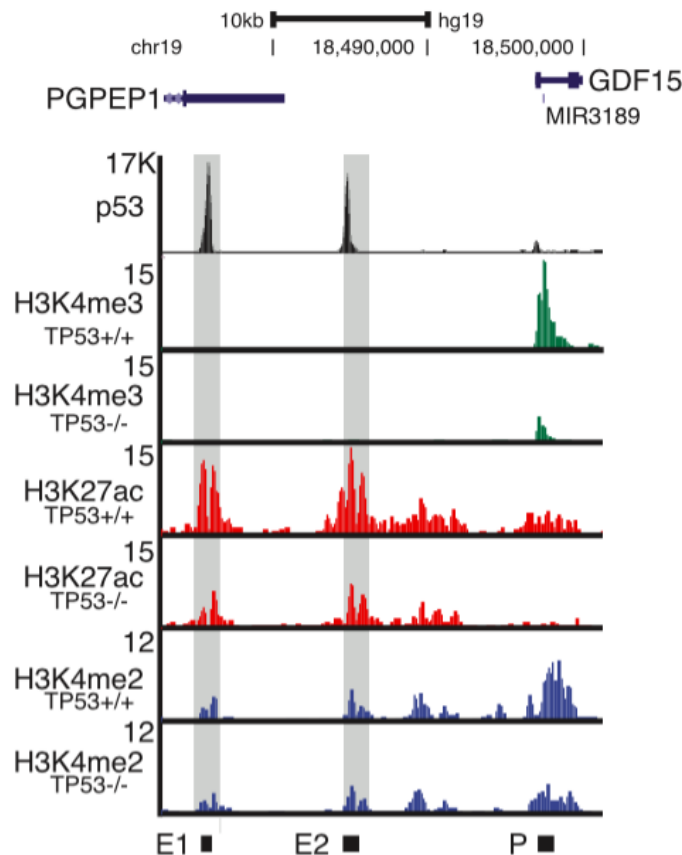


Figure 49: GDF15 has two putative p53 bound enhancers upstream of the gene body

Genome browser view of the *GDF15* locus showing p53, H3K4me3, H3K27ac, and H3K4me2 enrichment in HCT116 p53^{+/+} or HCT116 p53^{-/-} cell lines. E1 = enhancer 1, E2 = enhancer 2, and P = *GDF15* promoter. Grey shaded boxes are placed over the E1 and E2 regions.

p53-dependent transcription of GDF15 requires regulatory factors at two separate distal CREs

Data from our MPRA approach and follow-up experiments demonstrate that p53-dependent transcriptional activity at CREs is altered when sequences flanking the p53RE are

perturbed. The CREs regulating *CCNG1* and *TP53TG1* are intragenic or proximal to the gene promoter similar to the majority of known p53-bound CREs directly controlling downstream gene expression (Andrysiak et al., 2017; Wei et al., 2006). In order to better understand the regulatory potential and mechanisms of gene distal p53 binding events, we searched our MPRA dataset for p53-dependent CREs distal to the promoters of known p53 target genes. One such region is approximately 11kb upstream of *GDF15*, which is well-characterized p53 target gene (Allen et al., 2014; Kannan et al., 2000). As predicted, basal and induced *GDF15* expression is strongly dependent on p53 (Figure 53).

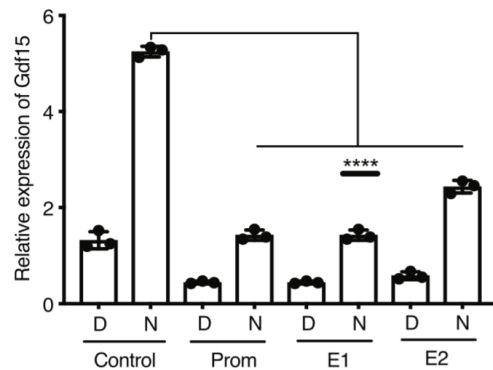


Figure 50: Repression of the two putative p53 enhancers upstream of GDF15 deplete endogenous GDF15 mRNA

qRT-PCR relative expression of GDF15 mRNA in control, promoter, E1, or E2-targeted dCas9-KRAB-expressing HCT116 p53+/+ cells treated with either DMSO (D) or 10uM Nutlin-3A (N) for 6 hours. (****P < 0.0001, one-way ANOVA).

GDF15 has also recently been identified as a key modulator of inflammatory and metabolic responses (Luan et al., 2019, p. 15; Patel et al., 2019, p. 15), but the CREs key to regulation after p53 activation are known. This putative CRE (called E2) is enriched with the histone modifications H3K27ac and H3K4me2 and depleted for H3K4me3, a pattern strongly associated with transcriptional CREs. p53 is strongly bound to this region *in vivo* (Figure 49). While examining the genomic context of this putative enhancer, we identified a second putative p53-bound CRE approximately 20kb upstream of *GDF15* in the 3'UTR of the *PGPEP1* gene, which we define as

E1. Both p53-bound regions are enriched for H3K27ac and H3K4me2 in the absence of p53 (Figure 49) suggesting potential CRE activity independent of p53. This observation is consistent with recent reports of basal enhancer RNA transcription and histone modification enrichment at potential CREs in the absence of p53 (Allen et al., 2014; Karsli Uzunbas et al., 2019; Sammons et al., 2015). We therefore wanted to determine whether these p53-bound regions act as CREs for the endogenous expression of *GDF15*. We took advantage of a recently described approach to inactivate enhancers (Thakore et al., 2015). In this approach, a catalytically inactive form of Cas9 (dCas9) was fused to the transcriptional repressor domain KRAB, and this strong repressor was targeted to either a control region (an enhancer for an unrelated gene, FGF2), the two p53-bound regions, or the *GDF15* promoter. Compared to the non-targeting control, targeting dCas9-KRAB to either p53-bound distal region (E1 or E2) reduced expression of endogenous GDF15 mRNA in both basal (DMSO) or p53-activated (Nutlin-3A) conditions (Figure 50). Repression of GDF15 mRNA levels when targeting either E1 or E2 was similar to that of targeting the *GDF15* promoter

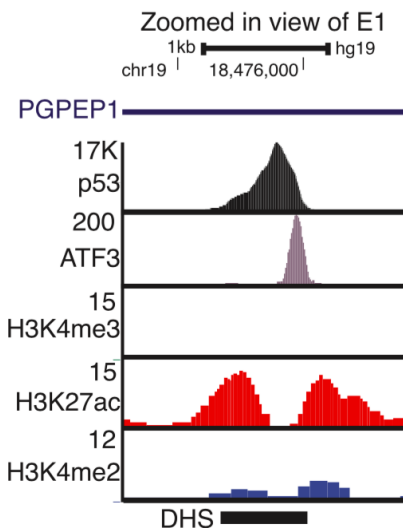


Figure 51: The stress factor ATF3 is strongly bound at the 3' *GDF15* enhancer

Genome browser view of the GDF15 E1 region showing ChIP-seq enrichment of p53, ATF3, H3K4me3, H3K27ac or H3K4me2. DHS = DNAse hypersensitive site.

region (Figure 50). These results provide evidence that the E1 and E2 regions, bound by p53, are likely CREs regulating the expression of *GDF15*.

We next wanted to determine whether potential sequences or transcription factors might regulate the activity of these p53-bound CREs for *GDF15*. We sought to use the breadth of publicly available ChIP-seq datasets to identify potential transcription factors bound the GDF15 E1 CRE. Using information from the CISTROME database (Mei et al., 2017), we found that ATF3, a member of the AP-1 family of transcription factors, strongly binds to the GDF15 E1 CRE in HCT116 cells (Figure 51). The summit of the ATF3 binding event coincides with an ATF3 DNA motif, approximately 125bp downstream of the p53RE (Figure 51). We therefore focused on ATF3 because of its previous association as a positive regulator of p53 activity and its well-known role as a modulator of the inflammatory response (Cui et al., 2016, p. 3; Gilchrist et al., 2006; Taketani et al., 2012, p. 3; Zhao et al., 2016, p. 3), of which GDF15 is a central regulator (Luan et al., 2019, p. 15).

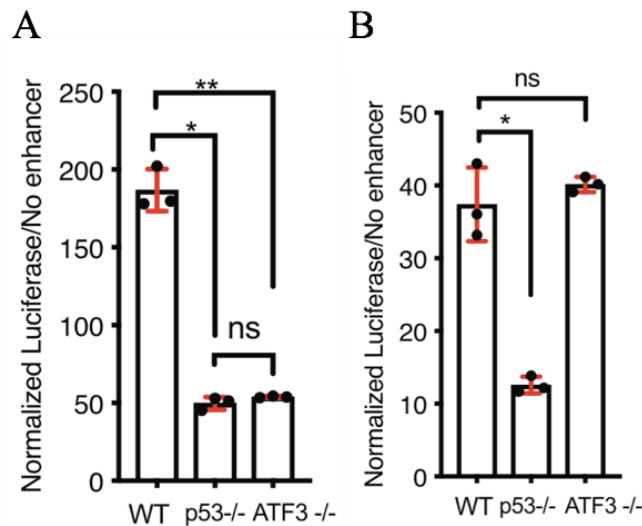


Figure 52: GDF15's 3' enhancer is dependent on ATF3 but not the 5' enhancer

Normalized Luciferase activity (relative to minimal promoter only) of the GDF15 E1 enhancer (**A**) or the GDF15 E2 enhancer (**B**) in wild-type, p53^{-/-} or ATF3^{-/-} HCT116 colon carcinoma cells (* $P < 0.05$, ** $P < 0.01$, one-way ANOVA).

Using a luciferase reporter approach, we assessed the activity of the GDF15 E1 enhancer in wild-type, p53-deficient, or ATF3-deficient HCT116 cells. Loss of either p53 or ATF3 leads to a substantial reduction of E1 enhancer activity (Figure 52A). As expected by the lack of binding *in*

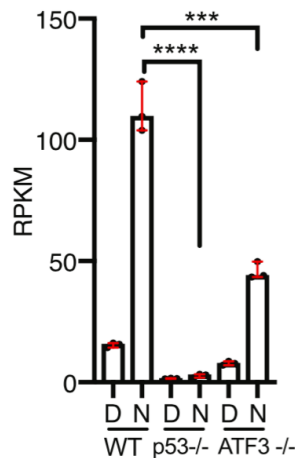


Figure 53: RNA-seq analysis confirms ATF3 protein expression is required for GDF15 mRNA production

Reads per kilobase per million (RPKM) expression value of GDF15 mRNA from three replicates of polyA+ RNAseq of wild-type, p53-/- or ATF3-/- HCT116 treated for 6 h with either DMSO or 5 μ M Nutlin-3A (***(P < 0.001, **** P < 0.0001, one-way ANOVA).

vivo, the activity of the GDF15 E2 enhancer was unaffected by the loss of ATF3, whereas it is strongly dependent on p53 for activity (Figure 52A, B). Interestingly, although GDF15 E2 contains multiple AP-1 family motifs, it is not bound by or regulated by AP-1 member ATF3.

Expression of endogenous GDF15 mRNA as determined by polyA+ RNAseq is reduced in either p53 or ATF3-deficient HCT116 cells consistent with *in vivo* binding and activity of ATF3 at the GDF15 E1 enhancer (Figure 53). Taken together, our data indicate combinatorial activity of both p53 and ATF3 is required for activity of the GDF15 E1 enhancer and that both the E1 and E2 enhancer directly regulate expression of *GDF15*.

Discussion

A number of high throughput analyses of p53 genomic occupancy revealed that p53 predominantly binds to *cis*-regulatory regions (CRE) like enhancers and promoters. The ability of p53 to activate transcription is well established, however, specific molecular mechanisms underlying p53 activity at CRE are less well studied. Here, we describe the use of a massively parallel reporter assay (MPRA) to characterize the effect of local sequence variation and transcription factor motifs on p53-dependent CRE activity. Our results support the canonical model of p53 activity where p53 primarily functions as a strong transcriptional activator at *cis*-regulatory elements (CRE) (Martin Fischer et al., 2014). Further, we confirmed that the p53 response element (p53RE) is a strong predictor of p53-dependent transcriptional regulation as has been observed across multiple experimental systems (El-Deiry et al., 1992; Verfaillie et al., 2016; Younger & Rinn, 2017). We then examined the contribution of local sequence context on enhancer activity by systematically altering sequences flanking the p53RE. Our results indicate that sequences outside of the core p53 binding site are required for optimal transcriptional activation. These functional sequences include both putative and confirmed transcription factor binding motifs, suggesting that p53 requires additional DNA-bound factors for its ability to activate transcription through CREs.

Two recent MPRA studies proposed a novel “single-factor” model for CRE regulation by p53 (Verfaillie et al., 2016; Younger & Rinn, 2017). In this model, p53 is solely responsible for transcriptional output of an individual p53-bound CRE and does not require other transcription factors. Our data suggest that loss of p53 through either genetic depletion or through alteration of a p53RE sequence severely diminishes p53-dependent CRE activity. Therefore, our data support the necessity of p53 for stimulus-dependent activation of p53-bound enhancers in

agreement with the single-factor model (Verfaillie et al., 2016; Younger & Rinn, 2017). Conversely, our results also demonstrate that additional transcription factors can co-regulate p53-dependent CRE activity. Our screening approach identified numerous motifs that positively or negatively affect CRE activity in a context-dependent manner, including those directly bound by other transcription factors. ATF3 binding to the GDF15 E1 enhancer is required for p53-dependent CRE activity and endogenous GDF15 mRNA expression. Additionally, a CRE regulating *CCNG1* transcription requires both a p53RE and an adjacent SP1/KLF family motif for activity. Loss of either motif diminishes native *CCNG1* transcription driven by the CRE. p53 occupancy at the *CCNG1* enhancer is reduced when sequences flanking the p53RE diverge from the wild type sequence as observed in our *in vivo* ChIP experiments. *In vitro* EMSA experiments suggest that only variation in the 3' adjacent sequence, which contains the SP1/KLF motif, alters p53 binding affinity. Similarly, only mutations within the SP1/KLF motif affected endogenous *CCNG1* mRNA levels. CRE activity is reduced when evolutionarily conserved residues in the SP1/KLF motif are altered in both wild type and p53-deficient cells. These data suggest the *CCNG1* CRE requires both p53 and an additional factor bound to the SP1/KLF family motif for optimal activity.

The requirement for other transcription factors in the co-regulation of p53-dependent transcriptional activity at CREs has not been characterized on a broad scale. Certainly, individual p53 CREs have been previously demonstrated to require co-regulatory factors in reporter assays, including the requirement for the p53RE and an AP-1 element bound by JunD for DNA damage-dependent activation of *GADD45A* transcription (Daino et al., 2006), amongst others. A recent *in vivo* CRISPR/Cas9-screening approach identified CEBPbeta binding within a p53-dependent CRE required for optimal transcription of *CDKN1A* and initiation of senescence (Korkmaz et al., 2016).

Single nucleotide polymorphisms associated with lung cancer risk found within a p53-regulated CRE disrupt canonical transcription factor motifs, reduce p53 binding, and alter expression of *TNFRSF19* (Shao et al., 2019). In this study, we identified both ATF3 and a likely member of the SP1/KLF family as co-regulatory transcription factors required for p53-dependent CRE activity. Of note, we have not identified specific transcription factors that bind to the *CCNG1* or *TP53TG1* CREs whose p53-dependent activity is altered upon variation in flanking sequence. In the case of *CCNG1*, the SP1/KLF family motif can be bound by over 12 family members, most of which are expressed in the cell type (HCT116 colon carcinoma) used in this study. Identification of specific transcription factors binding to individual DNA elements is often challenging, but updated approaches like the enhanced yeast 1-hybrid or quantitative mass spectrometry methods are now possible (Fuxman Bass et al., 2015; Reece-Hoyes et al., 2011). Importantly, we cannot rule out potential transcription factor-independent roles for these motifs in regulating p53-dependent CRE activity, such as the possibility that DNA shape or nucleosome positioning changes *in vivo* might be affected by changes in CRE sequence.

MPRAs are powerful tools for rapidly dissecting how sequence variation and context contributes to the activity of CREs. Despite their power, specific assay design choices and the non-native genomic context of the MPRA approach might help to explain some of the discrepancies between our work and previous reports (Verfaillie et al., 2016; Younger & Rinn, 2017). First, we used a random, lentiviral-based genomic integration strategy to deliver our MPRA constructs, whereas previous p53-based approaches have used transient, plasmid-based delivery (Verfaillie et al., 2016; Younger & Rinn, 2017). Genomic integration presumably allows for the greater influence of chromatin and higher-order genomic structure which directly influence transcription factor binding

and activity (Inoue et al., 2017). In direct comparison with episomal DNA, the activity of integrated massively parallel reporter constructs was more reproducible and more closely aligned with expected activity based on CRE-associated biochemical patterns like histone modification and accessible chromatin in previous MPRA analyses (Inoue et al., 2017). Second, our assay was specifically designed to test the effect of sequence variation on p53-dependent CRE activity while *post hoc* computational approaches were previously used to identify sequence features defining CRE activity. In both the primary MPRA screen and in traditional plasmid-based enhancer assays, we observed that variation in transcription factor motif sequences flanking the p53RE could alter CRE activity. Altering p53RE-adjacent TF motif sequences did not always alter CRE activity, suggesting sequence and context-dependent effects. Our MPRA approach was limited to assaying the activity of short segments (100bp) of p53-bound CREs during the early phase of p53 activity and in only one cell type. Given that CREs regulate transcription in space and time, in addition to abundance, additional cell types and contexts may ultimately reveal additional TF requirements for p53-bound CREs. Further, CREs are typically larger than 100bp in length suggesting additional transcription factors are likely involved in their regulation that were not directly tested in this study.

Our data suggest that p53 activity at CREs often requires additional transcription factors. However, we cannot rule out that the recently proposed single factor model explains p53 activity at other locations, such as at the hundreds of p53 binding sites that lack evidence of CRE-associated histone modifications or features like eRNA transcription (Azofeifa et al., 2018; Sammons et al., 2015; Younger & Rinn, 2017). The most likely scenario is that p53-bound CREs exist in a spectrum and have variable co-factor requirements, such that both the single factor and multi-factor model

underlie the activity of different sets of p53-bound CREs. Ultimately, additional work is needed to dissect the specific motif features, transcription factor requirements, and context-dependence of p53-bound CREs and how they function to enact the broad tumor suppressor activity of p53.

Previous reports could not identify sequence-based features beyond the p53RE that predicted p53-bound CRE activity using machine learning and traditional motif enrichment approaches (Verfaillie et al., 2016; Younger & Rinn, 2017). While accurate to say that there are no other transcription factor motifs or sequence-features that are as enriched as the p53RE (Supplemental Tables 6-7 from Catizone et. al. 2020), we find that other transcription factor motifs are well represented in the CREs we studied and within a previously identified core set of p53-bound CREs (Supplemental Tables 6-7 from Catizone et. al. 2020). This includes overrepresentation of the motif for the stress-dependent transcription factor ATF3 (Supplemental Table 6 from Catizone et. al. 2020), which binds to a number of p53-dependent CREs and regulates activity of a CRE for *GDF15*. ATF3 is a well-studied regulator of p53-dependent transcription through control of p53 stability and co-factor recruitment (Cui et al., 2016, p. 3; Taketani et al., 2012, p. 3; Zhao et al., 2016, p. 3). Previous reports clearly demonstrate that ATF3 can directly alter p53 stability and modulate p53 activity through interactions with histone modifying enzymes (Cui et al., 2016, p. 3; Taketani et al., 2012, p. 3; Yan et al., 2005). Our work uniquely identifies a direct role for ATF3 DNA binding within a p53-bound CRE and demonstrates a positive effect on p53-dependent transcriptional activity. Given that ATF3 binds to numerous p53-bound regions of the genome (Zhao et al., 2016, p. 3) and their previously reported relationship, further examination into the local interplay between p53 and ATF3 at DNA is warranted.

p53 is a pioneer transcription factor and can mediate context-dependent chromatin remodeling at CREs (Karsli Uzunbas et al., 2019; Sammons et al., 2015; Younger & Rinn, 2017). Despite this activity, the large majority of p53 genomic binding events occur within regions that are accessible before p53 engagement (Karsli Uzunbas et al., 2019; Sammons et al., 2015; Su et al., 2015; Younger & Rinn, 2017), similar to what is observed for glucocorticoid receptor binding (McDowell et al., 2018). These regions also contain chromatin modifications associated with active CRE, including H3K27ac and H3K4me1/2 before p53 binding (Andrysiak et al., 2017; Karsli Uzunbas et al., 2019; Sammons et al., 2015; Su et al., 2015; Younger et al., 2015, 2015). Further, p53 depletion does not alter basal CRE-associated chromatin modifications or chromatin structure at the large majority of CRE (Karsli Uzunbas et al., 2019; Sammons et al., 2015) suggesting that other transcription factors mediate chromatin accessibility at most p53-bound CREs. Consistent with this model, we observe enrichment of enhancer-associated histone modifications H3K27ac and H3K4me2 at GDF15 E1 and E2 enhancers in the absence of p53. Enhancer-derived RNA (eRNA) has also been identified as a strong predictor of transcription factor binding and CRE activity (Azofeifa et al., 2018). Our data suggest that those CREs with eRNA transcription are more likely to be bound by p53 and are more likely to see p53-dependent gains in enhancer activity. In further support of a multi-factor model, eRNA are transcribed from p53-regulated CREs in the absence of p53 (Allen et al., 2014; Sammons et al., 2015) suggesting other transcription factors are bound and active as previously suggested (Azofeifa et al., 2018). These data suggest that other factors are likely responsible for establishing and maintaining chromatin structure and basal activity at the majority of p53-bound CREs. Recent reports suggest that p53 binding and activity is strongly influenced by cell type-specific chromatin accessibility (Allen et al., 2014; Andrysiak et al., 2017; Karsli Uzunbas et al., 2019), which itself is controlled by differential DNA binding

transcription factor activity (Reiter et al., 2017; Shlyueva et al., 2014; Spitz & Furlong, 2012; Zaret & Carroll, 2011; Zaret & Mango, 2016). Indeed, we recently identified p63, a p53 family member, as a factor required for chromatin accessibility and activity of certain p53-bound enhancers in epithelial cell types (Karsli Uzunbas et al., 2019). How p53 functions across various cell and tissue contexts is still a vital and open question, but recent reports suggested that p53 binding and activity can be influenced by cell type suggest significant work remains to address the broad scope of p53-dependent transcription (Allen et al., 2014; Karsli Uzunbas et al., 2019; Nguyen et al., 2018).

We propose that the lack of a core set of commonly enriched transcription factors within p53-dependent CREs is a potentially important regulatory feature of the p53 network. By utilizing different sets of transcription factor co-regulators, we hypothesize that global p53 transcriptional activity is buffered against loss of any one regulatory partner. This hypothesis for p53 is strongly reminiscent of the “billboard” model seen at many *Drosophila* developmental enhancers (Kulkarni & Arnosti, 2003; Spitz & Furlong, 2012), whereby different combinations of factors can bind to a CRE and produce similar transcriptional outputs. The flexible billboard model for p53-bound enhancers is also consistent with a recently proposed “distributed p53 network” model whereby p53 transcriptionally controls many genes, but that any one p53 target gene is dispensable for tumor suppression (Andrysk et al., 2017).

CHAPTER 4: p63 and p53 co-regulate transcriptional activity at enhancers

Introduction

Gene paralogs normally result from gene duplication events. Over evolutionary timescales, paralogs can develop novel functions or might become inactive through accumulation of loss of function mutations (Joerger et al., 2009). Generally, only paralogs that are beneficial to the organisms persist throughout evolution. In the case of transcription factors (TF), paralogs can utilize pre-established regulatory region networks by recognizing similar DNA consensus sequences (Belyi et al., 2010)(Gonfloni et al., 2015). They can also bind to sub-optimal or novel DNA sequences that the ancestral protein could not previously bind due to acquired mutations over time. TF paralogs can also act in competition with the ancestral protein for the same binding loci, such that they can positively or negatively regulate each other (Shen et al., 2018). Changes in regulation of paralogs can result in differential activation or expression resulting in varied expression patterns across tissues. Further, sequence divergence means paralogs can ultimately interact with and be regulated by different cofactors ultimately leading to differential activity (Shen et al., 2018). How paralogs interact, cooperate, compete, and are regulated within an organism is a key open question, with specific for the p53 family of transcription factors.

Invertebrates, like sea anemones and Drosophilids, contain a p53 “like” protein that closely resembles the p53 family member, p63 (Lion et al., 2015)(Chillemi et al., 2017). This ancestral p53 “like” protein gives rise to modern, vertebrate p53 with its tumor suppressor functions (Biscotti et al., 2019). However, its structure and domains more closely resemble p63/p73 suggesting that these paralogs might have existed far back in evolution, and that the tumor suppressor role of modern p53 gained new functions over time (Chillemi et al., 2017). The vertebrate p63 maintains some tumor suppressor function through its isoform Tap63 that is

activated upon DNA damage. However, p63's main role lies in maintaining the identity of epithelial cell types (Soares & Zhou, 2017)(Carroll et al., 2006). While p53 is expressed in all cells and is stimulus dependent, p63 is exclusively expressed in epithelial cells. The deltaNp63 isoform is constitutively active in these cells. Loss of p63 in mice results in severe limb and skin abnormalities (A. Yang et al., 1999)(Yoh et al., 2016). Loss of p53 in mice, as well as humans, allows for normal development and viable organisms; however, animals lacking p53 are increasingly more susceptible to tumor formation as they age (Yoh et al., 2016). p53 and p63 bind to highly similar DNA elements. In most cases, this is not an issue as p63 is restricted to just one lineage (Annie Yang et al., 2006). p63 and p53 can bind at the same DNA locations in epithelial cells, except where p63 optimal/p53 sub-optimal consensus sequences are found. Some locations that can be bound by either p53 or p63, p63 appears necessary for p53 binding. Depletion of p63 prevents binding of p53 at numerous locations, likely through alterations in chromatin structure. This suggests that p53 and p63 collaborate at particular locations in the genome (Karsli Uzunbas et al., 2019). Conversely, depletion of p63 can also lead to an increase in p53 binding and activity at another subset of binding sites, suggesting p63 can also act antagonistically to p53. p53 therefore loses access to regulatory regions to drive gene expression (Flores et al., 2002).

We previously developed a massively parallel reporter assay (MPRA) to study p53 activity at enhancer elements in a non-epithelial cell type HCT116 colorectal cancer cells (Chapter 2, (Catizone et al., 2020). We used this tool to examine the role of p63 at both p53 and p63-bound enhancers in an epithelial cell type. Our study focused on the differences between “p63- only” bound enhancers and enhancers that are bound by both p53 and p63 in a native p63 cell type mammary epithelial cells (MCF10a). We chose these cells for their ability to withstand p63 knockdown without dying or total loss of epithelial identity. We determined that enhancers bound

by both paralogs, were affected by the loss of both p53 and p63, as well as the p53 family motif. p63-bound enhancers were only affected by the loss of p63 and transcriptional activity was uninhibited by p53 knockdown. This suggested that both p53 and p63 might be influencing the same regulatory regions (Karsli Uzunbas et al., 2019). After dissecting these enhancers, we addressed the question of whether p63 alone was sufficient to drive the activity of these regulatory regions. We found that similar to its paralog, p53, p63 requires the presence and activity of local transcription factors and lineage specific proteins. We also find that p53 dependent enhancers rely on p63's activity in native epithelial cells but not in non-epithelial cell types. This raises the question of how p63 and p53 may regulate each other at enhancer and promoter regions. We are just beginning to elucidate how the p53 family of transcription factors may both positively and negatively regulate each other when present in the same cell type.

Results

Execution of an MPRA for enhancer activity in MCF10a cells lines

The 296 putative p53 binding locations from the original HCT116 experiment (Chapter 2) were K-means clustered into 3 groups: cluster 1, 2 and 3. The 20bp p53/p63 family motif was centered in a 100bp region. 32 out of 296 regions were bound strongly by p53 (cluster 1), 136 out of 296 were moderately bound by p53 (cluster 3), and 128 out of 296 showed little or no binding of p53 (cluster 2) in HCT116. This pattern was consistent for p53 in MCF10a cells. p63 was found strongly bound in clusters 1 and 2 and moderately bound in cluster 3 (Figure 54). All clusters

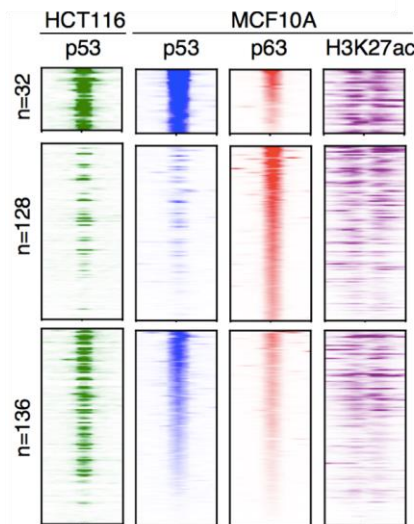


Figure 54: Motif containing enhancers have varied p53 and p63 occupancy in vivo

Heatmaps are split into three clusters: p53 strongly bound/p63 bound (top), p63 only bound (middle), and p53/p63 bound moderately bound enhancers (bottom). Heatmap of p53 ChIP-seq enrichment from Nutlin-3A-treated HCT116 colon carcinoma cell lines for regions found in the MPRA pool (left). Heatmap of p53 ChIP-seq from Nutlin 3A treatment and p63-ChIP-seq from untreated MCF10a mammary epithelial cells (next right). Heatmap of H3K27ac ChIP-seq in untreated MCF10a cells (far right).

show enrichment of canonical enhancer-associated histone modifications H3K27ac in MCF10A both in p53 bound and p63 bound regions. The average position weight matrices are highly similar in composition (Figure 55A), however, all three clusters score higher as an optimal p63 consensus

motifs (Figure 55B). These data suggest that CREs present in MCF10A that bind p63 show DNA accessibility and have chromatin modifications associated with transcription.

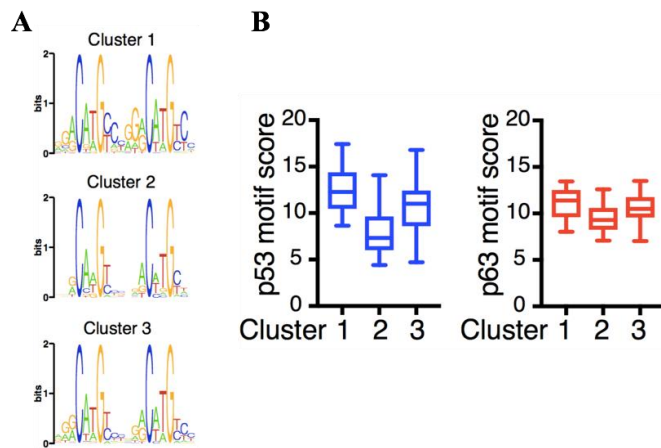


Figure 55: p53RE motifs within the three clusters have differently scored binding sites

(A) DNA sequence weight motifs for cluster 1 (top), cluster 2 (middle), and cluster 3 (bottom) regions from the MPRA pool. (B) Box plots of scores from p53scan depicting the adherence to a canonical p53 family motif sequence for Clusters 1, 2, and 3 (left) and box plots of scores from p63scan depicting the adherence to a canonical p53 family motif sequence for Clusters 1, 2, and 3 (right).

We then performed duplicate biological measurements of p53-dependent enhancer activity in MCF10A wildtype cells using our MPRA approach. MPRA-transduced cells were treated for 6 hours with DMSO or 5 μ M Nutlin-3A and expressed RNA barcodes were sequenced as described in Chapter 2 and in Materials and Methods. Nutlin 3A strongly increases enhancer activity of

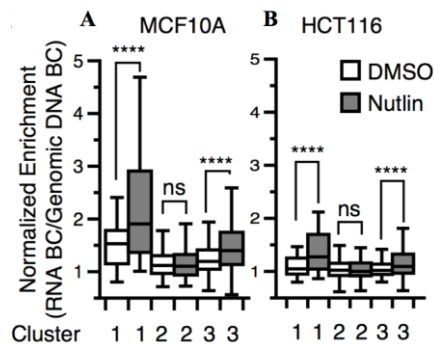


Figure 56: Cluster 2 enhancers bound only by p63 do not respond to Nutlin 3A treatment

Normalized transcriptional activity of clusters 1, 2 and 3 from the MPRA assay after 6 h of either DMSO or 5 μ M Nutlin-3A treatment. Data are depicted as enrichment of the 3'UTR-encoded barcode linked to each putative regulatory region normalized to the enrichment of that same sequence integrated into the genome and represent the averages from three biological replicates of each condition (HCT116) and two biological replicates (MCF10A) (****P < 0.0001 by one-way ANOVA). (A) MCF10a cells (B) HCT116 p53 +/+ cells

cluster 1 in MCF10A cells (Figure 56A) which is comparable to what we have seen previously in HCT116 (Figure 56B).

Importantly, enhancer activity trends across the three clusters is conserved across cell types. Cluster 1 has the most robust response to Nutlin 3A treatment, cluster 3 has the next most response, and cluster 2 has no response to Nutlin 3A treatment (Figure 56A-B, **** p<0.0001, one way ANOVA). As expected from our analysis of p53 occupancy, p53-bound enhancers have the strongest response to Nutlin 3A treatment over p63 bound enhancers. These data suggest that only enhancers bound by p53 will be affected by Nutlin 3A treatment and p63 bound enhancers maintain activity regardless of treatment or increased p53 protein levels.

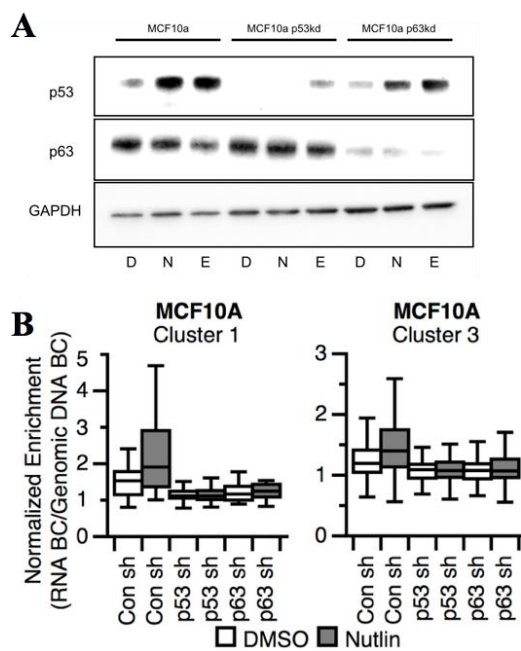


Figure 57: Enhancer activity was significantly reduced compared to expression in wildtype cells

(A) Immunoblotting for p53 (top), p63 (middle), or GAPDH (bottom) expression in MCF10a con sh, p53 sh, or p63 after 6 hours of treatment with DMSO (D), 5 μ M Nutlin-3A (N) or 100 μ M etoposide (E). (B) Normalized transcriptional activity of MCF10a con sh, p53 sh, or p63 sh after 6 hours of treatment with DMSO (white) or 5 μ M Nutlin-3A (grey). Data are depicted as enrichment of the 3'UTR-encoded barcode linked to each putative regulatory region normalized to the enrichment of that same sequence integrated into the genome and represent the averages from two biological replicates of each condition

p53-enhancers require direct-interaction of p53 and p63-bound require direct-interaction of p63

In order to determine if enhancer activity was dependent on either p53 or p63 protein expression, we assessed their transcriptional outputs in MCF10A control short hairpin (sh), p53sh, and p63sh cells (Karsli Uzunbas et al., 2019)(Figure 57A). Nutlin-3A-induced activity of clusters with the most p53 occupancy (clusters 1 and 3) were diminished in MCF10Ap p53sh cell lines cells suggesting enhancers depend on p53 protein presence. Interestingly, activity of enhancers in the p63sh cell lines was also reduced suggesting that the binding of p63 may influence some of the overall enhancer activity (Fig. 57A-B). To test whether enhancer activity is direct or indirectly dependent on p53 or p63, we compared the original enhancer sequences to those with either the p53/p63 family motif (Mid) or the entire enhancer sequence (Scr) mutated (Figure 58A).

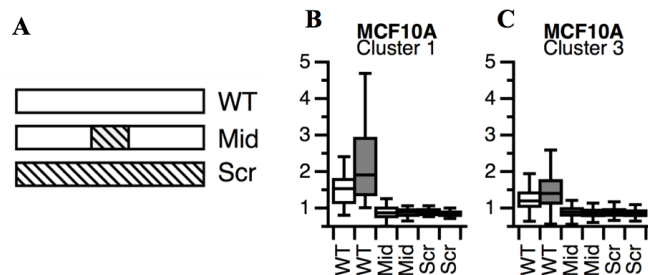


Figure 58: Loss of the p53RE disrupted enhancer activity in MCF10a cells

(A) Sequences within the wild-type clusters 1 and 3 from the MPRA were shuffled (while preserving GC content) to alter either the 20 bp p53 binding site (Mid) or the entire 100 bp MPRA sequence. (B) Normalized transcriptional activity of cluster 1 and 3 for the wild-type (WT), p53-binding site scramble (Mid), or the full scramble (Scr) regions in MCF10a control sh cells after a 6-h treatment of either DMSO or 5 μ M Nutlin-3A. Data are depicted as enrichment of the 3'UTR-encoded barcode linked to each putative regulatory region normalized to the enrichment of that same sequence integrated into the genome and represent the averages from three biological replicates of each condition.

In clusters 1 and 3, loss of the p53/p63 family motif or the entire sequence composition (Scr) depleted enhancer activity (Figure 58B-C). These data suggest that Nutlin3A and basal

enhancer activity in MCF10A requires direct binding of p53 or p63. Cluster 2 enhancers (strong p63 and little to no p53 occupancy) are unaffected by the loss of p53 (Figure 59A) suggesting that p53 does not bind this set of enhancers. However, loss of p63 does reduce enhancer activity, regardless of cell or treatment (Figure 59A). Loss of the p53/p63 family motif or fully mutating the enhancer (Scr) decreases enhancer activity (Figure 59B), suggesting the presence and binding of p63 protein is required for cluster 2 enhancers. However, p53 is not required.

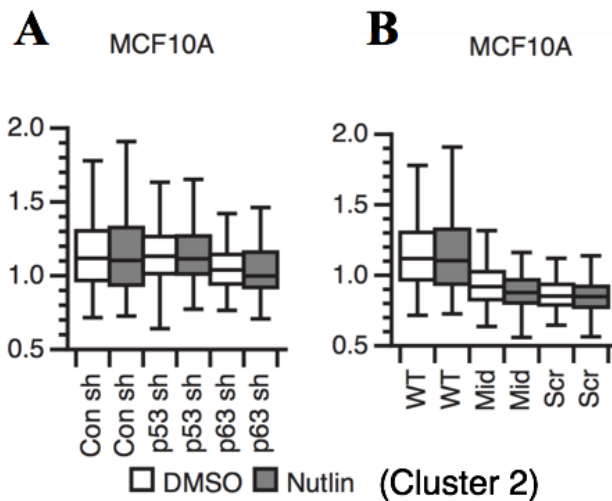


Figure 59: Loss of p63 but not p53 affects cluster 2 enhancers

(A) Normalized transcriptional activity cluster 2 enhancers in MCF10a con sh, p53 sh, or p63 sh after 6 hours of treatment with DMSO (white) or 5 μ M Nutlin-3A (grey). Data are depicted as enrichment of the 3'UTR-encoded barcode linked to each putative regulatory region normalized to the enrichment of that same sequence integrated into the genome and represent the averages from two biological replicates of each condition. (B) Normalized transcriptional activity of cluster 2 enhancers for the wild-type (WT), p53-binding site scramble (Mid), or the full scramble (Scr) regions in MCF10a control sh cells after a 6-h treatment of either DMSO or 5 μ M Nutlin-3A. Data are depicted as enrichment of the 3'UTR-encoded barcode linked to each putative regulatory region normalized to the enrichment of that same sequence integrated into the genome and represent the averages from three biological replicates of each condition.

p63 is required, but not sufficient, to drive p63-mediated enhancer activity in a p63 non-native cell type

We next validated our observation that the absence of p63 protein affected enhancer activity of cluster 2. We sought to validate these MPRA results by utilizing a standard Luciferase

reporter-based assay. Expanding from the 100bp sequence used in the MPRA, we determined the enhancer activity of a sequence encompassing the entire DNase hypersensitivity (DHS) region as

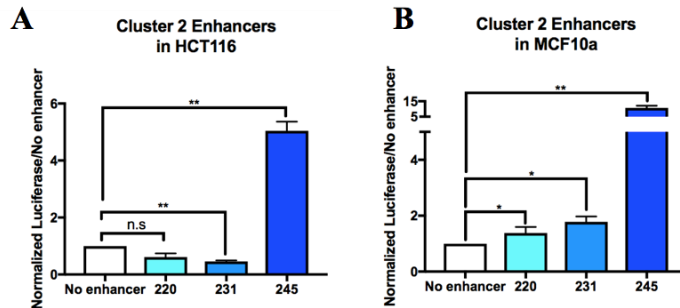


Figure 60: Cluster 2 enhancers are only strongly active in native p63 expressing cells

Normalized Luciferase activity (test sequence Firefly versus constitutive Renilla) of full length DNase hypersensitivity sites for MPRA regions #220, #231, and #241 in (A) HCT116 p53^{+/+} and in (B) MCF10A mammary epithelial cell line (****P < 0.0001 paired t-test).

determined by ENCODE. DHS are putative regulatory regions but may not actually possess enhancer activity in all contexts. We chose enhancers 220, 231, and 245 which were members of cluster 2.

Using the traditional luciferase assay, we measured the activity of cluster 2 enhancers in HCT116 p53^{+/+} and MCF10A control sh cells (Figure 60A-B). Enhancer 245 served as a control because it shows enhancer activity above the “no enhancer” control in both cell types, while 220 and 231 were below the no enhancer control in HCT116 (Figure 60A). When all three enhancers

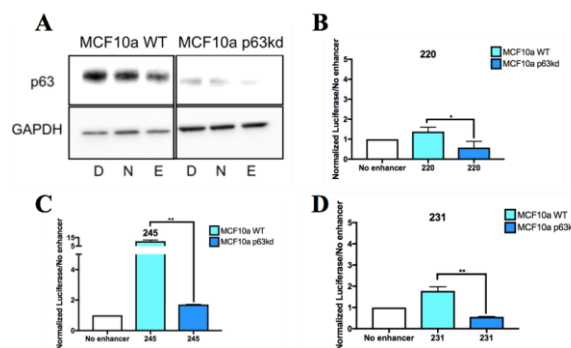


Figure 61: Cluster 2 enhancers have reduced activity in absence of p63 protein

(A) Immunoblotting for p63 (top) or GAPDH (bottom) expression in MCF10a WT and MCF10a p63sh cells after 6 hours of treatment with DMSO (D), 5 μ M Nutlin-3A (N) or 100 μ M etoposide (E). Normalized Luciferase activity (test sequence Firefly versus constitutive Renilla) of full length DNase hypersensitivity sites for MPRA regions #220, #231, and #241 in (A) MCF10a wildtype cells and in (B) MCF10A p63 sh cells (****P < 0.0001 paired t-test).

were expressed in MCF10A control sh cells, they displayed significantly increased activity compared to the no enhancer control suggesting that the presence of p63 or some other cell type-specific factor is responsible for the activation of the region (Figure 60B). Utilizing the same full-length DHS luciferase vectors, we tested enhancer activity in both MCF10A control sh and p63sh cell lines (Figure 61A). Activity of cluster 2 enhancers were significantly reduced upon knock down of p63 protein suggesting that p63 is required for optimal enhancer activity of these regions (Figure 61B-D).

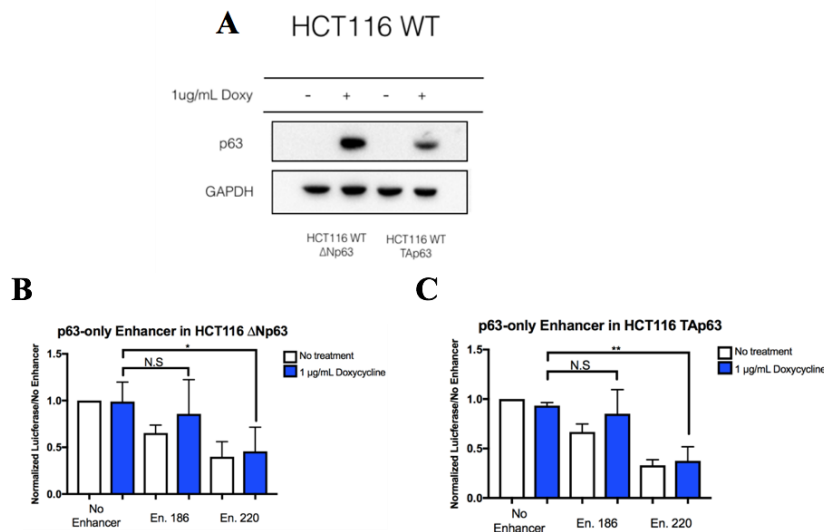


Figure 62: p63 expression is not sufficient to activate cluster 2 enhancers

(A) Immunoblotting for p63 (top) or GAPDH (bottom) expression in HCT116 ΔNp63 and Tap63 expressing cells with tet-on inducible expression treated with either water or 1ug/mL doxycycline. Normalized Luciferase activity (test sequence Firefly versus constitutive Renilla) of full length DNase hypersensitivity sites for MPRA regions #186 and #220 from cluster 2 in (B) HCT116 ΔNp63 and (C) Tap63 expressing cells with tet-on inducible expression treated with either water or 1ug/mL doxycycline. (**P < 0.0001 paired t-test).

Finally, we wanted to investigate whether p63 protein alone was sufficient to influence the activity of these p63 dependent enhancers. HCT116 p53+/+ cells were transduced with a doxycycline inducible version of two p63 isoforms: ΔNp63 and TAp63 (Figure 62A). Upon addition of 1ug/mL doxycycline for 4 hours, both isoforms were highly expressed compared to untreated cells (Figure 62A). Utilizing the same full DHS cluster 2 enhancer luciferase vectors, we measured the overall transcriptional activity after the induction of p63 isoforms. We found that

over expression of either p63 isoform had no significant effect on enhancer activity (Figure 62B-C, **** $P < 0.0001$ paired t-test). This suggests that although p63 is required for enhancer activity in epithelial cells, none of the p63 isoforms are sufficient in a cell not natively expressing p63 to drive transcriptional activity of these regions. Taken together, these data demonstrate that p63-bound enhancers require both p63 and other, as-of-yet unknown co-factors found only in epithelial cell types.

Discussion

Recent studies have shown the p63 both positively and negatively regulates p53 pathways (Karsli Uzunbas et al., 2019). Because their DNA binding domains share 80% similarity, one proposed mechanism of regulation involves direct competition or cooperativity between p53 and p63 at shared regulatory regions(Levrero et al., 2000)(Annie Yang et al., 2006). The exact mechanism by which p63 regulates p53 is still unclear. p63 has more flexibility than p53 in interacting with DNA binding sites and is found at a larger number of locations than p53. This is confirmed by our small sample size of 296 enhancers (Figure 54). p63 binds a higher percentage of the MPRA regions than does p53. As expected from data in Chapter 3, knock down of p53 in MCF10A cells reduced the Nutlin 3A response in p53-bound enhancers. Interestingly, loss of p63 also significantly reduced the activity of these regions (Figure 57B). This observation is in line with recent work suggesting that p63 is required for binding and activity of a subset of p53 binding sites in epithelial cells (Karsli Uzunbas et al., 2019)(Rizzo et al., 2016). Importantly, these same enhancers are perfectly active in HCT116 cell, which lack endogenous expression of p63. These results provide additional evidence that p53 activity is altered in a cell type-

dependent manner and that this is mechanistically may be due to changes in co-factor and transcription factor expression across cell types.

Alternatively, these observations could be due an indirect effect of the loss of p63 from MCF10A cells. Most epithelial cells lines do not tolerate p63 knock down well, and complete loss of p63 in these cell lines can be lethal. It is possible that global transcriptional activity is reduced due to the depletion of p63 and subsequent loss of other p63 controlled gene products(Truong et al., 2006)(Qu et al., 2018). We would need to do parallel studies to test the transcriptional capacity of these p63 knock down cells and due rescue experiments with p63 protein to see if p53-bound enhancer optimal activity was recovered. Further, use of rapid protein depletion approaches, like inducible degron systems, would allow an acute depletion of p63 (Sathyan et al., 2019)(Natsume et al., 2016). This may circumvent any ill effects of long-term p63 depletion and would allow a more in-depth and time resolved analysis of p63 enhancer activity in the absence of the paralog p63.

Independent of p53, p63 bound to a set of enhancers in our MPRA (cluster 2) that were inactive in our previous experiments in HCT116. This led us to believe these represented *bona fide* p63-dependent, p53-independent enhancers. To test whether p63 was both required and sufficient for cluster 2 enhancer activity, we expressed the p63 isoforms ΔNp63 and TAp63 under the control of a doxycycline inducible promoter in cells normally lacking p63. We found that overexpression of either isoform was not sufficient to activate the enhancers via an enhancer luciferase assay. However, the same enhancers were active in the native p63 expressing cell type MCF10A. This suggests that other factors besides p63 may be required for optimal p63-mediated transcription to occur. We see these same trends from our previous study with our MPRA studying p53-mediated activity (Chapter 2). Recently published studies demonstrate some

cooperative factors that are required for p63 to maintain epithelial cell identity, such as KLF4 (Lin-Shiao et al., 2018). Indeed, certain p63-dependent cell fate conversions and chromatin remodeling cascades require both p63 and KLF4 (Lin-Shiao et al., 2019). Future work will examine which factors are required for transcriptional activity of p63-bound enhancers. One approach is to examine p63-bound enhancers activity in non-epithelial cell lines by concurrent expression of other transcription factors along with p63 isoforms. We can also knockdown other potentially cooperating factors in native p63-expressing epithelial cells to determine which may be required for optimal transcriptional activation. Finally, either a more high-resolution MPRA or *in vivo* CRISPR-based screening approach could be designed to identify transcription factors flanking p63 binding sites that are ultimately required for enhancer activity. These data suggest that the p53 family of transcription factors possess both ‘pioneer’ transcription factor activity as well as work in combination with other transcription factors at enhancers. This observation has broad implications into the maintenance of cell identity like in epithelial cells and the process of tumor suppression.

CHAPTER 5: Discussion and Future Directions

p53 was given the nickname “the guardian of the genome” specifically for its role in protecting the organism from the spread of DNA damage and mutations. p53 is able to do this by regulating a large and diverse set of target gene networks whose expression leads to phenotypic outcomes such as apoptosis, cell cycle arrest and senescence. These cell fates after p53 activation are mutually exclusive and it is unclear how these decisions are made within individual cells and within the context of the entire organism. Some mechanisms that have been proposed include differential dosage of p53, stochastic differences in target gene expression, or broad differential p53 binding and gene activation. Each of these can feasibly drive differential gene expression and engagement of various pathway outcomes. For example, HCT116 carcinoma cells were more likely to commit to an apoptosis fate if they reached a threshold of p53 protein levels by a certain time point after exposure to p53 activators (Paek et al., 2016). If cells failed to reach this p53 threshold, cells stayed in a state of cell cycle arrest (Paek et al., 2016). This would suggest that the amount of p53 present in the cell may determine the downstream response. Other data suggested that the mechanism of p53 activation could alter p53 protein expression kinetics, and that how p53 expression levels reached their threshold was as important as whether the threshold was met. For example, exposure to a single dose of gamma irradiation leads to pulsatile p53 expression levels while UV irradiation leads to a prolonged and consistent amount of p53 expression (Purvis et al., 2012). Further, recent work suggested that pulsatile activation of p53 altered the specificity of target gene activation relative to sustained p53 activation without altering DNA binding (Hafner et al., 2017).

We investigated these questions using a different approach and by investigating an alternative hypothesis. We hypothesized that activation of p53 by different means altered gene expression patterns due to inherent differences in chromatin structure and activity due to the method used to activate p53. So, we asked if p53 activity was different between two common activators, Nutlin 3A (non-genotoxic) and Etoposide (genotoxic). We found that locations where p53 was bound and the chromatin landscapes were highly similar between both treatment conditions. We also showed that RNA polymerase II enrichment and general accessibility at these p53-bound regions were nearly identical. However, when we looked at differential gene expression, we found a number of etoposide-specific genes. Upon further investigation, we found that these genes were p53-independent and under the control of a different transcription factor, NF- κ B. The majority of these etoposide-specific genes are involved in inflammatory and immune responses, which may have roles in altering the fate of cells exposed to etoposide relative to Nutlin 3A. Many of these genes are considered part of the SASP cascade of extracellular ligands that support senescence and tumor suppression (Coppé et al., 2008, 2010). These data suggest that different types of cellular insults or chemotherapeutics may turn on multiple, parallel stress pathways governed by multiple stress dependent transcription factors.

The results of this chapter have multiple implications for the use of chemotherapeutics and other small molecule in the treatment of cancer. The MDM2 inhibitor Nutlin 3A was viewed as a potential breakthrough cancer therapy due to its ability to activate p53 without first causing DNA damage (Vassilev et al. 2004). This initial promise turned out to be more complicated than initially thought, with cancer lines and tumors often gaining resistance to Nutlin 3A through induction of mutations in MDM2 (Khoo et al., 2014; Wei et al., 2013). Our results suggest

Nutlin 3A fails to engage a DNA damage-dependent inflammatory axis controlled by NF- κ B. This pathway is activated by etoposide and other DNA damage-inducing chemotherapies in a p53-independent manner. Combination drug therapies including Nutlin 3A (and its clinical derivatives) and other agents may increase success rate for reaching remission in certain types of cancers (Kocik et al., 2019).

Understanding parallel stress pathways is certainly important to understand their effect on cell and organismal phenotypes. Further, understanding that cell signaling does not exist in an isolated manner is an important future direction for studying p53-mediated pathways. It is possible that different activation methods of p53 result in differential regulation of proteins and RNA that interact with the p53 pathway and its downstream targets. For example, differences in DNA repair and the activation of the DNA damage-response kinase ATM can alter p53-dependent cell fates (Stewart-Ornstein and Lahav, 2017). We investigated whether differential activation might alter p53's interaction with DNA and chromatin. Our results suggested that within the same cell type, the activation method has little to no effect on p53's ability to bind to its DNA targets and activate gene expression. Our data, though, were focused on an acute phase of p53 activation and future experiments can examine whether differential p53 activity at different timepoints results from varied p53 activation methods. Different insults like UV damage, pollutions, chemicals, and nutrient deprivation may induce parallel pathways that directly affect p53-mediated transcription at regulatory regions. Additional work is still required to unravel the role of activation method and parallel activated pathways on p53-dependent cell fates.

While our work indicates that p53 genomic occupancy is conserved within one cell type, recent evidence suggested that p53 activity varies dramatically across cell types (Hafner et al., 2020; Karsli Uzunbas et al., 2019). These results open up an entire new area of p53 biology, in that mechanisms beyond p53 oscillations and protein expression might explain p53-dependent gene expression and cell fates. These studies, much like our initial observations about p53 occupancy in response to differential activation methods, suggest that the local chromatin environment plays a massive role in p53-dependent activities and cell fates. Differential chromatin structure is likely controlled by other cell type-specific transcription factors that may bind and cooperate with p53 at regulatory regions, like promoters and enhancers. Through this hypothesis, we decided to investigate the mechanisms that regulate and occur at p53 bound regulatory regions.

p53 activity at promoters has been rigorously studied over the years. However, in the past 5 years, we have learned that p53 primarily binds to distal enhancer elements. The influence of this binding on target gene activation is relatively understudied, as are the specific mechanisms in action at enhancers. In order to study the mechanisms that occur at p53 enhancers we chose to utilize a high throughput reporter assay to study hundreds of p53 enhancers in parallel. By mutating flanking regions outside the p53RE, we were able to successfully disrupt other TF binding sites and measure their effect on p53-mediated transcription. Combinatorial activity of p53 and other transcription factors at enhancers had not been previously tested. We found a number of highly conserved and primate-emergent transcription factor binding sites that directly affected the transcriptional output of the p53-bound regions. These data form the basis for future studies into p53-mediated regulation through enhancer and promoter elements. Loss of a single factor, through mutation to its binding site or loss of expression, can completely diminish p53-

dependent activation of enhancer elements and seriously reduce target gene expression. This has direct implications in cancer biology. First, we can now examine cancer cell lines for DNA variation at p53 binding sites. Second, we can examine whether known DNA-binding cofactors of p53 have altered expression patterns. Both of these approaches have the potential to reveal how tumorigenesis occurs in the presence of genetically wild type p53, providing significant insight into at least 50% of cancers.

Two common transcription factor families (AP-1 and SP1/KLF) were involved in regulation of multiple p53-bound enhancer. From the AP-1 family, we were able to confirm that ATF3, a stress transcription factor, and p53 both bound a region upstream of the metabolic factor *GDF15*. Loss of either protein via RNA-seq significantly reduced *GDF15* levels in the cell. ATF3 is a stress transcription factor that is regulated by p53, however, it responds to many types of p53 independent cellular stress like viral infection. It is possible that the presence of varied locally acting transcription factors influences downstream target expression through these distal enhancers can produce different p53 pathway outputs (i.e. apoptosis vs senescence). The cofactors that work with p53 at these enhancers may be products of parallel stress pathways, so in turn, the type of stress produces cooperative factors that influence p53-mediated gene expression. p53 seems to have the flexibility to work with a number of different cofactors at enhancers. Through our analysis, we did not find a single enriched binding partner or family that was specific to p53. This makes evolutionary sense because the more binding partners p53 has the more protection the p53 pathways has from loss of function due to protein mutations. This could allow for redundancy in certain pathways or allow independent pathways to function downstream of p53 activation.

Due to p53's influence in cellular reprogramming and identity (Chang et al., 2011; Karsli Uzunbas et al., 2019), we decided to investigate the idea that cofactors influencing p53 activity may be cell type specific. The p53 family member, p63, is an epithelial specific lineage factor and has strong pioneer factor activities (Kouwenhoven et al., 2015; Li et al., 2019; Lin-Shiao et al., 2019; Pattison et al., 2018). Previous studies have eluded to p63 and p53 both positively and negatively regulating each other (Karsli Uzunbas et al., 2019; McDade et al., 2014). We utilized the same MPRA strategy from Chapter 2 but performed the assay in the p63-positive mammary epithelial cell type MCF10A. We also performed this study in p53 and p63 knockdown cell lines. We found interestingly that p53 dependent enhancer activity was affected by the loss of both p63 and p53, confirming that cofactors bound at p53 enhancers are required for activity. These results are consistent with other work suggesting that p63 can positively regulate p53 activity through control of chromatin structure and enhancer activity (Karsli Uzunbas et al., 2019). A number of important questions still remain, though. One such question is how differences in cell type and cofactor availability alter p53-dependent enhancers. p63 is not present in the large majority of cell types and is not necessary for activity of the same regulatory regions in those other cells. What, then, is the mechanism for the requirement in one cell type but not in another? We anticipate that other DNA-bound cofactors are present in non-p63-expressing cell types that serve the same function as p63 in epithelial cell types. A more detailed genetic and biochemical dissection of the roles of p63 and these other cofactors is highly warranted, including high-resolution analysis of DNA sequence requirements for p53-bound enhancer function. The development of locus-specific proteomic should also be able to directly answer these questions

as well (Gao et al., 2018, 2019; Korthout et al., 2018), although they are still in their infancy or only applicable to model organisms.

Our data confirmed that p63 was required for the activity of its bound enhancers. Interestingly, p63 is not sufficient to drive enhancer activity in a non-native cell type, with over expression of either of the two N-terminal p63 isoforms in HCT116 colon carcinoma cells did not activate enhancer function at all. However, these same enhancers work well in the native epithelial cell line MCF10A. These data suggest that p63, despite its pioneer factor activity, still requires epithelial specific factors to drive transcription through enhancers. These results would that the p53 family of transcription factors has both “pioneer activity” as well as combinatorial activity like we see in enhanceosome and billboard enhancer models. This has direct and clear implications for fields studying p53 and p63 biology. We need to gain a better understanding of how these proteins work independently, work together, or work with other as-of-yet unknown cofactors. The ultimate goal being how this complex interplay regulates gene expression in different disease and cell states. Overall, the p53 family of transcription factors has control over an expansive gene expression network, with p53 as the “guardian of the genome” in tumor suppression and p63 acting as a master regulator of epithelial cell fate. Certainly, p73 will have some of the same functions and outstanding questions as its family members. However, without knowledge of the sequence-specific transcription factors that bind along with p53 family members at gene regulatory regions, the study of the p53 family and its control over gene expression is lacking key context for investigating their broad cell type-dependent activities. As such, this work provides a novel framework for the study of p53 family activities, including how

multiple stress pathways and context-specific factors work together to yield powerful organismal phenotypes like tumor suppression.

CHAPTER 6: Detailed materials and methods of CHAPTERS 2, 3, and 4

Model System

Cell Culture:

IMR90 fetal lung fibroblasts were cultured at 37°C with 5% CO₂/3% O₂ in DMEM (Gibco, Waltham, MA, USA) with 10% fetal bovine serum and penicillin/streptomycin. Experiments were performed between cell population doublings 20 and 35. HCT116 parental, TP53^{-/-} and ATF3^{-/-} lines were cultured in McCoy's 5A media with 10% fetal bovine serum. HCT116 ATF3^{-/-} cell line was a kind gift of Chunhong Yan (Augusta University). HEK293FT cells were used for virus preparation and were cultured in DMEM with 10% FBS without antibiotic. MCF10A cells were grown in HuMEC media (Gibco). Mouse embryonic fibroblasts (MEFs) were grown in DMEM with 10% FBS and were a kind gift of Jing Huang (National Cancer Institute, NIH). All cell lines were cultured at 37°C and 5% CO₂ in a water-jacketed incubator.

Cell Treatments:

Treatments for qPCR, western, and sequencing experiments with Dimethyl sulfoxide (DMSO), Nutlin (5 μM final, Calbiochem, St. Louis, MO, USA), etoposide (100 μM final) or Bay 11-7082 (10 μM final, Cayman Chemical, Ann Arbor, MI, USA) were performed for 6 h before processing cells for downstream experiments. ELISA treatments with either DMSO (as a control), 5μM Nutlin-3a, 100μM Etoposide, 2mM Histidinol (Acros organics, Product ID: 228830010), and 2μM Tunicamycin (Cayman Chemicals, item number: 11445) in 3mLs of McCoy media (as stated previously). All treatments were dissolved in DMSO.

Molecular Biology

Quantitative real time PCR:

Total RNA was isolated using the Omega E.Z RNA kit with an on-column treatment with 50 units of RNase-free DNase I for 30 min. Single-stranded cDNA was generated with the High Capacity cDNA Reverse Transcription reagents (Applied Biosystems), and qPCR was performed on an Applied Biosystems 7900HT with the relative standard curve method and iTaq Universal SYBR Green Supermix reagents (Biorad). Primers are found in Methods Table 1.

Western blotting:

Total protein was isolated using RIPA buffer, followed by a 15-min incubation on ice, and pelleting of and centrifugation to remove insoluble debris. Protein lysate samples were run at 150V on NuPAGE 10% Bis–Tris protein gels from Invitrogen. Samples were blotted onto 0.2 µm nitrocellulose membrane. Membranes were process with SuperSignal Chemi- luminescent reagents (Thermo Scientific) and imaged on a BioRad Chemidoc imager.

Enzyme-linked immunosorbent assay (ELISA):

HCT116 p53^{+/+} and HCT116 p53^{-/-} cells were seeded in 6-well tissue culture treated plates at 8 x 10⁵ cells per well. After 24 hours, 1 mL of media was collected per sample. 50uL of media was diluted 6x and run on pre-coated ELISA plates (R&D Biosystems, catalog #: DGD150). Samples were measured in duplicate across three biological replicates. Wells were read at 450nm and normalized to a 540nm reading to account for optical differences between the wells. Relative values were calculated for GDF15 protein expression in media across treatments. Oligos are found in Methods Table 2.

Antibodies:

Western blot antibodies: p53 (clone DO1, BD Biosciences, #554923), GAPDH (Cell signaling #5174S) antibodies. Proteins were visualized with HRP-conjugated secondary antibodies, Rabbit Anti-Mouse IgG H&L (HRP) (ab6728), Goat Anti-Rabbit IgG H&L (HRP) (ab6721). Immunoprecipitation was performed using the following: p53 (Abcam, Cambridge, MA, USA, ab80645, clone DO1), histone H3 (Abcam ab1791), H3K4me1 (Abcam, ab8895), H3K4me2 (Millipore, St. Louis, MO, USA, 07-030), H3K4me3 (Abcam, ab8580), H3K27ac (Active Motif, Carlsbad, CA, USA, #39133), H4K16ac (Millipore, 07-329), and POLR2A (RNA pol II, Santa Cruz, Santa Cruz, CA, USA, #sc-56767, GDF15 (Mic-1) (Cell signaling, mAb #8479), Tp63 (BioLegend, cat no. 687202)

Luciferase plasmid cloning and expression assays:

Candidate enhancer sequences were synthesized as dsDNA (IDT) and cloned into the pGL4.24 destabilized Luciferase reporter vector (Promega) using the HiFi DNA Assembly method (NEB). Enhancer variants were created using the inverse PCR method with Hot Start Q5 Polymerase (NEB) and barcoded primers. Plasmids were reverse transfected according to manufacturer's recommendations (JetPrime, Polyplus Transfection) in triplicate in a 96-well plate. Plasmid DNA (0.2 µg) was transfected at a ratio of 9:1 for the candidate enhancer:constitutive promoter driving Renilla luciferase (pGL4.75, Promega). Luciferase activity was determined using the Promega Dual-Luciferase® Reporter Assay System according to manufacturer specifications on a Synergy HI plate reader (Bio-Tek). Cloning primers are found in Methods Table 3.

Sequencing

ATAC-seq:

Assay for transposase-accessible chromatin (ATAC-seq) was performed in proliferating IMR90 cells treated with DMSO, Nutlin 3A, or etoposide as described above and harvested by centrifugation. In total, 50,000 cells were resuspended in ATAC lysis buffer and incubated on ice for 5 min before pelleting at $500 \times G$ for 5 min at 4°C . Lysis buffer was then removed, and nuclei were immediately resuspended in 50 μL of transposase reaction mix (1X TD buffer, 2.5 μL of Nextera transposase, Illumina, San Diego, CA, USA). The transposase reaction was incubated at 37°C for 30 min before the reaction was stopped by purification with Qiagen MinElute columns. Transposed DNA fragments were PCR amplified using custom indexing primers before sequencing on the Illumina NextSeq 500.

ChIP-seq:

10 million cells were crosslinked with formaldehyde (1% final concentration) for 10 min at room temperature with gentle rotation and quenched with glycine. Cells were isolated, washed twice with ice-cold phosphate-buffered saline, and snap-frozen on dry ice. Chromatin was extracted from isolated nuclei and sheared to 300 bp average size using a Diagenode Bioruptor Plus. All reactions were performed overnight at 4°C with rotation. Immunoprecipitated DNA was purified by phenol: chloroform extraction, and indexed sequencing libraries were prepared using the NEBNext Ultra DNA Library reagents (New England Biolabs, Ipswich, MA, USA). An Agilent BioAnalyzer was used to determine library sizes, and the Invitrogen Qubit fluorimeter was used to quantify library mass. Finally, absolute molarity calculations were determined using the KAPA Library Quantification method, and libraries were pooled for sequencing per manufacturer's

recommendations.

All ChIP-seq libraries (Catizone et. al 2019) were run with 100-bp single-end reads on an Illumina HiSeq 2000 with the exception of H3K4me2 which was performed with 75-bp single-end reads on an Illumina NextSeq 500. Raw FastQ files were aligned to the hg19 reference assembly (downloaded from the Illumina iGenomes repository) using bowtie2, and data were analyzed/visualized using Homer, deepTools, and a local installation of UCSC Genome Browser. ChIP-seq for histone modifications for Catizone et. al 2020 were performed in HCT116 colon carcinoma cells treated for 6 h with 5uM Nutlin-3A and then crosslinked with methanol-free formaldehyde (1% nal) at room temperature for 5 min. The reaction was then quenched with 2.5 M glycine for 5 min, followed by two washes with ice-cold PBS. Nuclear extraction and sonication were performed as previously described above, with an average fragment size of 500 bp. Crosslinked material was then immunoprecipitated with 5 ug of either anti-H3K27ac (Active Motif 39133) or anti-H3K4me2 (Millipore 07-030) coupled to Protein A/G Dynabeads (Invitrogen) overnight at 4°C. Beads were then washed 3x with low-salt buffer, 1× with high-salt buffer, and 1× with LiCl buffer, followed by elution with 1% SDS and 500 mM NaCl at 65°C with shaking. Eluted DNA was then quantified and used for Illumina-compatible library preparation using the New England Biolabs NEBNext Ultra II DNA Library prep reagents. Libraries were sequenced on an Illumina NextSeq 500. Raw data were aligned to the human hg19 genome assembly using hisat2. DNase- seq, H3K4me1 and H3K4me3 histone modification data were obtained from the ENCODE Reference Epigenome Series for HCT116 colon carcinoma cell lines under accession ENCSR309SGV. eRNA data were obtained from GEO GSE53966 and GEO GSE86165. Normalized read counts within MPRA region coordinates were quantified using HOMER.

RNA-seq:

For Catizone et. al 2019, DNA-free, total RNA was isolated using RNeasy columns (Qiagen, Germantown, MD, USA) and 1 µg was used to extract polyA+ RNA using magnetic poly(d)T beads (New England Biolabs). Strand-specific RNA libraries were constructed using NEBNext Ultra Directional RNA and BioO NextFlex Rapid reagents. RNA-seq libraries were sequenced with 100-bp single-end reads on an Illumina HiSeq 2000 (initial comparison of DMSO, Nutlin, etoposide) and with 75-bp single-end reads on an Illumina NextSeq 500 (NF-κB inhibitor experiments). Resulting raw data were aligned to the hg19 assembly using TopHat2/Bowtie2. Differentially expressed genes were those with at least twofold difference between the treated condition and the comparable DMSO-treated condition.

For Catizone et. al 2020, HCT116 parental, TP53^{-/-} or ATF3^{-/-} cells were treated at 80% confluence in a six-well plate with either DMSO or 5 M Nutlin-3A for 6 h and total RNA was isolated (EZ RNA, Omega Biotek). PolyA+ RNA was purified using poly dT magnetic beads (Perkin Elmer) and fragmented at 90°C for 15 min. Fragmented RNA was used as the template for double-stranded cDNA production using random hexamers (first strand synthesis) and the dUTP method to preserve strandedness (second strand synthesis). The resulting double-stranded cDNA was then used to construct an Illumina-compatible sequencing library (BioO NextFlex RNA Library Kit, Perkin Elmer). Libraries were quantified using qPCR (NEBNext Library Quantification, New England Biolabs) and an Agilent Bioanalyzer and then pooled for sequencing on an Illumina NextSeq 500. Sequencing reads were aligned to the hg19/GRCh37 assembly and transcript counts were determined using quantMode in STAR. Differential gene expression and normalized gene counts were determined using DESeq2.

Massively Parallel Reporter Assay

Selection of candidate enhancers:

Candidate enhancer regions were selected starting with regions of the hg19 genome assembly containing DNAse Hypersensitive Sites (DHS) (wgEncodeRegDnaseClusteredV3 downloaded from <http://hgdownload.cse.ucsc.edu/goldenPath/hg19/encodeDCC/wgEncodeRegDnaseClustered/>). DHS were then altered by the presence of a p53 family motif using gimmeMotifs (29). Ultimately, 296 DHS containing a p53 family motif and falling within 100 kb of a coding sequence transcriptional start site (TSS) were randomly selected for MPRA analysis. In parallel, 196 enhancers from the FANTOM Ubiquitous Enhancer group were selected as positive controls, with the central 100 bp segment of each enhancer used in the MPRA ([http://enhancer.binf.ku.dk/presets/Ubiquitous enhancers S9.bed](http://enhancer.binf.ku.dk/presets/Ubiquitous%20enhancers%20S9.bed)). Candidate p53-bound enhancers were shortened to 100 bp with the 20 bp p53 response element motif at the center with 40 bp of flanking genomic context on each side. Each candidate p53-bound enhancer was scrambled in 20 bp sections from 5' to 3' across the entire length producing. Nucleotide randomization preserved GC content and was performed using EMBOSS shuffle-seq. As negative controls for regulatory activity, the entire 100 bp sequence for all candidate or ubiquitous enhancers was scrambled while preserving GC content.

Massively Parallel Reporter Assay (MPRA) oligo design:

Each candidate 100 bp regulatory sequence was coupled to five separate 12 nucleotide unique molecular identifier (UMI) sequences. Replicates of the test sequences plus controls totaled the

library at 12 035 unique oligos in the orientation of: a 5' Primer binding overlap, a 100 bp enhancer sequence, a spacer for restriction enzyme sites EcoRI and SbfI, a unique enhancer associated 12 bp barcode, and a 3' Primer binding overlap. All sequences for the MPRA oligo library are found in Supplemental Table S1 of Catizone et. al. 2020. The final 12,035 unique oligo-pool was synthesized by CustomArray.

Two-step vector library cloning and verification:

The MPRA lentiviral vector pLs-mP was a gift from Nadav Ahituv (Addgene plasmid # 81225; <http://n2t.net/addgene: 81225>; RRID: Addgene 81225). pLs-mP was digested with the restriction enzymes EcoRI and SbfI yielding two fragments representing the plasmid backbone and the minimal promoter/eGFP. The candidate enhancer pool was PCR amplified using primers SL468 and SL469 in 3 separate re- actions of 50 ng at 21 cycles each, gel purified, and combined (Supplemental Table S2, cloning primers tab). The resulting PCR product was ligated to the EcoRI–SbfI digested pLs-mP backbone in three separate Gibson assembly reactions (HiFi DNA Assembly, NEB). 2l of each Gibson assembly reaction were transformed into Stbl4 electro-competent Escherichia coli (Invitrogen) in three separate transformation reactions (1200 V, 200, BioRad). Transformation reactions were plated on 10 separate 15 cm LB- agar plates with 100 µg/ml ampicillin selection at 30°C for 48 h. Colonies were isolated directly from plates and plasmid DNA was individually prepped (ZymoPURE II Midi Plasmid Kit). The resulting DNA was combined to create the Step 1 library. This plasmid pool was then digested with EcoRI and SbfI in three separate reactions at 1 g each and gel purified. The 780 bp fragment from the original EcoRI–SbfI reaction (containing the minimal promoter/EGFP fragment), was ligated into the digested Step 1 plasmid using T4 ligase. Ligation products were transformed as above and the

resulting MPRA library was sequence verified by Illumina sequencing.

MPRA virus production and transduction:

To make virus, 4×10^6 cells were seeded in 10 cm plates 24 h before transfection. Per 10 cm plate, cells were transfected with 8 μg of MPRA lentiviral backbone, 4 μg of M2G helper plasmid and 8 μg of ps-PAX helper plasmid using Jet-Prime transfection reagent according to manufacturer's recommendations. Virus was collected from supernatant at 24 and 48 h, pooled, and filtered using 0.45 μm syringe filters. HCT116 TP53^{+/+} and TP53^{-/-} cell lines were seeded 24 h before viral transduction in three 10 cm plates at a concentration of 2.0×10^6 cells/plate. Virus supernatant was combined with 8 g/ml polybrene, added to the seeded cells, and incubated for 48 h. Cells were then treated for 6 h with DMSO (as a control) or 5 μM Nutlin-3A (45-SML0580, Millipore Sigma) to induce p53 activity. One plate was left untreated as the infection control plate for genomic DNA isolation. After 6 h of treatment, cells were collected in ice- cold 1x PBS, snap-frozen on liquid nitrogen, and stored at -80°C until analysis. Three biological replicates were performed for each condition. MCF10a cells were transduced and prepared in the same manner.

MPRA Amplicon enrichment and RNA-seq library preparation:

Total RNA was isolated from DMSO or Nutlin-3A treated cells (EZ RNA Kit, Omega Biotek) with on-column DNaseI treatment. 6 μg of resulting total RNA was then taken through an additional round of TurboDNase treatment (ThermoFisher) to ensure complete removal of contaminating genomic DNA. The resulting RNA was split into three first strand reverse transcription reactions each using custom barcoded primers to identify the cell line, treatment, and

replicate number. All three cDNA reactions were combined and taken through a two-step PCR amplification process. In Round 1, each cDNA sample was amplified in 22 separate PCR reactions of three cycles each using barcoded primers. PCR reactions were then pooled and purified using 2.5x AMPure XP beads (Beckman-Coulter). The purified Round 1 PCR product went through a second round of PCR in eight reactions for 15 cycles each using barcoded primers as described in Supplemental Table S2. Step 2 PCR product was run on a 2% agarose gel and gel purified. Genomic DNA controls were prepared in a similar manner. 500 ng of genomic DNA was PCR amplified across 16 separate reactions of three cycles each using barcoded primers. The pooled PCR product was combined and purified using 2.5× volume AMPure XP beads. The resulting purified DNA was then separated into 16 separate PCR reactions of 15 cycles each, pooled, and gel purified. After the two-step PCR reaction, DNA amplicons representing the expressed mRNA barcode and the genomic DNA infection control within each biological replicate were combined at equal molarity. An Illumina-compatible sequencing library was generated (NEBNext Ultra II DNA Library Kit, New England Biolabs) for each biological replicate and sequenced using the NextSeq 500 at the University at Albany Center for Functional Genomics. MCF10a cell libraries were produced in the same manner in 2 biological replicates each. Barcoded sequencing primers can be found in Methods Table 5.

CRISPR-Cas9 Cell Lines

In vivo CRISPR/Cas9 mutagenesis and amplicon ChIP- sequencing:

HCT116 colon carcinoma cells were transduced with lentiCas9-Blast and cells stably expressing wild-type spCas9 were selected using 2 g/ml blasticidin. LentiCas9-Blast was a gift from Feng Zhang (Addgene plasmid #52962; <http://n2t.net/addgene:52962>; RRID: Addgene 52962).

Streptomyces pyogenes (sp) guide RNA sequences were cloned into the LentiGuide-Puro plasmid (plasmid #52963, Addgene). lentiGuide-Puro was a gift from Feng Zhang (Addgene plasmid # 52963; <http://n2t.net/addgene:52963>; RRID:Addgene 52963). Viral particles from LentiGuide-Puro were made by transfecting HEK293FT cells with the pack- aging plasmids psPax2 and pMD2.G and the respective guide RNA viral backbone cloned into pLS-mP. psPAX2 was a gift from Didier Trono (Addgene plasmid # 12260; <http://n2t.net/addgene:12260>; RRID:Addgene 12260). pMD2.G was a gift from Didier Trono (Addgene plasmid # 12259; <http://n2t.net/addgene:12259>; RRID:Addgene 12259).

HCT116 cells stably expressing spCas9 were selected with 2 g/ml puromycin 48 h after infection. The heterogeneous cell pool was then treated for 6 h with either DMSO or 5 M Nutlin-3A for either qPCR-mediated gene expression measurements or for ChIP. For ChIP, 10 million cells were crosslinked on plate with 1% formaldehyde for 10 min at room temperature until the reaction was quenched with 2.5% glycine. Crosslinked cells were processed using standard lysis procedures and chromatin was sonicated using a probe sonicator (Qsonica) at 25% amp for 10 pulses total; 10 seconds on, 50 s off for a total of 10 min at 4°C. Sheared chromatin was then used in a ChIP assay for p53 (clone DO1, BD Biosciences). 50 ng of purified DNA per experimental sample was used in a barcoding PCR reaction (Supplemental Table S2, barcode primers tab), and amplicons were then used as template for created Illumina- compatible sequencing libraries (NEBNext Ultra II DNA Library Kit). Libraries were quantified by qPCR and run on an Illumina NextSeq 500 (150 bp single-end). Raw FastQ reads containing the amplicon primers were altered (fastx-barcode-splitter, FastX-toolkit, <http://hannonlab.cshl.edu>) and used in subsequent analysis. The number of reads per DNA variant were quantified (fastX-collapser, FastX-toolkit) and the ChIP values were

normalized to genomic DNA input. DNA variants were then sorted by the presence or absence of p53 or Sp1/KLF family motifs as determined by gimmeMotifs. Barcoded library primers can be found in Methods Table 5.

Targeting KRAB to enhancers at genomic loci:

HCT116 colon carcinoma cells were transduced with Lenti-EF1a-dCas9-KRAB-Puro (Addgene Plasmid #99372) containing annealed oligos targeting the GDF15 E1, E2, promoter, FGF enhancer (as a control) and PGPEP1 promoter and selected with 2 μ g/mL puromycin. Viral particles were made in HEK293FT cells as described above. Cells were seeded at 8x10⁵ cells per well in 3mLs and treated with DMSO (as a control) or 100 μ M Etoposide. Samples were measured in 3 technical replicates across 3 biological replicates via relative qPCR as described above.

Generation of doxycycline inducible p63 isoform cell lines

HCT116 p53 $^{+/+}$ cells were transduced with Δ Np63 and TAp63 in PGK-rtTA-2A-puro (Addgene plasmid (#41393). Cells were selected for 24 hours with 2 ug/mL puromycin and validated with western blot for p63. Cells were treated with 1ug/mL doxycycline (Sigma Aldrich, #D9891-1G) for 4 hours to induce p63 protein levels. Primers for cloning can be found in Methods Table 3.

Biochemistry

Protein expression and purification:

Human p53_{1–393} in pGEX-2TK (Ampicillin) coding for an in-frame N-terminal GST tag was a gift from Cheryl Arrow- smith (Addgene plasmid # 24860; <http://n2t.net/addgene: 24860>;

RRID:Addgene 24860. p53_{1–393} was expressed in Rosetta 2 DE3 cells (EMD Millipore) in 2YT media. Cells were grown at 37°C with shaking at 225 rpm until OD_{600 nm} = 0.4–0.6, then shifted to 22°C and induced with 1 mM IPTG for 4 h. Cells were harvested by centrifugation at 4800 rpm for 15 min. Cell pellets were lysed in GST Buffer A (20 mM Tris–HCl pH 7.3 (RT), 300 mM NaCl, 0.2 mM EDTA, 1 mM DTT, 5% glycerol, 10 mM Na-butyrate and supplemented with Complete protease inhibitor cocktail (Roche) and 0.1% NP40. Cells were lysed by sonication. Cell lysates were cleared by centrifugation at 18 000 rpm for 45 min at 4°C. Cell lysates were filtered with a 0.45 µM syringe filter and loaded on to an equilibrated 5 ml GStrap HP column (GE Healthcare) using an Akta Purifier FPLC (GE Healthcare). The column was washed with GST Buffer A; bound protein was eluted using a linear gradient of 0–100% GST Buffer B (GST Buffer A + 10 mM glutathione (reduced)). Purity was determined by SDS PAGE using a 4–12% Bis–Tris gel run in 1× MOPS SDS buffer. Eluted fractions containing p53_{1–393} constructs were pooled and concentrated using a Vivaspin 10 kDa MWCO centrifugal concentrator (GE healthcare). Concentrated protein was dialyzed overnight into GST-Buffer D (GST Buffer A + 20% glycerol). Protein concentration was determined using a nanodrop with calculated extinction co-efficient and molecular weight parameters. Purified protein was divided into single use aliquots, ash frozen in liquid nitrogen and stored at –80°C.

CCNG1 p53 electrophoretic mobility shift assay:

Binding of p53 to CCNG1 enhancer sequences was tested by electrophoretic mobility shift assays (EMSA). 60 bp HPLC purified DNA sequences were resuspended at 100 M in 1× TE buffer. Equal volumes of complementary oligonucleotides were heated at 95°C for 5 min and annealed by

cooling to 21°C for 30 min. Binding reactions were assembled in DNase/RNase free, low adhesion microcentrifuge tubes. Reactions contained 1× p53 binding buffer (50 mM Tris– HCl pH 7.3, 150 mM NaCl, 2 mM DTT, 0.1 mg/ml BSA). Unless otherwise stated, 50 nM of annealed DNA was added to each reaction. Binding reactions were started by adding the required concentration of p53_{1–393} and allowed to proceed for 30 min at 21°C. Reactions were loaded immediately on a vertical 0.7% Agarose gel (Ultrapure agarose, Life Technologies) buffered with 1× TBE. Gels were run for 45 min at 60 V in 1× TBE buffer. Gels were stained for 10 min with 1× SYBR gold nucleic acid stain (ThermoFisher) in 1× TBE buffer and imaged on a G:box blue light transilluminator (Syngene). Densitometric analysis was carried out in Fiji; binding curves were fitted using the Hill equation with a two-site binding model (Hill coefficient = 2) using non-linear regression (nls) in R.

Data analysis

Massively Parallel Reporter Assay (MPRA) data analysis:

Sequencing reads for each individual experimental condition were flanked by a unique 5' and 3' amplicon barcode to allow separation from the pooled raw sequencing reads. Barcoded, experimental condition-specific reads were separated into individual files for further analysis using the FastX toolkit (fastx-barcode-splitter, <http://hannonlab.cshl.edu>). The number of reads containing unique enhancer identifying sequences were then parsed and counted using fastX-collapser from the FastX-toolkit. Raw read counts for each enhancer sequence across cell lines, treatment conditions, and biological replicates be found in Supplemental Table S3. Differential enhancer activity across experimental conditions and cell lines was calculated from raw enhancer barcode read counts using DESeq2. To account for differences in representation across the original

viral enhancer sequence library, raw enhancer barcode read counts scaled to transcripts per million (TPM) and were then normalized to the read counts from genomic DNA (fold-change, RNA barcode/ DNA barcode). Normalized enhancer count values for mutant enhancer sequences were then compared to wild-type values using a one-way ANOVA with a post-hoc Tukey HSD test implemented in R.

Transcription factor peak intersections:

Transcription factor peak les were obtained from the Cistrome database, <http://cistrome.org/db>, accessed 1 July 2019). MPRA regions were converted into the hg38 genome assembly coordinates using liftOver from hg19 to hg38 (UCSC). Transcription factor peak summits were then intersected with MPRA regions using BedTools (intersectBed). Peak intersection data were clustered by row (MPRA regions) and column (transcription factor) by One minus Pearson Correlation with complete linkage using Morpheus (<https://software.broadinstitute.org/morpheus>).

Transcription factor motif analysis:

Three tools were used to identify motifs either present or enriched within the 100 bp regions from the MPRA p53- bound and p53-unbound peaks. Additionally, we analyzed transcription factor motif presence and enrichment within a set of p53 binding sites identified across multiple cell types in Verfaillie et al. For the Verfaillie p53 set, we considered only the 1001/1149 (87%) p53 peaks found within DNase Hypersensitive Clusters (UCSC GenomeBrowser, ENCODE Regulation Track. Motif analysis was then performed on the entire DNase Hypersensitive Cluster region. Known Motif enrichment using HOMER was performed using the findMotifsGenome module (find- MotifsGenome.pl -nomotif -size given) against the hg19 genome. Analysis for the

presence of known motifs within MPRA regions and the Verfaillie p53 set was performed using the 2018 release of JASPAR Vertebrate Transcription Factor Motif Database and both gimmeMotifs and UCSC TableBrowser. Analysis of transcription factor motif enrichment using gimmeMotifs was run using the scan module (options -t -g hg19 -p JASPAR2018 vertebrates.pfm). The presence of hg19-based JASPAR vertebrate transcription factor motifs within p53-bound MPRA peaks and within the Verfaillie p53 set was performed using the UCSC TableBrowser and the JASPAR 2018 hg19 Track Hub. Only motifs with an enrichment score of 400 or higher ($P < 0.0001$) were considered for analysis. Histograms of motif enrichment within MPRA p53 or Verfaillie p53 peak sets were generated using bedTools (coverage Bed-d option) and Morpheus.

Data Availability

Catizone et. al 2019 and Chapter 2:

Datasets found in this manuscript are available without restriction through Gene Expression Omnibus GSE58740 (DMSO and Nutlin 3A) and GSE115940 (etoposide).

Catizone et. al 2020 and Chapters 3-4:

All sequencing data generated as part of this manuscript are available under Gene Expression Omnibus (GEO) Accession GSE137297. p53 ChIP data from Nutlin-3A-treated cells were obtained from GSE86222. Conserved element data (bigWig) from PhyloP and PhastCon were obtained from the UCSC Genome Browser and plots were generated using deepTools.

Reagent tables

Table 1: QPCR primers

Lab code:	Sequence:	Description:
SL790	TGTAAAATCAATAGAAGAGGAAAGGAATG	CCNG1 qrtPCR
SL791	CTCATCAAGTCTGAAACCGTAAACC	CCNG1 qrtPCR
SL47	CCAGGTGGTCTCCTGACTTC	GAPDH qrtPCR
SL48	GTGGTCGTTGAGGGCAATG	GAPDH qrtPCR
SL71	ACCTGCTAACCAAGGCTGCG	GDF15 qrtPCR
SL72	CGGTGTTCGAATCTTCCCAG	GDF15 qrtPCR
SL55	AGCGATGGAACCTCGACTTTG	Hs p21 expression F
SL56	CGAAGTCACCCCTCAGTGGT	H2 p21 expression R
SL63	AAATGAATCCCCCCCCTCC	Hs MDM2 FWD
SL64	CACGAAGGGCCAACATCT	Hs MDM2 REV
SL1389	GCGGCCTTCAGCCAAAATCT	PUMA (bbc3) QPCR primers FWD #1
SL1390	CCCCATCAATCCATTG	PUMA (bbc3) QPCR primers REV #1
SL163	GGCAGCCTTCCTGATTCTG	Human IL8 for RTqPCR FWD
SL164	CTTGGCAAAACTGCACCTCA	Human IL8 for RTqPCR REV
SL165	TGTAAGCTATGCCCACTCCA	Human IL1A for RTqPCR FWD
SL166	AGAGACACAGATTGATCCATGCA	Human IL1A for RTqPCR REV
SL167	CACCACTACAGCAAGGGCTC	Human IL1B for RTqPCR FWD
SL168	CATGGCCACAACAACGTGACG	Human IL1B for RTqPCR REV

Table 2: EMSA oligo sequences

Name	Oligo Sequence
CCNG1_WT_TOP	AAACTCTACCGCTTGTGAGCACAGCCAGGCTAGTCGAGGCTGGAGGGCGGAGCC
CCNG1_WT_BOTTOM	GGCTCCGCCCTCCAGCCTCGGACTAGCCTGGCTTGCTCACACAGCGGTAGAGTT
CCNG1_L2_TOP	TACAAGGGAGGCTTTCATCCGACAAGCCAGGCTAGTCGAGGCTGGAGGGCGGAGCC
CCNG1_L2_BOTTOM	GGCTCCGCCCTCCAGCCTCGGACTAGCCTGGCTTGCGGATGAAAGCCTCTGTA
CCNG1_R2_TOP	AAACTCTACCGCTTGTGAGCACAGCCAGGCTAGTCGGGGCGGGACACGTGAGG
CCNG1_R2_BOTTOM	CCTGCACGTGCCCCGCCGGACTAGCCTGGCTTGCTCACACAGCGGTAGAGTT

Table 3: Plasmid Cloning primers

Lab code:	Sequence:	Description:
Cloning MPRA Library		
SL468	ggccgcgttagacctgcaACCTAGGACGGATCAAC	Primers for Gibson Assembly of ESB into PLSMP (generated from NEB and snap gene; not from paper) FWD
SL469	agtattatggcttcgtacCATTCGGTGAAACCGACAATT	Primers for Gibson Assembly of ESB into PLSMP (generated from NEB and snap gene; not from paper) REV
Cloning for Validating MPRA (CCNG1 and TP53TG1)		
SL721	ctggccaaactggccgtacAGTAGGTCTGGCCCCGCG	Gibson primer to insert CCNG1 into pGL4.24 forward
SL722	cattatacccttagtgtctaCATAACACAACATGTCCCGGC	Gibson primer to insert CCNG1 into pGL4.24 reverse
SL745	caactgcaggGATCCGGCCTCTGAAGGT	CCNG1 mutagenesis primer MR2 fwd
SL746	tccggccccCGACTAGCCTGGGCTTG	CCNG1 mutagenesis primer MR2 rev
SL747	gcggccaggGATCCGGCCTCTGAAGGT	CCNG1 mutagenesis primer NR2 fwd
SL748	ccccgcctgtCGACTAGCCTGGGCTTG	CCNG1 mutagenesis primer NR2 rev
SL1119	cgccggccggGATCCGGCCTCTGAAGGT	Mutagenesis primers to mutate 2nd highly conserved g in CCNG1 enhancer R2 region FWD
SL1120	cttcacggcctGGACTAGCCTGGGCTTG	Mutagenesis primers to mutate 2nd highly conserved g in CCNG1 enhancer R2 region REV
SL1121	gcggggccggGATCCGGCCTCTGAAGGT	Mutagenesis primers to mutate 3rd highly conserved g in CCNG1 enhancer R2 region REV
SL1122	ctcccaagccctCGACTAGCCTGGGCTTG	Mutagenesis primers to mutate 3rd highly conserved g in CCNG1 enhancer R2 region REV
SL982	ctggccaaactggccgtacGTTACTCCATATGCTTGTTC	Enhancer 46 forward gibson primer for pgl4.24 cutting with KPN1 and HINDIII
SL983	cattatacccttagtgtctaCTGACAGCATGATGATCATC	Enhancer 46 reverse gibson primer for pgl4.24 cutting with KPN1 and HINDIII
SL1101	actcggtggTTAGGCAAGCCCCCTG	Mutagenesis primers for enhancer 46 making R1 version full enhancer FWD
SL1102	ccgtcgaaagGATAAAGAAAGGCTAACAGGTGACTTGC	Mutagenesis primers for enhancer 46 making R1 version full enhancer REV
Cloning for GDF15E2		
SL1107	CATCCCCTCAAATCCAAGGTTGG	Primer to amplify full gdf15e2 out of genome FWD
SL1108	TGGGTTCTCCCTGCTCTTC	Primer to amplify full gdf15e2 out of genome REV
SL1109	ctggccaaactggccgtacCATCCCTCAAATCCAAGGTTGG	Gibson primer to add full gdf15e2 into pgl4.24 FWD
SL1110	tatatacccttagtgtctaTCGGTTCTCCCTGCTCTTC	Gibson primer to add full gdf15e2 into pgl4.24 REV
Cloning for tet-on inducible p63 isoforms		
SL776	cagatcgccggagaatggATGTTGTACTGGAAAAC	Gibson fwd primer for deltap63 into 41393 tet on plasmid backbone
SL777	ttatgttgtgggttgttgttgcACTTGTATCGTCGTC	Gibson rev primer for deltap63 into 41393 tet on plasmid backbone
SL778	cagatcgccggagaatggATGTCAGACACAG	Gibson fwd primer for TAp63 into 41393 tet on plasmid backbone
SL779	ttatgttgtgggttgttgttgcATACTTGTATCGTCGTC	Gibson rev primer for TAp63 into 41393 tet on plasmid backbone
Cloning for cluster 2 enhancers for luciferase		
SL694	ctggccaaactggccgtacTGGTACTCTGATCTAGC	Enhancer 245 from MPRA into pGL4.24 gibson primer FWD
SL695	cattatacccttagtgtctaCTTAATTAAGTAGTCTATGAAGCTG	Enhancer 245 from MPRA into pGL4.24 gibson primer REV
SL696	ctggccaaactggccgtacATTAAATGAGATAAAACTGTAGAG	Enhancer 186 from MPRA into pGL4.24 gibson primer FWD
SL697	cattatacccttagtgtctaTCGTTATGGTGTACATAG	Enhancer 186 from MPRA into pGL4.24 gibson primer REV
SL698	ctggccaaactggccgtacATAAAAATTTAACATGATTTTGTG	Enhancer 231 from MPRA into pGL4.24 gibson primer FWD
SL699	cattatacccttagtgtctaTCTGGTTTCCACAATTTC	Enhancer 231 from MPRA into pGL4.24 gibson primer REV
SL700	ctggccaaactggccgtacATCAAATGTTAAAATCATCCAG	Enhancer 220 from MPRA into pGL4.24 gibson primer FWD
SL701	cattatacccttagtgtctaAAACAAACCCAGACATT	Enhancer 220 from MPRA into pGL4.24 gibson primer REV

Table 4: CRISPR guide primers

Lab code:	Sequence:	Description:
GDF15 Enhancers in vivo		
SL243	CACCGTGGATGGGGAAAGTGATCTA	FGF2_enhancer1 at p53BS_Guide1_F (CACCG)
SL244	AAACTAGATCACTCCCCCATCAC	FGF2_enhancer1 at p53BS_Guide1_R (AAAC-C)
SL245	CACCGGAGGGCATGTCAGGACTTC	FGF2_enhancer1 at p53BS_Guide2_F (CACCG)
SL246	AAACGCAAGTCTGACATGCCCTCC	FGF2_enhancer1 at p53BS_Guide2_R (AAAC-C)
SL247	CACCGCTGGCTCCGGAGAACGAGA	FGF2_enhancer1 at p53BS_Guide7_F (CACCG)
SL248	AAACATTCTCTCTCCGGAGCCAGC	FGF2_enhancer1 at p53BS_Guide7_R (AAAC-C)
SL265	CACCGCCATGCCGGCAAGAACTC	GDF15_promoter at p53BS_Guide2_F (CACCG)
SL266	AAACGAGTTCTGCCCCGGCATGGC	GDF15_promoter at p53BS_Guide2_R (AAAC-C)
SL267	CACCGTGAGGTTCGGGCTGAGC	GDF15_promoter at p53BS_Guide6_F (CACCG)
SL268	AAACGCTCAGAGCCCAACCTGCAC	GDF15_promoter at p53BS_Guide6_R (AAAC-C)
SL269	CACCGGAATGCTCTAGATGCTCC	GDF15_promoter at p53BS_Guide7_F (CACCG)
SL270	AAACGGAGCATCTGAGAGCCATTCC	GDF15_promoter at p53BS_Guide7_R (AAAC-C)
SL271	CACCGGACTTGGACATGTCGGGC	GDF15_enhancer1 at p53BS_Guide1_F (CACCG)
SL272	AAACGCCGGACATGCTCAAAGTCCC	GDF15_enhancer1 at p53BS_Guide1_R (AAAC-C)
SL273	CACCGGAGGCACTCTGGTAAAAAC	GDF15_enhancer1 at p53BS_Guide2_F (CACCG)
SL274	AAACGTTTACCAAGGAGTGCCTCC	GDF15_enhancer1 at p53BS_Guide2_R (AAAC-C)
SL275	CACCGGGTAAAACGGTGTGATTGCC	GDF15_enhancer1 at p53BS_Guide5_F (CACCG)
SL276	AAACGGCAATCACCAAGTTTACCC	GDF15_enhancer1 at p53BS_Guide5_R (AAAC-C)
SL277	CACCGGAGGAATTGGGGCGGGCAA	GDF15_enhancer2 at p53BS_Guide1_F (CACCG)
SL278	AAACTGGCCGCCGGATTCTCC	GDF15_enhancer2 at p53BS_Guide1_R (AAAC-C)
SL279	CACCGATGTCCCCGATGTCAGC	GDF15_enhancer2 at p53BS_Guide4_F (CACCG)
SL280	AAACGCTCAGACATGCCGGACATC	GDF15_enhancer2 at p53BS_Guide4_R (AAAC-C)
SL281	CACCGAAACGGGGCGGGGGC	GDF15_enhancer2 at p53BS_Guide5_F (CACCG)
SL282	AAACGCCCGCGCCCCGTTTGC	GDF15_enhancer2 at p53BS_Guide5_R (AAAC-C)
CCNG1 in vivo		
SL814	CACCGGCTGTTGAGCACAAGCCC	CCNG1 Crispr Guide p53RE 1 (CACCG)
SL815	AAACGGGTTGTCACAACAGCC	CCNG1 Crispr Guide p53RE 1 (AAAC-C)
SL816	CACCGCTCAGCCTCGGACTAGCCT	CCNG1 Crispr Guide p53RE 2 (CACCG)
SL817	AAACAGGCTAGTCCGAGGCTGGAGC	CCNG1 Crispr Guide p53RE 2 (AAAC-C)
SL818	CACCGAGGCTAGTCCGAGGCTGGAG	CCNG1 Crispr Guide R2 position 1 (CACCG)
SL819	AAACCTCAGCCTCGGACTAGCCTC	CCNG1 Crispr Guide R2 position 1 (AAAC-C)
SL820	CACCGCAGGCTAGTCCGAGGCTGG	CCNG1 Crispr Guide R2 position 2 (CACCG)
SL821	AAACTCCAGCCTCGGACTAGCCTG	CCNG1 Crispr Guide R2 position 2 (AAAC-C)
SL822	CACCGGACCTCAGGAGGCCGATC	CCNG2 Crispr Guide R2 postion 3 (CACCG)
SL823	AAACGATCCGGCTCTGAGGTGCC	CCNG2 Crispr Guide R2 postion 3 (AAAC-C)
SL1001	CACCGTGGCTTGTCTACAAACAG	CRISPR guide 1 L2 position in CCNG1 FWD
SL1002	AAACCTTGTGAGCACAAAGCCAC	CRISPR guide 1 L2 position in CCNG1 rev
SL1003	CACCGAACAGCGGTAGAGTTAGTG	CRISPR guide 2 L2 position in CCNG1 FWD
SL1004	AAACCACTAAACTCACCGCTGTT	CRISPR guide 2 L2 position in CCNG1 rev
SL1005	CACCGGGTAGAGTTAGTGTGAAA	CRISPR guide 3 L2 position in CCNG1 FWD
SL1006	AAACTTCCACACTAAACTCACCC	CRISPR guide 3 L2 position in CCNG1 rev

Table 5: Barcoded Library primers

Lab code:	Sequence:	Description:	Cell Line	Treatment	Replicate
Barcoded amplicon sequencing primers					
SL592	AAC GGT CTC GGC ATG GAC GAG CTG TAC AAG TAG	MPRA FWD primers BC1	HCT116 p53+/-	DMSO	3
SL593	ACA TGT CTC GGC ATG GAC GAG CTG TAC AAG TAG	MPRA FWD primers BC2	HCT116 p53+/-	Nutlin	3
SL594	AGA CTC CTC GGC ATG GAC GAG CTG TAC AAG TAG	MPRA FWD primers BC3	HCT116 p53+/-	DMSO	3
SL595	ATC GCA CTC GGC ATG GAC GAG CTG TAC AAG TAG	MPRA FWD primers BC4	HCT116 p53+/-	Nutlin	3
SL596	ATG TCC CTC GGC ATG GAC GAG CTG TAC AAG TAG	MPRA FWD primers BC5	HCT116 p53+/-	DMSO	2
SL597	CAA TTG CTC GGC ATG GAC GAG CTG TAC AAG TAG	MPRA FWD primers BC6	HCT116 p53+/-	Nutlin	2
SL598	CAT CAG CTC GGC ATG GAC GAG CTG TAC AAG TAG	MPRA FWD primers BC7	HCT116 p53+/-	DMSO	2
SL599	CCA CTT CTC GGC ATG GAC GAG CTG TAC AAG TAG	MPRA FWD primers BC8	HCT116 p53+/-	Nutlin	2
SL600	CGA AAC CTC GGC ATG GAC GAG CTG TAC AAG TAG	MPRA FWD primers BC9	HCT116 p53+/-	DMSO	1
SL601	GAC CAA CTC GGC ATG GAC GAG CTG TAC AAG TAG	MPRA FWD primers BC10	HCT116 p53+/-	Nutlin	1
SL602	GTC TAT CTC GGC ATG GAC GAG CTG TAC AAG TAG	MPRA FWD primers BC11	HCT116 p53+/-	DMSO	1
SL603	GCA GAA CTC GGC ATG GAC GAG CTG TAC AAG TAG	MPRA FWD primers BC12	HCT116 p53+/-	Nutlin	1
SL604	GTT CAG CTC GGC ATG GAC GAG CTG TAC AAG TAG	MPRA FWD primers BC13	HCT116 p53+/-	Genomic	3
SL605	GAT ACA CTC GGC ATG GAC GAG CTG TAC AAG TAG	MPRA FWD primers BC14	HCT116 p53+/-	Genomic	3
SL606	TAAC GAC CTC GGC ATG GAC GAG CTG TAC AAG TAG	MPRA FWD primers BC15	HCT116 p53+/-	Genomic	2
SL607	TCA ATC CTC GGC ATG GAC GAG CTG TAC AAG TAG	MPRA FWD primers BC16	HCT116 p53+/-	Genomic	2
SL608	TGC TCA CTC GGC ATG GAC GAG CTG TAC AAG TAG	MPRA FWD primers BC17	HCT116 p53+/-	Genomic	1
SL609	TTC TGG CTC GGC ATG GAC GAG CTG TAC AAG TAG	MPRA FWD primers BC18	HCT116 p53+/-	Genomic	1
SL610	AAC GTG ACG AAG TTA TTA GGT CCC TCG AC	MPRA REV primers BC1	HCT116 p53+/-	DMSO	3
SL611	ACA TGT ACG AAG TTA TTA GGT CCC TCG AC	MPRA REV primers BC2	HCT116 p53+/-	Nutlin	3
SL612	AGA CTC ACG AAG TTA TTA GGT CCC TCG AC	MPRA REV primers BC3	HCT116 p53+/-	DMSO	3
SL613	ATC GCA ACG AAG TTA TTA GGT CCC TCG AC	MPRA REV primers BC4	HCT116 p53+/-	Nutlin	3
SL614	ATG TCC ACG AAG TTA TTA GGT CCC TCG AC	MPRA REV primers BC5	HCT116 p53+/-	DMSO	2
SL615	CAA TTG ACG AAG TTA TTA GGT CCC TCG AC	MPRA REV primers BC6	HCT116 p53+/-	Nutlin	2
SL616	CAT CAG ACG AAG TTA TTA GGT CCC TCG AC	MPRA REV primers BC7	HCT116 p53+/-	DMSO	2
SL617	CCA CTT ACG AAG TTA TTA GGT CCC TCG AC	MPRA REV primers BC8	HCT116 p53+/-	Nutlin	2
SL618	CGA AAC ACG AAG TTA TTA GGT CCC TCG AC	MPRA REV primers BC9	HCT116 p53+/-	DMSO	1
SL619	GAC CAA ACG AAG TTA TTA GGT CCC TCG AC	MPRA REV primers BC10	HCT116 p53+/-	Nutlin	1
SL620	GTC TAT ACG AAG TTA TTA GGT CCC TCG AC	MPRA REV primers BC11	HCT116 p53+/-	DMSO	1
SL621	GCA GAA ACG AAG TTA TTA GGT CCC TCG AC	MPRA REV primers BC12	HCT116 p53+/-	Nutlin	1
SL622	GCA GAA ACG AAG TTA TTA GGT CCC TCG AC	MPRA REV primers BC13	HCT116 p53+/-	Genomic	3
SL623	GAT ACA ACG AAG TTA TTA GGT CCC TCG AC	MPRA REV primers BC14	HCT116 p53+/-	Genomic	3
SL624	TAA GAC ACG AAG TTA TTA GGT CCC TCG AC	MPRA REV primers BC15	HCT116 p53+/-	Genomic	2
SL625	TCA ATC ACG AAG TTA TTA GGT CCC TCG AC	MPRA REV primers BC16	HCT116 p53+/-	Genomic	2
SL626	TGC TCA ACG AAG TTA TTA GGT CCC TCG AC	MPRA REV primers BC17	HCT116 p53+/-	Genomic	1
SL627	TTC TGG ACG AAG TTA TTA GGT CCC TCG AC	MPRA REV primers BC18	HCT116 p53+/-	Genomic	1
Column1	Column2	Column3	Column4	Column5	Column6
Lab code:	Sequence:	Description:			
Barcoded ChIP amplicon primers				Conditions	
SL1079	CGAACAGTAGGTCTGGCCCCGCG	CCNG1 BARCODED CHIP PRIMERS FWD 1	DMSO	p53 ChIP	
SL1080	GACAAAGTAGGTCTGGCCCCGCG	CCNG1 BARCODED CHIP PRIMERS FWD 2	Nutlin	p53 ChIP	
SL1081	GTCATAGTAGGTCTGGCCCCGCG	CCNG1 BARCODED CHIP PRIMERS FWD 3	DMSO	Input	
SL1082	GCAGAAAGTAGGTCTGGCCCCGCG	CCNG1 BARCODED CHIP PRIMERS FWD 4	Nutlin	Input	
SL1083	CGAAACCATAACACAAACCATGTCCCCGGC	CCNG1 BARCODED CHIP PRIMERS REV 1	DMSO	p53 ChIP	
SL1084	GACCAACATAACACACACCATGTCCCCGGC	CCNG1 BARCODED CHIP PRIMERS REV 2	Nutlin	p53 ChIP	
SL1085	GTCATATCAAACACACACCATGTCCCCGGC	CCNG1 BARCODED CHIP PRIMERS REV 3	DMSO	Input	
SL1086	GCAGAACATAACACACACCATGTCCCCGGC	CCNG1 BARCODED CHIP PRIMERS REV 4	Nutlin	Input	

Table 6: Plasmid list

Plasmid name	Plasmid use	Chapter use
MPRA pooled plasmid library	MPRA screen	2
CCNG1-fulllength-pgl4.24	luciferase vector	2
TP53TG1-fulllength-pgl4.24	luciferase vector	2
CCNG1-R2SCR-fulllength-pgl4.24	luciferase vector	2
CCNG1-R2*SCR-fulllength-pgl4.24	luciferase vector	2
CCNG1-G3-fulllength-pgl4.24	luciferase vector	2
CCNG1-G4-fulllength-pgl4.24	luciferase vector	2
L2-gRNA-lentiguidepuro	CRISPR mutations	2
MID-gRNA-lentiguidepuro	CRISPR mutations	2
R2-gRNA-lentiguidepuro	CRISPR mutations	2
FGF-dcas9KRAB	targeting KRAB to enhancer	2
GDF15promoter-dcas9KRAB	targeting KRAB to enhancer	2
GDF15E1-dcas9KRAB	targeting KRAB to enhancer	2
GDF15E2-dcas9KRAB	targeting KRAB to enhancer	2
GDF15E1-fulllength-pgl4.24	luciferase vector	2
GDF15E2-fulllength-pgl4.24	luciferase vector	2
Cluster2#220-pgl4.24	luciferase vector	3
Cluster2#231-pgl4.24	luciferase vector	3
Cluster2#245-pgl4.24	luciferase vector	3
ΔNp63-tet-on-lentiviral	tet-on protein expression	3
TAp63-tet-on-lentiviral	tet-on protein expression	3

CHAPTER 7: Copyright details

The text and figures from Chapter 2 have been reused from “Comparison of genotoxic vs. non-genotoxic stabilization of p53 provides insight into parallel stress-responsive transcriptional networks” in accordance with *Cell Cycle*’s CC-BY-NC 4.0 license. To view a copy of this license, visit <http://creativecommons.org/licenses/by/4.0>

Link to original work:

<https://www.tandfonline.com/doi/full/10.1080/15384101.2019.1593643>

The text and figures from Chapter 3 have been reused from “Locally acting transcription factors regulate p53-dependent *cis*-regulatory element activity” in accordance with *Nucleic Acid Research*’s CC-BY-NC 4.0 license. To view a copy of this license, visit <http://creativecommons.org/licenses/by/4.0>

Link to original work:

<https://doi.org/10.1093/nar/gkaa147>

These published articles are being included because they were part of the programmatic line of research that comprised the dissertation and including them provides a coherent and appropriately sequenced investigation of the topic being studied.

CHAPTER 8: Contributions

The data from Chapters 2 and 3 are published, the data from Chapter 4 is unpublished.

The data from Chapter 2 was completed by Allison N Catizone. The other contributors to the paper were: Charly Ryan Good, Katherine A. Alexander, and Shelley L. Berger.

The data from Chapter 3 was completed by Allison N Catizone. The other contributors to the paper were: Gizem Karsli Uzunbas, Petra Celadova, Sylvia Kuang, and Daniel Bose.

The data from Chapter 4 was completed by Allison N Catizone. The other contributors for this chapter were Sylvia Kuang.

CHAPTER 9: References

- Abraham, R. T. (2001). Cell cycle checkpoint signaling through the ATM and ATR kinases. *Genes & Development*, 15(17), 2177–2196. <https://doi.org/10.1101/gad.914401>
- Allen, B. L., & Taatjes, D. J. (2015). The Mediator complex: A central integrator of transcription. *Nature Reviews Molecular Cell Biology*, 16(3), 155–166. <https://doi.org/10.1038/nrm3951>
- Allen, M. A., Andrysik, Z., Dengler, V. L., Mellert, H. S., Guarnieri, A., Freeman, J. A., Sullivan, K. D., Galbraith, M. D., Luo, X., Kraus, W. L., Dowell, R. D., & Espinosa, J. M. (2014a). Global analysis of p53-regulated transcription identifies its direct targets and unexpected regulatory mechanisms. *eLife*, 3. <https://doi.org/10.7554/eLife.02200>
- Allen, M. A., Andrysik, Z., Dengler, V. L., Mellert, H. S., Guarnieri, A., Freeman, J. A., Sullivan, K. D., Galbraith, M. D., Luo, X., Kraus, W. L., Dowell, R. D., & Espinosa, J. M. (2014b). Global analysis of p53-regulated transcription identifies its direct targets and unexpected regulatory mechanisms. *eLife*, 3. <https://doi.org/10.7554/eLife.02200>
- Andrysik, Z., Galbraith, M. D., Guarnieri, A. L., Zaccara, S., Sullivan, K. D., Pandey, A., MacBeth, M., Inga, A., & Espinosa, J. M. (2017). Identification of a core TP53 transcriptional program with highly distributed tumor suppressive activity. *Genome Research*, 27(10), 1645–1657. <https://doi.org/10.1101/gr.220533.117>
- Appella, E., Nagaich, A. K., Zhurkin, V. B., & Harrington, R. E. (1998). Analysis of the interaction between the p53 binding domain and the p21/CiP1 DNA response element: A novel architectural organization. *J Protein Chem*, 17, 527–528.

- Arnosti, D. N., & Kulkarni, M. M. (2005). Transcriptional enhancers: Intelligent enhanceosomes or flexible billboards? *Journal of Cellular Biochemistry*, 94(5), 890–898.
<https://doi.org/10.1002/jcb.20352>
- Azofeifa, J. G., Allen, M. A., Hendrix, J. R., Read, T., Rubin, J. D., & Dowell, R. D. (2018). Enhancer RNA profiling predicts transcription factor activity. *Genome Research*, 28(3), 334–344. <https://doi.org/10.1101/gr.225755.117>
- Baldwin, E. L., & Osheroff, N. (2005). Etoposide, topoisomerase II and cancer. *Current Medicinal Chemistry. Anti-Cancer Agents*, 5(4), 363–372.
- Barlev, N. A., Liu, L., Chehab, N. H., Mansfield, K., Harris, K. G., Halazonetis, T. D., & Berger, S. L. (2001). Acetylation of p53 activates transcription through recruitment of coactivators/histone acetyltransferases. *Molecular Cell*, 8(6), 1243–1254.
- Barski, A., Cuddapah, S., Cui, K., Roh, T.-Y., Schones, D. E., Wang, Z., Wei, G., Chepelev, I., & Zhao, K. (2007). High-Resolution Profiling of Histone Methylation in the Human Genome. *Cell*, 129(4), 823–837. <https://doi.org/10.1016/j.cell.2007.05.009>
- Beckerman, R., & Prives, C. (2010). Transcriptional Regulation by P53. *Cold Spring Harbor Perspectives in Biology*, 2(8). <https://doi.org/10.1101/cshperspect.a000935>
- Behera, V., Evans, P., Face, C. J., Hamagami, N., Sankaranarayanan, L., Keller, C. A., Giardine, B., Tan, K., Hardison, R. C., Shi, J., & Blobel, G. A. (2018). Exploiting genetic variation to uncover rules of transcription factor binding and chromatin accessibility. *Nature Communications*, 9(1). <https://doi.org/10.1038/s41467-018-03082-6>
- Belyi, V. A., Ak, P., Markert, E., Wang, H., Hu, W., Puzio-Kuter, A., & Levine, A. J. (2010). The Origins and Evolution of the p53 Family of Genes. *Cold Spring Harbor Perspectives in Biology*, 2(6). <https://doi.org/10.1101/cshperspect.a001198>

Bentley, D. R., Balasubramanian, S., Swerdlow, H. P., Smith, G. P., Milton, J., Brown, C. G., Hall, K. P., Evers, D. J., Barnes, C. L., Bignell, H. R., Boutell, J. M., Bryant, J., Carter, R. J., Keira Cheetham, R., Cox, A. J., Ellis, D. J., Flatbush, M. R., Gormley, N. A., Humphray, S. J., ... Smith, A. J. (2008). Accurate whole human genome sequencing using reversible terminator chemistry. *Nature*, 456(7218), 53–59.
<https://doi.org/10.1038/nature07517>

Biddie, S. C., John, S., Sabo, P. J., Thurman, R. E., Johnson, T. A., Schiltz, R. L., Miranda, T. B., Sung, M.-H., Trump, S., Lightman, S. L., Vinson, C., Stamatoyannopoulos, J. A., & Hager, G. L. (2011). Transcription factor AP1 potentiates chromatin accessibility and glucocorticoid receptor binding. *Molecular Cell*, 43(1), 145–155.
<https://doi.org/10.1016/j.molcel.2011.06.016>

Biscotti, M. A., Barucca, M., Carducci, F., Forconi, M., & Canapa, A. (2019). The p53 gene family in vertebrates: Evolutionary considerations. *Journal of Experimental Zoology Part B: Molecular and Developmental Evolution*, 0(0). <https://doi.org/10.1002/jez.b.22856>
Blaser, H., Dostert, C., Mak, T. W., & Brenner, D. (2016). TNF and ROS Crosstalk in Inflammation. *Trends in Cell Biology*, 26(4), 249–261.
<https://doi.org/10.1016/j.tcb.2015.12.002>

Boettcher, S., Miller, P. G., Sharma, R., McConkey, M., Leventhal, M., Krivtsov, A. V., Giacomelli, A. O., Wong, W., Kim, J., Chao, S., Kurppa, K. J., Yang, X., Milenkovic, K., Piccioni, F., Root, D. E., Rücker, F. G., Flamand, Y., Neuberg, D., Lindsley, R. C., ... Ebert, B. L. (2019). A dominant-negative effect drives selection of TP53 missense mutations in myeloid malignancies. *Science*, 365(6453), 599–604.
<https://doi.org/10.1126/science.aax3649>

- Botcheva, K., McCorkle, S. R., McCombie, W., Dunn, J. J., & Anderson, C. W. (2011). Distinct p53 genomic binding patterns in normal and cancer-derived human cells. *Cell Cycle*, 10(24), 4237–4249. <https://doi.org/10.4161/cc.10.24.18383>
- Bowen, M. E., McClendon, J., Long, H. K., Sorayya, A., Van Nostrand, J. L., Wysocka, J., & Attardi, L. D. (2019). The Spatiotemporal Pattern and Intensity of p53 Activation Dictates Phenotypic Diversity in p53-Driven Developmental Syndromes. *Developmental Cell*, 50(2), 212-228.e6. <https://doi.org/10.1016/j.devcel.2019.05.015>
- Brady, C. A., Jiang, D., Mello, S. S., Johnson, T. M., Jarvis, L. A., Kozak, M. M., Kenzelmann Broz, D., Basak, S., Park, E. J., McLaughlin, M. E., Karnezis, A. N., & Attardi, L. D. (2011). Distinct p53 transcriptional programs dictate acute DNA-damage responses and tumor suppression. *Cell*, 145, 571–583. <https://doi.org/10.1016/j.cell.2011.03.035>
- Buenrostro, J. D., Giresi, P. G., Zaba, L. C., Chang, H. Y., & Greenleaf, W. J. (2013). Transposition of native chromatin for fast and sensitive epigenomic profiling of open chromatin, DNA-binding proteins and nucleosome position. *Nat Methods*, 10, 1213–1218. <https://doi.org/10.1038/nmeth.2688>
- Burgess, A., Chia, K. M., Haupt, S., Thomas, D., Haupt, Y., & Lim, E. (2016a). Clinical Overview of MDM2/X-Targeted Therapies. *Frontiers in Oncology*, 6. <https://doi.org/10.3389/fonc.2016.00007>
- Burgess, A., Chia, K. M., Haupt, S., Thomas, D., Haupt, Y., & Lim, E. (2016b). Clinical Overview of MDM2/X-Targeted Therapies. *Frontiers in Oncology*, 6. <https://doi.org/10.3389/fonc.2016.00007>

Cadet, J., & Wagner, J. R. (2013). DNA Base Damage by Reactive Oxygen Species, Oxidizing Agents, and UV Radiation. *Cold Spring Harbor Perspectives in Biology*, 5(2).

<https://doi.org/10.1101/cshperspect.a012559>

Candau, R., Scolnick, D. M., Darpino, P., Ying, C. Y., Halazonetis, T. D., & Berger, S. L. (1997). Two tandem and independent sub-activation domains in the amino terminus of p53 require the adaptor complex for activity. *Oncogene*, 15(7), 807–816.

<https://doi.org/10.1038/sj.onc.1201244>

Carninci, P., Sandelin, A., Lenhard, B., Katayama, S., Shimokawa, K., Ponjavic, J., Semple, C. A. M., Taylor, M. S., Engström, P. G., Frith, M. C., Forrest, A. R. R., Alkema, W. B., Tan, S. L., Plessy, C., Kodzius, R., Ravasi, T., Kasukawa, T., Fukuda, S., Kanamori-Katayama, M., ... Hayashizaki, Y. (2006). Genome-wide analysis of mammalian promoter architecture and evolution. *Nature Genetics*, 38(6), 626–635.

<https://doi.org/10.1038/ng1789>

Carroll, D. K., Carroll, J. S., Leong, C.-O., Cheng, F., Brown, M., Mills, A. A., Brugge, J. S., & Ellisen, L. W. (2006). P63 regulates an adhesion programme and cell survival in epithelial cells. *Nature Cell Biology*, 8(6), 551. <https://doi.org/10.1038/ncb1420>

Catizone, A. N., Good, C. R., Alexander, K. A., Berger, S. L., & Sammons, M. A. (2019). Comparison of genotoxic versus nongenotoxic stabilization of p53 provides insight into parallel stress-responsive transcriptional networks. *Cell Cycle (Georgetown, Tex.)*, 18(8), 809–823. <https://doi.org/10.1080/15384101.2019.1593643>

Catizone, A. N., Uzunbas, G. K., Celadova, P., Kuang, S., Bose, D., & Sammons, M. A. (2019). Locally acting transcription factors are required for p53-dependent *cis*-regulatory element activity. *BioRxiv*, 761387. <https://doi.org/10.1101/761387>

Catizone, A. N., Uzunbas, G. K., Celadova, P., Kuang, S., Bose, D., & Sammons, M. A. (2020a).

Locally acting transcription factors regulate p53-dependent cis-regulatory element activity. *Nucleic Acids Research*. <https://doi.org/10.1093/nar/gkaa147>

Catizone, A. N., Uzunbas, G. K., Celadova, P., Kuang, S., Bose, D., & Sammons, M. A. (2020b).

Locally acting transcription factors regulate p53-dependent cis-regulatory element activity. *Nucleic Acids Research*. <https://doi.org/10.1093/nar/gkaa147>

Chang, C.-J., Chao, C.-H., Xia, W., Yang, J.-Y., Xiong, Y., Li, C.-W., Yu, W.-H., Rehman, S.

K., Hsu, J. L., Lee, H.-H., Liu, M., Chen, C.-T., Yu, D., & Hung, M.-C. (2011a). P53 regulates epithelial–mesenchymal transition and stem cell properties through modulating miRNAs. *Nature Cell Biology*, 13(3), 317–323. <https://doi.org/10.1038/ncb2173>

Chang, C.-J., Chao, C.-H., Xia, W., Yang, J.-Y., Xiong, Y., Li, C.-W., Yu, W.-H., Rehman, S.

K., Hsu, J. L., Lee, H.-H., Liu, M., Chen, C.-T., Yu, D., & Hung, M.-C. (2011b). P53 regulates epithelial–mesenchymal transition and stem cell properties through modulating miRNAs. *Nature Cell Biology*, 13(3), 317–323. <https://doi.org/10.1038/ncb2173>

Chang, G. S., Chen, X. A., Park, B., Rhee, H. S., Li, P., Han, K. H., Mishra, T., Chan-Salis, K.

Y., Li, Y., Hardison, R. C., Wang, Y., & Pugh, B. F. (2014a). A Comprehensive and High Resolution Genome-wide Response of p53 to Stress. *Cell Reports*, 8(2), 514–527. <https://doi.org/10.1016/j.celrep.2014.06.030>

Chang, G. S., Chen, X. A., Park, B., Rhee, H. S., Li, P., Han, K. H., Mishra, T., Chan-Salis, K.

Y., Li, Y., Hardison, R. C., Wang, Y., & Pugh, B. F. (2014b). A Comprehensive and High Resolution Genome-wide Response of p53 to Stress. *Cell Reports*, 8(2), 514–527. <https://doi.org/10.1016/j.celrep.2014.06.030>

Chen, J. (2016). The Cell-Cycle Arrest and Apoptotic Functions of p53 in Tumor Initiation and Progression. *Cold Spring Harbor Perspectives in Medicine*, 6(3), a026104.

<https://doi.org/10.1101/cshperspect.a026104>

Chen, X., Farmer, G., Zhu, H., Prywes, R., & Prives, C. (1993). Cooperative DNA binding of p53 with TFIID (TBP): A possible mechanism for transcriptional activation. *Genes & Development*, 7(10), 1837–1849. <https://doi.org/10.1101/gad.7.10.1837>

Chen, Xi, Chen, J., Gan, S., Guan, H., Zhou, Y., Ouyang, Q., & Shi, J. (2013). DNA damage strength modulates a bimodal switch of p53 dynamics for cell-fate control. *BMC Biology*, 11(1), 73. <https://doi.org/10.1186/1741-7007-11-73>

Chien, Y., Scuoppo, C., Wang, X., Fang, X., Balgley, B., Bolden, J. E., Premsrirut, P., Luo, W., Chicas, A., Lee, C. S., Kogan, S. C., & Lowe, S. W. (2011a). Control of the senescence-associated secretory phenotype by NF-κB promotes senescence and enhances chemosensitivity. *Genes & Development*, 25(20), 2125–2136.

<https://doi.org/10.1101/gad.17276711>

Chien, Y., Scuoppo, C., Wang, X., Fang, X., Balgley, B., Bolden, J. E., Premsrirut, P., Luo, W., Chicas, A., Lee, C. S., Kogan, S. C., & Lowe, S. W. (2011b). Control of the senescence-associated secretory phenotype by NF-κB promotes senescence and enhances chemosensitivity. *Genes & Development*, 25(20), 2125–2136.

<https://doi.org/10.1101/gad.17276711>

Childs, B. G., Baker, D. J., Kirkland, J. L., Campisi, J., & van Deursen, J. M. (2014). Senescence and apoptosis: Dueling or complementary cell fates? *EMBO Reports*, 15(11), 1139–1153. <https://doi.org/10.15252/embr.201439245>

- Chillemi, G., Kehrloesser, S., Bernassola, F., Desideri, A., Dötsch, V., Levine, A. J., & Melino, G. (2017). Structural Evolution and Dynamics of the p53 Proteins. *Cold Spring Harbor Perspectives in Medicine*, 7(4). <https://doi.org/10.1101/cshperspect.a028308>
- Cohen, D. M., Lim, H.-W., Won, K.-J., & Steger, D. J. (2018). Shared nucleotide flanks confer transcriptional competency to bZip core motifs. *Nucleic Acids Research*, 46(16), 8371–8384. <https://doi.org/10.1093/nar/gky681>
- Coppé, J.-P., Desprez, P.-Y., Krtolica, A., & Campisi, J. (2010). The Senescence-Associated Secretory Phenotype: The Dark Side of Tumor Suppression. *Annual Review of Pathology*, 5, 99–118. <https://doi.org/10.1146/annurev-pathol-121808-102144>
- Coppé, J.-P., Patil, C. K., Rodier, F., Sun, Y., Muñoz, D. P., Goldstein, J., Nelson, P. S., Desprez, P.-Y., & Campisi, J. (2008). Senescence-Associated Secretory Phenotypes Reveal Cell-Nonautonomous Functions of Oncogenic RAS and the p53 Tumor Suppressor. *PLOS Biology*, 6(12), e301. <https://doi.org/10.1371/journal.pbio.0060301>
- Cui, H., Li, X., Han, C., Wang, Q.-E., Wang, H., Ding, H.-F., Zhang, J., & Yan, C. (2016). The Stress-responsive Gene ATF3 Mediates Dichotomous UV Responses by Regulating the Tip60 and p53 Proteins. *The Journal of Biological Chemistry*, 291(20), 10847–10857. <https://doi.org/10.1074/jbc.M115.713099>
- Daino, K., Ichimura, S., & Nenoi, M. (2006). Both the basal transcriptional activity of the GADD45A gene and its enhancement after ionizing irradiation are mediated by AP-1 element. *Biochimica et Biophysica Acta (BBA) - Gene Structure and Expression*, 1759(10), 458–469. <https://doi.org/10.1016/j.bbagen.2006.09.005>
- D'Errico, M., Teson, M., Calcagnile, A., Proietti De Santis, L., Nikaido, O., Botta, E., Zambruno, G., Stefanini, M., & Dogliotti, E. (2003). Apoptosis and efficient repair of

DNA damage protect human keratinocytes against UVB. *Cell Death Differ*, 10, 754–756.

<https://doi.org/10.1038/sj.cdd.4401224>

Donehower, L. A., Soussi, T., Korkut, A., Liu, Y., Schultz, A., Cardenas, M., Li, X., Babur, O.,

Hsu, T.-K., Lichtarge, O., Weinstein, J. N., Akbani, R., & Wheeler, D. A. (2019).

Integrated Analysis of TP53 Gene and Pathway Alterations in The Cancer Genome Atlas.

Cell Reports, 28(5), 1370-1384.e5. <https://doi.org/10.1016/j.celrep.2019.07.001>

El-Deiry, W. S., Kern, S. E., Pietenpol, J. A., Kinzler, K. W., & Vogelstein, B. (1992a).

Definition of a consensus binding site for p53. *Nature Genetics*, 1(1), 45–49.

<https://doi.org/10.1038/ng0492-45>

El-Deiry, W. S., Kern, S. E., Pietenpol, J. A., Kinzler, K. W., & Vogelstein, B. (1992b).

Definition of a consensus binding site for p53. *Nature Genetics*, 1(1), 45–49.

<https://doi.org/10.1038/ng0492-45>

Espinosa, Joaquin M, & Emerson, B. M. (2001). Transcriptional Regulation by p53 through

Intrinsic DNA/Chromatin Binding and Site-Directed Cofactor Recruitment. *Molecular*

Cell, 8(1), 57–69. [https://doi.org/10.1016/S1097-2765\(01\)00283-0](https://doi.org/10.1016/S1097-2765(01)00283-0)

Espinosa, Joaquín M., Verdun, R. E., & Emerson, B. M. (2003). P53 functions through stress- and promoter-specific recruitment of transcription initiation components before and after DNA damage. *Molecular Cell*, 12(4), 1015–1027.

Fischer, M. (2017). Census and evaluation of p53 target genes. *Oncogene*, 36(28), 3943–3956.

<https://doi.org/10.1038/onc.2016.502>

Fischer, M. (2017). Census and evaluation of p53 target genes. *Oncogene*, 36(28), 3943–3956.

<https://doi.org/10.1038/onc.2016.502>

- Fischer, Martin. (2019). Conservation and divergence of the p53 gene regulatory network between mice and humans. *Oncogene*. <https://doi.org/10.1038/s41388-019-0706-9>
- Fischer, Martin, Quaas, M., Steiner, L., & Engeland, K. (2016). The p53-p21-DREAM-CDE/CHR pathway regulates G2/M cell cycle genes. *Nucleic Acids Research*, 44(1), 164–174. <https://doi.org/10.1093/nar/gkv927>
- Fischer, Martin, Steiner, L., & Engeland, K. (2014). The transcription factor p53: Not a repressor, solely an activator. *Cell Cycle (Georgetown, Tex.)*, 13(19), 3037–3058. <https://doi.org/10.4161/15384101.2014.949083>
- Flores, E. R., Tsai, K. Y., Crowley, D., Sengupta, S., Yang, A., McKeon, F., & Jacks, T. (2002). P63 and p73 are required for p53-dependent apoptosis in response to DNA damage. *Nature*, 416(6880), 560–564. <https://doi.org/10.1038/416560a>
- Freed-Pastor, W. A., & Prives, C. (2012). Mutant p53: One name, many proteins. *Genes & Development*, 26(12), 1268–1286. <https://doi.org/10.1101/gad.190678.112>
- Frith, M. C., Ponjavic, J., Fredman, D., Kai, C., Kawai, J., Carninci, P., Hayashizaki, Y., Hayashizaki, Y., & Sandelin, A. (2006). Evolutionary turnover of mammalian transcription start sites. *Genome Research*, 16(6), 713–722. <https://doi.org/10.1101/gr.5031006>
- Furlong, E. E. M., & Levine, M. (2018). Developmental enhancers and chromosome topology. *Science (New York, N.Y.)*, 361(6409), 1341–1345. <https://doi.org/10.1126/science.aau0320>
- Fuxman Bass, J. I., Sahni, N., Shrestha, S., Garcia-Gonzalez, A., Mori, A., Bhat, N., Yi, S., Hill, D. E., Vidal, M., & Walhout, A. J. M. (2015). Human Gene-Centered Transcription

Factor Networks for Enhancers and Disease Variants. *Cell*, 161(3), 661–673.

<https://doi.org/10.1016/j.cell.2015.03.003>

Gaertner, B., & Zeitlinger, J. (2014). RNA polymerase II pausing during development.

Development, 141(6), 1179–1183. <https://doi.org/10.1242/dev.088492>

Gao, X. D., Rodríguez, T. C., & Sontheimer, E. J. (2019). Adapting dCas9-APEX2 for subnuclear proteomic profiling. In *Methods in Enzymology* (Vol. 616, pp. 365–383). Elsevier. <https://doi.org/10.1016/bs.mie.2018.10.030>

Gao, X. D., Tu, L.-C., Mir, A., Rodriguez, T., Ding, Y., Leszyk, J., Dekker, J., Shaffer, S. A., Zhu, L. J., Wolfe, S. A., & Sontheimer, E. J. (2018). C-BERST: Defining subnuclear proteomic landscapes at genomic elements with dCas9–APEX2. *Nature Methods*, 15(6), 433–436. <https://doi.org/10.1038/s41592-018-0006-2>

Georgakopoulou, E., Evangelou, K., Havaki, S., Townsend, P., Kanavaros, P., & Gorgoulis, V. G. (2016). Apoptosis or senescence? Which exit route do epithelial cells and fibroblasts preferentially follow? *Mechanisms of Ageing and Development*, 156, 17–24.

<https://doi.org/10.1016/j.mad.2016.03.010>

Gilchrist, M., Thorsson, V., Li, B., Rust, A. G., Korb, M., Roach, J. C., Kennedy, K., Hai, T., Bolouri, H., & Aderem, A. (2006). Systems biology approaches identify ATF3 as a negative regulator of Toll-like receptor 4. *Nature*, 441(7090), 173–178.

<https://doi.org/10.1038/nature04768>

Gonfloni, S., Caputo, V., & Iannizzotto, V. (2015). P63 in health and cancer. *International Journal of Developmental Biology*, 59(1-2-3), 87–93.

<https://doi.org/10.1387/ijdb.150045sg>

- Guertin, M. J., & Lis, J. T. (2013). Mechanisms by which transcription factors gain access to target sequence elements in chromatin. *Current Opinion in Genetics & Development*, 23(2), 116–123. <https://doi.org/10.1016/j.gde.2012.11.008>
- Haferkamp, S., Tran, S. L., Becker, T. M., Scurr, L. L., Kefford, R. F., & Rizos, H. (2009). The relative contributions of the p53 and pRb pathways in oncogene-induced melanocyte senescence. *Aging (Albany NY)*, 1, 542–556. <https://doi.org/10.18632/aging.100051>
- Hafner, A., Bulyk, M. L., Jambhekar, A., & Lahav, G. (2019). The multiple mechanisms that regulate p53 activity and cell fate. *Nature Reviews Molecular Cell Biology*. <https://doi.org/10.1038/s41580-019-0110-x>
- Hafner, A., Kublo, L., Tsabar, M., Lahav, G., & Stewart-Ornstein, J. (2020). Identification of universal and cell-type specific p53 DNA binding. *BMC Molecular and Cell Biology*, 21(1), 5. <https://doi.org/10.1186/s12860-020-00251-8>
- Hafner, A., Lahav, G., & Stewart-Ornstein, J. (2017). Stereotyped p53 binding tuned by chromatin accessibility. *BioRxiv*, 177667.
- Hafner, A., Stewart-Ornstein, J., Purvis, J. E., Forrester, W. C., Bulyk, M. L., & Lahav, G. (2017a). P53 pulses lead to distinct patterns of gene expression albeit similar DNA-binding dynamics. *Nature Structural & Molecular Biology*, 24(10), 840–847. <https://doi.org/10.1038/nsmb.3452>
- Hafner, A., Stewart-Ornstein, J., Purvis, J. E., Forrester, W. C., Bulyk, M. L., & Lahav, G. (2017b). P53 pulses lead to distinct patterns of gene expression albeit similar DNA-binding dynamics. *Nature Structural & Molecular Biology*, 24(10), 840–847. <https://doi.org/10.1038/nsmb.3452>

- Haupt, Y., Maya, R., Kazaz, A., & Oren, M. (1997). Mdm2 promotes the rapid degradation of p53. *Nature*, 387(6630), 296–299. <https://doi.org/10.1038/387296a0>
- Hayden, M. S., & Ghosh, S. (2008). Shared principles in NF-kappaB signaling. *Cell*, 132(3), 344–362. <https://doi.org/10.1016/j.cell.2008.01.020>
- Heinz, S., Benner, C., Spann, N., Bertolino, E., Lin, Y. C., Laslo, P., Cheng, J. X., Murre, C., Singh, H., & Glass, C. K. (2010a). Simple combinations of lineage-determining transcription factors prime cis-regulatory elements required for macrophage and B cell identities. *Molecular Cell*, 38(4), 576–589. <https://doi.org/10.1016/j.molcel.2010.05.004>
- Heinz, S., Benner, C., Spann, N., Bertolino, E., Lin, Y. C., Laslo, P., Cheng, J. X., Murre, C., Singh, H., & Glass, C. K. (2010b). Simple combinations of lineage-determining transcription factors prime cis-regulatory elements required for macrophage and B cell identities. *Molecular Cell*, 38(4), 576–589. <https://doi.org/10.1016/j.molcel.2010.05.004>
- Heinz, S., Romanoski, C. E., Benner, C., & Glass, C. K. (2015). The selection and function of cell type-specific enhancers. *Nature Reviews Molecular Cell Biology*, 16(3), 144–154. <https://doi.org/10.1038/nrm3949>
- Henseleit, U., Zhang, J., Wanner, R., Haase, I., Kolde, G., & Rosenbach, T. (1997). Role of p53 in UVB-induced apoptosis in human HaCaT keratinocytes. *J Invest Dermatol*, 109, 722–727. <https://doi.org/10.1111/1523-1747.ep12340708>
- Herz, H. M., Hu, D., & Shilatifard, A. (2014). Enhancer malfunction in cancer. *Mol Cell*, 53, 859–866. <https://doi.org/10.1016/j.molcel.2014.02.033>
- Herzog, G., Joerger, A. C., Shmueli, M. D., Fersht, A. R., Gazit, E., & Segal, D. (2012). Evaluating Drosophila p53 as a Model System for Studying Cancer Mutations. *Journal of Biological Chemistry*, 287(53), 44330–44337. <https://doi.org/10.1074/jbc.M112.417980>

- Horn, H. F., & Vousden, K. H. (2007). Coping with stress: Multiple ways to activate p53. *Oncogene*, 26(9), 1306–1316. <https://doi.org/10.1038/sj.onc.1210263>
- Hu, Z., & Tee, W.-W. (2017). Enhancers and chromatin structures: Regulatory hubs in gene expression and diseases. *Bioscience Reports*, 37(2). <https://doi.org/10.1042/BSR20160183>
- Iannetti, A., Ledoux, A. C., Tudhope, S. J., Sellier, H., Zhao, B., Mowla, S., Moore, A., Hummerich, H., Gewurz, B. E., Cockell, S. J., Jat, P. S., Willmore, E., & Perkins, N. D. (2014). Regulation of p53 and Rb Links the Alternative NF- κ B Pathway to EZH2 Expression and Cell Senescence. *PLOS Genetics*, 10(9), e1004642. <https://doi.org/10.1371/journal.pgen.1004642>
- Inoue, F., Kircher, M., Martin, B., Cooper, G. M., Witten, D. M., McManus, M. T., Ahituv, N., & Shendure, J. (2017). A systematic comparison reveals substantial differences in chromosomal versus episomal encoding of enhancer activity. *Genome Research*, 27(1), 38–52.
- Itahana, K., Dimri, G., & Campisi, J. (2001). Regulation of cellular senescence by p53. *European Journal of Biochemistry*, 268(10), 2784–2791. <https://doi.org/10.1046/j.1432-1327.2001.02228.x>
- Iwafuchi-Doi, M., & Zaret, K. S. (2016). Cell fate control by pioneer transcription factors. *Development*, 143, 1833–1837. <https://doi.org/10.1242/dev.133900>
- Jain, A. K., & Barton, M. C. (2018). p53: Emerging roles in stem cells, development and beyond. *Development*, 145(8). <https://doi.org/10.1242/dev.158360>

- Jain, D., Baldi, S., Zabel, A., Straub, T., & Becker, P. B. (2015). Active promoters give rise to false positive ‘Phantom Peaks’ in ChIP-seq experiments. *Nucleic Acids Research*, 43(14), 6959–6968. <https://doi.org/10.1093/nar/gkv637>
- Joerger, A. C., Rajagopalan, S., Natan, E., Veprintsev, D. B., Robinson, C. V., & Fersht, A. R. (2009). Structural evolution of p53, p63, and p73: Implication for heterotetramer formation. *Proceedings of the National Academy of Sciences*, 106(42), 17705–17710. <https://doi.org/10.1073/pnas.0905867106>
- Jolma, A., Yan, J., Whitington, T., Toivonen, J., Nitta, K. R., Rastas, P., Morgunova, E., Enge, M., Taipale, M., Wei, G., Palin, K., Vaquerizas, J. M., Vincentelli, R., Luscombe, N. M., Hughes, T. R., Lemaire, P., Ukkonen, E., Kivioja, T., & Taipale, J. (2013). DNA-binding specificities of human transcription factors. *Cell*, 152(1–2), 327–339. <https://doi.org/10.1016/j.cell.2012.12.009>
- Kannan, K., Amariglio, N., Rechavi, G., & Givol, D. (2000). Profile of gene expression regulated by induced p53: Connection to the TGF-beta family. *FEBS Letters*, 470(1), 77–82. [https://doi.org/10.1016/s0014-5793\(00\)01291-6](https://doi.org/10.1016/s0014-5793(00)01291-6)
- Karsli Uzunbas, G., Ahmed, F., & Sammons, M. A. (2019a). Control of p53-dependent transcription and enhancer activity by the p53 family member p63. *The Journal of Biological Chemistry*. <https://doi.org/10.1074/jbc.RA119.007965>
- Karsli Uzunbas, G., Ahmed, F., & Sammons, M. A. (2019b). Control of p53-dependent transcription and enhancer activity by the p53 family member p63. *The Journal of Biological Chemistry*. <https://doi.org/10.1074/jbc.RA119.007965>
- Kastenhuber, E. R., & Lowe, S. W. (2017). Putting p53 in Context. *Cell*, 170(6), 1062–1078. <https://doi.org/10.1016/j.cell.2017.08.028>

- Khan, A., Fornes, O., Stigliani, A., Gheorghe, M., Castro-Mondragon, J. A., van der Lee, R., Bessy, A., Chèneby, J., Kulkarni, S. R., Tan, G., Baranasic, D., Arenillas, D. J., Sandelin, A., Vandepoele, K., Lenhard, B., Ballester, B., Wasserman, W. W., Parcy, F., & Mathelier, A. (2018). JASPAR 2018: Update of the open-access database of transcription factor binding profiles and its web framework. *Nucleic Acids Research*, 46(D1), D1284. <https://doi.org/10.1093/nar/gkx1188>
- Khoo, K. H., Hoe, K. K., Verma, C. S., & Lane, D. P. (2014). Drugging the p53 pathway: Understanding the route to clinical efficacy. *Nature Reviews Drug Discovery*, 13(3), 217–236. <https://doi.org/10.1038/nrd4236>
- Khoo, K. H., Verma, C. S., & Lane, D. P. (2014). Drugging the p53 pathway: Understanding the route to clinical efficacy. *Nature Reviews Drug Discovery*, 13(3), 217. <https://doi.org/10.1038/nrd4236>
- Kocik, J., Machula, M., Wisniewska, A., Surmiak, E., Holak, T. A., & Skalniak, L. (2019). Helping the Released Guardian: Drug Combinations for Supporting the Anticancer Activity of HDM2 (MDM2) Antagonists. *Cancers*, 11(7). <https://doi.org/10.3390/cancers11071014>
- Korkmaz, G., Lopes, R., Ugalde, A. P., Nevedomskaya, E., Han, R., Myacheva, K., Zwart, W., Elkon, R., & Agami, R. (2016). Functional genetic screens for enhancer elements in the human genome using CRISPR-Cas9. *Nature Biotechnology*, 34(2), 192–198. <https://doi.org/10.1038/nbt.3450>
- Korthout, T., Poramba-Liyanage, D. W., van Kruijsbergen, I., Verzijlbergen, K. F., van Gemert, F. P. A., van Welsem, T., & van Leeuwen, F. (2018). Decoding the chromatin proteome

of a single genomic locus by DNA sequencing. *PLOS Biology*, 16(7), e2005542.

<https://doi.org/10.1371/journal.pbio.2005542>

Koster, M. I., Kim, S., Mills, A. A., DeMayo, F. J., & Roop, D. R. (2004). P63 is the molecular switch for initiation of an epithelial stratification program. *Genes & Development*, 18(2), 126–131. <https://doi.org/10.1101/gad.1165104>

Kotler, E., Shani, O., Goldfeld, G., Lotan-Pompan, M., Tarcic, O., Gershoni, A., Hopf, T. A., Marks, D. S., Oren, M., & Segal, E. (2018). A Systematic p53 Mutation Library Links Differential Functional Impact to Cancer Mutation Pattern and Evolutionary Conservation. *Molecular Cell*, 71(1), 178-190.e8.

<https://doi.org/10.1016/j.molcel.2018.06.012>

Koutsodontis, G., Tentes, I., Papakosta, P., Moustakas, A., & Kardassis, D. (2001). Sp1 Plays a Critical Role in the Transcriptional Activation of the Human Cyclin-dependent Kinase Inhibitor p21^{WAF1/Cip1} Gene by the p53 Tumor Suppressor Protein. *Journal of Biological Chemistry*, 276(31), 29116–29125. <https://doi.org/10.1074/jbc.M104130200>

Kouwenhoven, E. N., Oti, M., Niehues, H., van Heeringen, S. J., Schalkwijk, J., Stunnenberg, H. G., van Bokhoven, H., & Zhou, H. (2015). Transcription factor p63 bookmarks and regulates dynamic enhancers during epidermal differentiation. *EMBO Reports*, 16(7), 863–878. <https://doi.org/10.15252/embr.201439941>

Kress, M., May, E., Cassingena, R., & May, P. (1979). Simian virus 40-transformed cells express new species of proteins precipitable by anti-simian virus 40 tumor serum. *Journal of Virology*, 31(2), 472–483.

Kruse, J.-P., & Gu, W. (2008). SnapShot: P53 Posttranslational Modifications. *Cell*, 133(5), 930-30.e1. <https://doi.org/10.1016/j.cell.2008.05.020>

- Kulkarni, M. M., & Arnosti, D. N. (2003). Information display by transcriptional enhancers. *Development*, 130(26), 6569–6575. <https://doi.org/10.1242/dev.00890>
- Levine, A. J. (1997). P53, the Cellular Gatekeeper for Growth and Division. *Cell*, 88(3), 323–331. [https://doi.org/10.1016/S0092-8674\(00\)81871-1](https://doi.org/10.1016/S0092-8674(00)81871-1)
- Levrero, M., Laurenzi, V. D., Costanzo, A., Gong, J., Wang, J. Y., & Melino, G. (2000). The p53/p63/p73 family of transcription factors: Overlapping and distinct functions. *J Cell Sci*, 113(10), 1661–1670.
- Li, H., Zhang, Y., Ströse, A., Tedesco, D., Gurova, K., & Selivanova, G. (2014). Integrated high-throughput analysis identifies Sp1 as a crucial determinant of p53-mediated apoptosis. *Cell Death and Differentiation*, 21(9), 1493–1502. <https://doi.org/10.1038/cdd.2014.69>
- Li, L., Wang, Y., Torkelson, J. L., Shankar, G., Pattison, J. M., Zhen, H. H., Fang, F., Duren, Z., Xin, J., Gaddam, S., Melo, S. P., Piekos, S. N., Li, J., Liaw, E. J., Chen, L., Li, R., Wernig, M., Wong, W. H., Chang, H. Y., & Oro, A. E. (2019). TFAP2C- and p63-Dependent Networks Sequentially Rearrange Chromatin Landscapes to Drive Human Epidermal Lineage Commitment. *Cell Stem Cell*. <https://doi.org/10.1016/j.stem.2018.12.012>
- Li, M., He, Y., Dubois, W., Wu, X., Shi, J., & Huang, J. (2012). Distinct Regulatory Mechanisms and Functions for p53-Activated and p53-Repressed DNA Damage Response Genes in Embryonic Stem Cells. *Molecular Cell*, 46(1), 30–42. <https://doi.org/10.1016/j.molcel.2012.01.020>
- Li, T., Kon, N., Jiang, L., Tan, M., Ludwig, T., Zhao, Y., Baer, R., & Gu, W. (2012). Tumor suppression in the absence of p53-mediated cell-cycle arrest, apoptosis, and senescence. *Cell*, 149, 1269–1283. <https://doi.org/10.1016/j.cell.2012.04.026>

- Li, X., Wu, L., Corsa, C. A. S., Kunkel, S., & Dou, Y. (2009). Two mammalian MOF complexes regulate transcription activation by distinct mechanisms. *Molecular Cell*, 36(2), 290–301. <https://doi.org/10.1016/j.molcel.2009.07.031>
- Lin-Shiao, E., Lan, Y., Coradin, M., Anderson, A., Donahue, G., Simpson, C. L., Sen, P., Saffie, R., Busino, L., Garcia, B. A., Berger, S. L., & Capell, B. C. (2018). KMT2D regulates p63 target enhancers to coordinate epithelial homeostasis. *Genes & Development*, 32(2), 181–193. <https://doi.org/10.1101/gad.306241.117>
- Lin-Shiao, E., Lan, Y., Welzenbach, J., Alexander, K. A., Zhang, Z., Knapp, M., Mangold, E., Sammons, M., Ludwig, K. U., & Berger, S. L. (2019). P63 establishes epithelial enhancers at critical craniofacial development genes. *Science Advances*, 5(5), eaaw0946. <https://doi.org/10.1126/sciadv.aaw0946>
- Linzer, D. I., & Levine, A. J. (1979). Characterization of a 54K dalton cellular SV40 tumor antigen present in SV40-transformed cells and uninfected embryonal carcinoma cells. *Cell*, 17(1), 43–52. [https://doi.org/10.1016/0092-8674\(79\)90293-9](https://doi.org/10.1016/0092-8674(79)90293-9)
- Lion, M., Raimondi, I., Donati, S., Jousson, O., Ciribilli, Y., & Inga, A. (2015). Evolution of p53 Transactivation Specificity through the Lens of a Yeast-Based Functional Assay. *PLOS ONE*, 10(2), e0116177. <https://doi.org/10.1371/journal.pone.0116177>
- Liu, X., Kraus, W. L., & Bai, X. (2015). Ready, Pause, Go: Regulation of RNA Polymerase II Pausing and Release by Cellular Signaling Pathways. *Trends in Biochemical Sciences*, 40(9), 516–525. <https://doi.org/10.1016/j.tibs.2015.07.003>
- Lo, K., & Smale, S. T. (1996). Generality of a functional initiator consensus sequence. *Gene*, 182(1–2), 13–22. [https://doi.org/10.1016/s0378-1119\(96\)00438-6](https://doi.org/10.1016/s0378-1119(96)00438-6)

Loewer, A., Batchelor, E., Gaglia, G., & Lahav, G. (2010a). Basal dynamics of p53 reveal transcriptionally attenuated pulses in cycling cells. *Cell*, 142(1), 89–100.

<https://doi.org/10.1016/j.cell.2010.05.031>

Loewer, A., Batchelor, E., Gaglia, G., & Lahav, G. (2010b). Basal dynamics of p53 reveal transcriptionally attenuated pulses in cycling cells. *Cell*, 142(1), 89–100.

<https://doi.org/10.1016/j.cell.2010.05.031>

Long, H. K., Prescott, S. L., & Wysocka, J. (2016). Ever-Changing Landscapes: Transcriptional Enhancers in Development and Evolution. *Cell*, 167(5), 1170–1187.

<https://doi.org/10.1016/j.cell.2016.09.018>

Lowe, J. M., Menendez, D., Bushel, P. R., Shatz, M., Kirk, E. L., Troester, M. A., Garantziotis, S., Fessler, M. B., & Resnick, M. A. (2014). P53 and NF-κB coregulate proinflammatory gene responses in human macrophages. *Cancer Research*, 74(8), 2182–2192.

<https://doi.org/10.1158/0008-5472.CAN-13-1070>

Luan, H. H., Wang, A., Hilliard, B. K., Carvalho, F., Rosen, C. E., Ahasic, A. M., Herzog, E. L., Kang, I., Pisani, M. A., Yu, S., Zhang, C., Ring, A. M., Young, L. H., & Medzhitov, R. (2019). GDF15 Is an Inflammation-Induced Central Mediator of Tissue Tolerance. *Cell*, 178(5), 1231-1244.e11. <https://doi.org/10.1016/j.cell.2019.07.033>

Maanen, V., S, J. M., Retèl, J., de Vries, J., & Pinedo, H. M. (1988). Mechanism of Action of Antitumor Drug Etoposide: A Review. *JNCI: Journal of the National Cancer Institute*, 80(19), 1526–1533. <https://doi.org/10.1093/jnci/80.19.1526>

Marión, R. M., Strati, K., Li, H., Murga, M., Blanco, R., Ortega, S., Fernandez-Capetillo, O., Serrano, M., & Blasco, M. A. (2009). A p53-mediated DNA damage response limits

reprogramming to ensure iPS cell genomic integrity. *Nature*, 460(7259), 1149–1153.

<https://doi.org/10.1038/nature08287>

Maximov, G. K., & Maximov, K. G. (2008). The Role of p53 Tumor-Suppressor Protein in

Apoptosis and Cancerogenesis. *Biotechnology & Biotechnological Equipment*, 22(2),

664–668. <https://doi.org/10.1080/13102818.2008.10817532>

McDade, S. S., Patel, D., Moran, M., Campbell, J., Fenwick, K., Kozarewa, I., Orr, N. J., Lord,

C. J., Ashworth, A. A., & McCance, D. J. (2014a). Genome-wide characterization reveals complex interplay between TP53 and TP63 in response to genotoxic stress. *Nucleic Acids Res*, 42, 6270–6285. <https://doi.org/10.1093/nar/gku299>

McDade, S. S., Patel, D., Moran, M., Campbell, J., Fenwick, K., Kozarewa, I., Orr, N. J., Lord,

C. J., Ashworth, A. A., & McCance, D. J. (2014b). Genome-wide characterization reveals complex interplay between TP53 and TP63 in response to genotoxic stress. *Nucleic Acids Res*, 42, 6270–6285. <https://doi.org/10.1093/nar/gku299>

McDowell, I. C., Barrera, A., D’Ippolito, A. M., Vockley, C. M., Hong, L. K., Leichter, S. M.,

Bartelt, L. C., Majoros, W. H., Song, L., Safi, A., Koçak, D. D., Gersbach, C. A.,

Hartemink, A. J., Crawford, G. E., Engelhardt, B. E., & Reddy, T. E. (2018a).

Glucocorticoid receptor recruits to enhancers and drives activation by motif-directed binding. *Genome Research*. <https://doi.org/10.1101/gr.233346.117>

McDowell, I. C., Barrera, A., D’Ippolito, A. M., Vockley, C. M., Hong, L. K., Leichter, S. M.,

Bartelt, L. C., Majoros, W. H., Song, L., Safi, A., Koçak, D. D., Gersbach, C. A.,

Hartemink, A. J., Crawford, G. E., Engelhardt, B. E., & Reddy, T. E. (2018b).

Glucocorticoid receptor recruits to enhancers and drives activation by motif-directed binding. *Genome Research*. <https://doi.org/10.1101/gr.233346.117>

- McKinley, K. L., & Cheeseman, I. M. (2017). Large-Scale Analysis of CRISPR/Cas9 Cell-Cycle Knockouts Reveals the Diversity of p53-Dependent Responses to Cell-Cycle Defects. *Developmental Cell*, 40(4), 405-420.e2. <https://doi.org/10.1016/j.devcel.2017.01.012>
- Meek, D. W. (2015). Regulation of the p53 response and its relationship to cancer. *The Biochemical Journal*, 469(3), 325–346. <https://doi.org/10.1042/BJ20150517>
- Mei, S., Qin, Q., Wu, Q., Sun, H., Zheng, R., Zang, C., Zhu, M., Wu, J., Shi, X., Taing, L., Liu, T., Brown, M., Meyer, C. A., & Liu, X. S. (2017). Cistrome Data Browser: A data portal for ChIP-Seq and chromatin accessibility data in human and mouse. *Nucleic Acids Research*, 45(D1), D658–D662. <https://doi.org/10.1093/nar/gkw983>
- Meikrantz, W., & Schlegel, R. (1995). Apoptosis and the cell cycle. *Journal of Cellular Biochemistry*, 58(2), 160–174. <https://doi.org/10.1002/jcb.240580205>
- Menendez, D., Nguyen, T. A., Freudenberg, J. M., Mathew, V. J., Anderson, C. W., Jothi, R., & Resnick, M. A. (2013). Diverse stresses dramatically alter genome-wide p53 binding and transactivation landscape in human cancer cells. *Nucleic Acids Res*, 41, 7286–7301. <https://doi.org/10.1093/nar/gkt504>
- Menendez, Daniel, Inga, A., & Resnick, M. A. (2009). The expanding universe of p53 targets. *Nature Reviews Cancer*, 9, 724–737. <https://doi.org/10.1038/nrc2730>
- Menendez, Daniel, Inga, A., Snipe, J., Krysiak, O., Schönfelder, G., & Resnick, M. A. (2007). A single-nucleotide polymorphism in a half-binding site creates p53 and estrogen receptor control of vascular endothelial growth factor receptor 1. *Molecular and Cellular Biology*, 27(7), 2590–2600. <https://doi.org/10.1128/MCB.01742-06>
- Menendez, Daniel, Snipe, J., Marzec, J., Innes, C. L., Polack, F. P., Caballero, M., Schurman, S. H., Kleeberger, S. R., & Resnick, M. A. (2019). P53-responsive TLR8 SNP enhances

human innate immune response to respiratory syncytial virus. *The Journal of Clinical Investigation*. <https://doi.org/10.1172/JCI128626>

Monteith, J. A., Mellert, H., Sammons, M. A., Kuswanto, L. A., Sykes, S. M., Resnick-Silverman, L., Manfredi, J. J., Berger, S. L., & McMahon, S. B. (2016). A rare DNA contact mutation in cancer confers p53 gain-of-function and tumor cell survival via TNFAIP8 induction. *Molecular Oncology*, 10(8), 1207–1220.
<https://doi.org/10.1016/j.molonc.2016.05.007>

Morris, S. A. (2016). Direct lineage reprogramming via pioneer factors; a detour through developmental gene regulatory networks. *Development*, 143, 2696–2705.
<https://doi.org/10.1242/dev.138263>

Natsume, T., Kiyomitsu, T., Saga, Y., & Kanemaki, M. T. (2016). Rapid Protein Depletion in Human Cells by Auxin-Inducible Degron Tagging with Short Homology Donors. *Cell Reports*, 15(1), 210–218. <https://doi.org/10.1016/j.celrep.2016.03.001>

Nguyen, T.-A. T., Grimm, S. A., Bushel, P. R., Li, J., Li, Y., Bennett, B. D., Lavender, C. A., Ward, J. M., Fargo, D. C., Anderson, C. W., Li, L., Resnick, M. A., & Menendez, D. (2018a). Revealing a human p53 universe. *Nucleic Acids Research*.

<https://doi.org/10.1093/nar/gky720>

Nguyen, T.-A. T., Grimm, S. A., Bushel, P. R., Li, J., Li, Y., Bennett, B. D., Lavender, C. A., Ward, J. M., Fargo, D. C., Anderson, C. W., Li, L., Resnick, M. A., & Menendez, D. (2018b). Revealing a human p53 universe. *Nucleic Acids Research*.

<https://doi.org/10.1093/nar/gky720>

Nikulenkov, F., Spinnler, C., Li, H., Tonelli, C., Shi, Y., Turunen, M., Kivioja, T., Ignatiev, I., Kel, A., Taipale, J., & Selivanova, G. (2012). Insights into p53 transcriptional function

via genome-wide chromatin occupancy and gene expression analysis. *Cell Death Differ*, 19, 1992–2002. <https://doi.org/10.1038/cdd.2012.89>

Paek, A. L., Liu, J. C., Loewer, A., Forrester, W. C., & Lahav, G. (2016a). Cell-to-Cell Variation in p53 Dynamics Leads to Fractional Killing. *Cell*, 165(3), 631–642.
<https://doi.org/10.1016/j.cell.2016.03.025>

Paek, A. L., Liu, J. C., Loewer, A., Forrester, W. C., & Lahav, G. (2016b). Cell-to-Cell Variation in p53 Dynamics Leads to Fractional Killing. *Cell*, 165(3), 631–642.
<https://doi.org/10.1016/j.cell.2016.03.025>

Paek, A. L., Liu, J. C., Loewer, A., Forrester, W. C., & Lahav, G. (2016c). Cell-to-Cell Variation in p53 Dynamics Leads to Fractional Killing. *Cell*, 165(3), 631–642.
<https://doi.org/10.1016/j.cell.2016.03.025>

Parrinello, S., Samper, E., Krtolica, A., Goldstein, J., Melov, S., & Campisi, J. (2003). Oxygen sensitivity severely limits the replicative lifespan of murine fibroblasts. *Nature Cell Biology*, 5(8), 741–747. <https://doi.org/10.1038/ncb1024>

Patel, S., Alvarez-Guaita, A., Melvin, A., Rimmington, D., Dattilo, A., Miedzybrodzka, E. L., Cimino, I., Maurin, A.-C., Roberts, G. P., Meek, C. L., Virtue, S., Sparks, L. M., Parsons, S. A., Redman, L. M., Bray, G. A., Liou, A. P., Woods, R. M., Parry, S. A., Jeppesen, P. B., ... O’Rahilly, S. (2019). GDF15 Provides an Endocrine Signal of Nutritional Stress in Mice and Humans. *Cell Metabolism*, 29(3), 707-718.e8.

<https://doi.org/10.1016/j.cmet.2018.12.016>

Pattison, J. M., Melo, S. P., Piekos, S. N., Torkelson, J. L., Bashkirova, E., Mumbach, M. R., Rajasingh, C., Zhen, H. H., Li, L., Liaw, E., Alber, D., Rubin, A. J., Shankar, G., Bao, X., Chang, H. Y., Khavari, P. A., & Oro, A. E. (2018). Retinoic acid and BMP4 cooperate

with p63 to alter chromatin dynamics during surface epithelial commitment. *Nature Genetics*, 50(12), 1658. <https://doi.org/10.1038/s41588-018-0263-0>

Phanstiel, D. H., Van Bortle, K., Spacek, D., Hess, G. T., Shamim, M. S., Machol, I., Love, M. I., Aiden, E. L., Bassik, M. C., & Snyder, M. P. (2017). Static and Dynamic DNA Loops form AP-1-Bound Activation Hubs during Macrophage Development. *Molecular Cell*, 67(6), 1037-1048.e6. <https://doi.org/10.1016/j.molcel.2017.08.006>

Pierce, J. W., Schoenleber, R., Jesmok, G., Best, J., Moore, S. A., Collins, T., & Gerritsen, M. E. (1997). Novel inhibitors of cytokine-induced IkappaBalpha phosphorylation and endothelial cell adhesion molecule expression show anti-inflammatory effects in vivo. *The Journal of Biological Chemistry*, 272(34), 21096–21103.

Platt, J. L., Salama, R., Smythies, J., Choudhry, H., Davies, J. O., Hughes, J. R., Ratcliffe, P. J., & Mole, D. R. (2016). Capture-C reveals preformed chromatin interactions between HIF-binding sites and distant promoters. *EMBO Reports*, 17(10), 1410–1421.
<https://doi.org/10.15252/embr.201642198>

Powell, E., Piwnica-Worms, D., & Piwnica-Worms, H. (2014). Contribution of p53 to metastasis. *Cancer Discovery*, 4(4), 405–414. <https://doi.org/10.1158/2159-8290.CD-13-0136>

Pucci, B., Kasten, M., & Giordano, A. (2000). Cell Cycle and Apoptosis. *Neoplasia (New York, N.Y.)*, 2(4), 291–299.

Purvis, J. E., Karhohs, K. W., Mock, C., Batchelor, E., Loewer, A., & Lahav, G. (2012a). P53 dynamics control cell fate. *Science (New York, N.Y.)*, 336(6087), 1440–1444.
<https://doi.org/10.1126/science.1218351>

Purvis, J. E., Karhohs, K. W., Mock, C., Batchelor, E., Loewer, A., & Lahav, G. (2012b). P53 dynamics control cell fate. *Science (New York, N.Y.)*, 336(6087), 1440–1444.
<https://doi.org/10.1126/science.1218351>

Qu, J., Tanis, S. E. J., Smits, J. P. H., Kouwenhoven, E. N., Oti, M., van den Bogaard, E. H., Logie, C., Stunnenberg, H. G., van Bokhoven, H., Mulder, K. W., & Zhou, H. (2018). Mutant p63 Affects Epidermal Cell Identity through Rewiring the Enhancer Landscape.

Cell Reports, 25(12), 3490-3503.e4. <https://doi.org/10.1016/j.celrep.2018.11.039>

Rahnamoun, H., Lu, H., Duttke, S. H., Benner, C., Glass, C. K., & Lauberth, S. M. (2017). Mutant p53 shapes the enhancer landscape of cancer cells in response to chronic immune signaling. *Nature Communications*, 8(1). <https://doi.org/10.1038/s41467-017-01117-y>
Raj, N., & Attardi, L. D. (2017). The Transactivation Domains of the p53 Protein. *Cold Spring Harbor Perspectives in Medicine*, 7(1), a026047.
<https://doi.org/10.1101/cshperspect.a026047>

Reece-Hoyes, J. S., Diallo, A., Lajoie, B., Kent, A., Shrestha, S., Kadreppa, S., Pesyna, C., Dekker, J., Myers, C. L., & Walhout, A. J. M. (2011). Enhanced yeast one-hybrid assays for high-throughput gene-centered regulatory network mapping. *Nature Methods*, 8(12), 1059–1064. <https://doi.org/10.1038/nmeth.1748>

Reiter, F., Wienerroither, S., & Stark, A. (2017a). Combinatorial function of transcription factors and cofactors. *Current Opinion in Genetics & Development*, 43, 73–81.
<https://doi.org/10.1016/j.gde.2016.12.007>

Reiter, F., Wienerroither, S., & Stark, A. (2017b). Combinatorial function of transcription factors and cofactors. *Current Opinion in Genetics & Development*, 43, 73–81.
<https://doi.org/10.1016/j.gde.2016.12.007>

- Rickels, R., & Shilatifard, A. (2018). Enhancer Logic and Mechanics in Development and Disease. *Trends in Cell Biology*, 28(8), 608–630.
<https://doi.org/10.1016/j.tcb.2018.04.003>
- Rinaldi, L., Datta, D., Serrat, J., Morey, L., Solanas, G., Avgustinova, A., Blanco, E., Pons, J. I., Matallanas, D., Von Kriegsheim, A., Di Croce, L., & Benitah, S. A. (2016). Dnmt3a and Dnmt3b Associate with Enhancers to Regulate Human Epidermal Stem Cell Homeostasis. *Cell Stem Cell*, 19(4), 491–501. <https://doi.org/10.1016/j.stem.2016.06.020>
- Rizzo, J. M., Oyelakin, A., Min, S., Smalley, K., Bard, J., Luo, W., Nyquist, J., Guttman-Yassky, E., Yoshida, T., & De Benedetto, A. (2016). ΔNp63 regulates IL-33 and IL-31 signaling in atopic dermatitis. *Cell Death & Differentiation*, 23(6), 1073–1085.
- Rufini, A., Tucci, P., Celardo, I., & Melino, G. (2013). Senescence and aging: The critical roles of p53. *Oncogene*, 32(43), 5129–5143. <https://doi.org/10.1038/onc.2012.640>
- Saifudeen, Z., Dipp, S., & El-Dahr, S. S. (2002). A role for p53 in terminal epithelial cell differentiation. *The Journal of Clinical Investigation*, 109(8), 1021–1030.
<https://doi.org/10.1172/JCI13972>
- Sainsbury, S., Bernecke, C., & Cramer, P. (2015). Structural basis of transcription initiation by RNA polymerase II. *Nature Reviews Molecular Cell Biology*, 16(3), 129–143.
<https://doi.org/10.1038/nrm3952>
- Sammons, M. A., Zhu, J., Drake, A. M., & Berger, S. L. (2015a). TP53 engagement with the genome occurs in distinct local chromatin environments via pioneer factor activity. *Genome Res*, 25, 179–188. <https://doi.org/10.1101/gr.181883.114>

- Sammons, M. A., Zhu, J., Drake, A. M., & Berger, S. L. (2015b). TP53 engagement with the genome occurs in distinct local chromatin environments via pioneer factor activity. *Genome Res.*, 25, 179–188. <https://doi.org/10.1101/gr.181883.114>
- Sathyan, K. M., McKenna, B. D., Anderson, W. D., Duarte, F. M., Core, L., & Guertin, M. J. (2019). An improved auxin-inducible degron system preserves native protein levels and enables rapid and specific protein depletion. *Genes & Development*. <https://doi.org/10.1101/gad.328237.119>
- Schoenfelder, S., & Fraser, P. (2019). Long-range enhancer-promoter contacts in gene expression control. *Nature Reviews. Genetics*, 20(8), 437–455. <https://doi.org/10.1038/s41576-019-0128-0>
- Schubert, J., & Brabertz, T. (2011). p53 spreads out further: Suppression of EMT and stemness by activating miR-200c expression. *Cell Research*, 21(5), 705–707. <https://doi.org/10.1038/cr.2011.62>
- Seto, E., Usheva, A., Zambetti, G. P., Momand, J., Horikoshi, N., Weinmann, R., Levine, A. J., & Shenk, T. (1992). Wild-type p53 binds to the TATA-binding protein and represses transcription. *Proceedings of the National Academy of Sciences of the United States of America*, 89(24), 12028–12032. <https://doi.org/10.1073/pnas.89.24.12028>
- Shao, L., Zuo, X., Yang, Y., Zhang, Y., Yang, N., Shen, B., Wang, J., Wang, X., Li, R., Jin, G., Yu, D., Chen, Y., Sun, L., Li, Z., Fu, Q., Hu, Z., Han, X., Song, X., Shen, H., & Sun, Y. (2019). The inherited variations of a p53-responsive enhancer in 13q12.12 confer lung cancer risk by attenuating TNFRSF19 expression. *Genome Biology*, 20(1), 103. <https://doi.org/10.1186/s13059-019-1696-1>

- Shen, J., Curtis, C., Tavaré, S., & Tower, J. (2009). A screen of apoptosis and senescence regulatory genes for life span effects when over-expressed in Drosophila. *Aging*, 1(2), 191–211. <https://doi.org/10.18632/aging.100018>
- Shen, N., Zhao, J., Schipper, J. L., Zhang, Y., Bepler, T., Leehr, D., Bradley, J., Horton, J., Lapp, H., & Gordan, R. (2018). Divergence in DNA Specificity among Paralogous Transcription Factors Contributes to Their Differential In Vivo Binding. *Cell Systems*, 6(4), 470-483.e8. <https://doi.org/10.1016/j.cels.2018.02.009>
- Shieh, S.-Y., Ikeda, M., Taya, Y., & Prives, C. (1997). DNA Damage-Induced Phosphorylation of p53 Alleviates Inhibition by MDM2. *Cell*, 91(3), 325–334. [https://doi.org/10.1016/S0092-8674\(00\)80416-X](https://doi.org/10.1016/S0092-8674(00)80416-X)
- Shlevkov, E., & Morata, G. (2012). A *dp53/JNK*-dependant feedback amplification loop is essential for the apoptotic response to stress in *Drosophila*. *Cell Death and Differentiation*, 19(3), 451–460. <https://doi.org/10.1038/cdd.2011.113>
- Shlyueva, D., Stampfel, G., & Stark, A. (2014). Transcriptional enhancers: From properties to genome-wide predictions. *Nature Reviews Genetics*, 15(4), 272–286. <https://doi.org/10.1038/nrg3682>
- Smeenk, L., van Heeringen, S. J., Koeppel, M., van Driel, M. A., Bartels, S. J. J., Akkers, R. C., Denissov, S., Stunnenberg, H. G., & Lohrum, M. (2008a). Characterization of genome-wide p53-binding sites upon stress response. *Nucleic Acids Research*, 36(11), 3639–3654. <https://doi.org/10.1093/nar/gkn232>
- Smeenk, L., van Heeringen, S. J., Koeppel, M., van Driel, M. A., Bartels, S. J. J., Akkers, R. C., Denissov, S., Stunnenberg, H. G., & Lohrum, M. (2008b). Characterization of genome-

wide p53-binding sites upon stress response. *Nucleic Acids Research*, 36(11), 3639–3654.

<https://doi.org/10.1093/nar/gkn232>

Smith, E., & Shilatifard, A. (2014). Enhancer biology and enhanceropathies. *Nat Struct Mol Biol*, 21, 210–219. <https://doi.org/10.1038/nsmb.2784>

Soares, E., & Zhou, H. (2017). Master regulatory role of p63 in epidermal development and disease. *Cellular and Molecular Life Sciences*. <https://doi.org/10.1007/s00018-017-2701-z>

Sogame, N., Kim, M., & Abrams, J. M. (2003). Drosophila p53 preserves genomic stability by regulating cell death. *Proceedings of the National Academy of Sciences*, 100(8), 4696–4701. <https://doi.org/10.1073/pnas.0736384100>

Soutourina, J. (2018). Transcription regulation by the Mediator complex. *Nature Reviews Molecular Cell Biology*, 19(4), 262–274. <https://doi.org/10.1038/nrm.2017.115>

Spitz, F., & Furlong, E. E. M. (2012a). Transcription factors: From enhancer binding to developmental control. *Nature Reviews Genetics*, 13(9), 613–626.

<https://doi.org/10.1038/nrg3207>

Spitz, F., & Furlong, E. E. M. (2012b). Transcription factors: From enhancer binding to developmental control. *Nature Reviews Genetics*, 13(9), 613–626.

<https://doi.org/10.1038/nrg3207>

Stewart-Ornstein, J., & Lahav, G. (2017). P53 dynamics in response to DNA damage vary across cell lines and are shaped by efficiency of DNA repair and activity of the kinase ATM. *Sci. Signal.*, 10(476), eaah6671.

Su, D., Wang, X., Campbell, M. R., Song, L., Safi, A., Crawford, G. E., & Bell, D. A. (2015). Interactions of Chromatin Context, Binding Site Sequence Content, and Sequence

Evolution in Stress-Induced p53 Occupancy and Transactivation. *PLOS Genetics*, 11(1), e1004885. <https://doi.org/10.1371/journal.pgen.1004885>

Sullivan, K. D., Galbraith, M. D., Andrysik, Z., & Espinosa, J. M. (2018). Mechanisms of transcriptional regulation by p53. *Cell Death & Differentiation*, 25(1), 133–143. <https://doi.org/10.1038/cdd.2017.174>

Surget, S., Khoury, M. P., & Bourdon, J.-C. (2013). Uncovering the role of p53 splice variants in human malignancy: A clinical perspective. *Oncotargets and Therapy*, 7, 57–68. <https://doi.org/10.2147/OTT.S53876>

Sykes, S. M., Mellert, H. S., Holbert, M. A., Li, K., Marmorstein, R., Lane, W. S., & McMahon, S. B. (2006). Acetylation of the p53 DNA binding domain regulates apoptosis induction. *Molecular Cell*, 24(6), 841–851. <https://doi.org/10.1016/j.molcel.2006.11.026>

Szak, S. T., Mays, D., & Pietenpol, J. A. (2001). Kinetics of p53 Binding to Promoter Sites In Vivo. *Molecular and Cellular Biology*, 21(10), 3375–3386. <https://doi.org/10.1128/MCB.21.10.3375-3386.2001>

Takahashi, K., & Yamanaka, S. (2016). A decade of transcription factor-mediated reprogramming to pluripotency. *Nature Reviews. Molecular Cell Biology*, 17(3), 183–193. <https://doi.org/10.1038/nrm.2016.8>

Taketani, K., Kawauchi, J., Tanaka-Okamoto, M., Ishizaki, H., Tanaka, Y., Sakai, T., Miyoshi, J., Maehara, Y., & Kitajima, S. (2012). Key role of ATF3 in p53-dependent DR5 induction upon DNA damage of human colon cancer cells. *Oncogene*, 31(17), 2210–2221. <https://doi.org/10.1038/onc.2011.397>

Tang, Y., Luo, J., Zhang, W., & Gu, W. (2006). Tip60-Dependent Acetylation of p53 Modulates the Decision between Cell-Cycle Arrest and Apoptosis. *Molecular Cell*, 24(6), 827–839.
<https://doi.org/10.1016/j.molcel.2006.11.021>

Teytelman, L., Thurtle, D. M., Rine, J., & Oudenaarden, A. van. (2013). Highly expressed loci are vulnerable to misleading ChIP localization of multiple unrelated proteins. *Proceedings of the National Academy of Sciences*, 110(46), 18602–18607.

<https://doi.org/10.1073/pnas.1316064110>

Thakore, P. I., D’Ippolito, A. M., Song, L., Safi, A., Shivakumar, N. K., Kabadi, A. M., Reddy, T. E., Crawford, G. E., & Gersbach, C. A. (2015). Highly specific epigenome editing by CRISPR-Cas9 repressors for silencing of distal regulatory elements. *Nat Methods*, 12, 1143–1149. <https://doi.org/10.1038/nmeth.3630>

Thanos, D., & Maniatis, T. (1995a). Virus induction of human IFN beta gene expression requires the assembly of an enhanceosome. *Cell*, 83(7), 1091–1100. [https://doi.org/10.1016/0092-8674\(95\)90136-1](https://doi.org/10.1016/0092-8674(95)90136-1)

Thanos, D., & Maniatis, T. (1995b). Virus induction of human IFN beta gene expression requires the assembly of an enhanceosome. *Cell*, 83(7), 1091–1100. [https://doi.org/10.1016/0092-8674\(95\)90136-1](https://doi.org/10.1016/0092-8674(95)90136-1)

The FANTOM Consortium, Andersson, R., Gebhard, C., Miguel-Escalada, I., Hoof, I., Bornholdt, J., Boyd, M., Chen, Y., Zhao, X., Schmidl, C., Suzuki, T., Ntini, E., Arner, E., Valen, E., Li, K., Schwarzfischer, L., Glatz, D., Raithel, J., Lilje, B., ... Sandelin, A. (2014). An atlas of active enhancers across human cell types and tissues. *Nature*, 507(7493), 455–461. <https://doi.org/10.1038/nature12787>

- Thurman, R. E., Rynes, E., Humbert, R., Vierstra, J., Maurano, M. T., Haugen, E., Sheffield, N. C., Stergachis, A. B., Wang, H., Vernot, B., Garg, K., John, S., Sandstrom, R., Bates, D., Boatman, L., Canfield, T. K., Diegel, M., Dunn, D., Ebersol, A. K., ... Stamatoyannopoulos, J. A. (2012). The accessible chromatin landscape of the human genome. *Nature*, 489, 75–82. <https://doi.org/10.1038/nature11232>
- Tripathi, S., Pohl, M. O., Zhou, Y., Rodriguez-Frandsen, A., Wang, G., Stein, D. A., Moulton, H. M., DeJesus, P., Che, J., Mulder, L. C. F., Yángüez, E., Andenmatten, D., Pache, L., Manicassamy, B., Albrecht, R. A., Gonzalez, M. G., Nguyen, Q., Brass, A., Elledge, S., ... Chanda, S. K. (2015). Meta- and Orthogonal Integration of Influenza “OMICs” Data Defines a Role for UBR4 in Virus Budding. *Cell Host & Microbe*, 18(6), 723–735. <https://doi.org/10.1016/j.chom.2015.11.002>
- Truong, A. B., Kretz, M., Ridky, T. W., Kimmel, R., & Khavari, P. A. (2006). P63 regulates proliferation and differentiation of developmentally mature keratinocytes. *Genes & Development*, 20(22), 3185–3197. <https://doi.org/10.1101/gad.1463206>
- Uzunbas, G. K., Ahmed, F., & Sammons, M. A. (2018a). Cell type-dependent control of p53 transcription and enhancer activity by p63. *BioRxiv*, 268649. <https://doi.org/10.1101/268649>
- Uzunbas, G. K., Ahmed, F., & Sammons, M. A. (2018b). Cell type-dependent control of p53 transcription and enhancer activity by p63. *BioRxiv*, 268649. <https://doi.org/10.1101/268649>
- van Heeringen, S. J., & Veenstra, G. J. C. (2011). GimmeMotifs: A de novo motif prediction pipeline for ChIP-sequencing experiments. *Bioinformatics (Oxford, England)*, 27(2), 270–271. <https://doi.org/10.1093/bioinformatics/btq636>

- Van Nostrand, J. L., Brady, C. A., Jung, H., Fuentes, D. R., Kozak, M. M., Johnson, T. M., Lin, C. Y., Lin, C. J., Swiderski, D. L., Vogel, H., Bernstein, J. A., Attie-Bitach, T., Chang, C. P., Wysocka, J., Martin, D. M., & Attardi, L. D. (2014). Inappropriate p53 activation during development induces features of CHARGE syndrome. *Nature*, 514, 228–232. <https://doi.org/10.1038/nature13585>
- Van Nostrand, Jeanine L, Bowen, M. E., Vogel, H., Barna, M., & Attardi, L. D. (2017). The p53 family members have distinct roles during mammalian embryonic development. *Cell Death and Differentiation*, 24(4), 575–579. <https://doi.org/10.1038/cdd.2016.128>
- Vassilev, L. T. (2004a). Small-molecule antagonists of p53-MDM2 binding: Research tools and potential therapeutics. *Cell Cycle (Georgetown, Tex.)*, 3(4), 419–421.
- Vassilev, L. T. (2004b). Small-molecule antagonists of p53-MDM2 binding: Research tools and potential therapeutics. *Cell Cycle (Georgetown, Tex.)*, 3(4), 419–421.
- Vassilev, L. T., Vu, B. T., Graves, B., Carvajal, D., Podlaski, F., Filipovic, Z., Kong, N., Kammlott, U., Lukacs, C., Klein, C., Fotouhi, N., & Liu, E. A. (2004). In vivo activation of the p53 pathway by small-molecule antagonists of MDM2. *Science (New York, N.Y.)*, 303(5659), 844–848. <https://doi.org/10.1126/science.1092472>
- Venkatesh, S., & Workman, J. L. (2015). Histone exchange, chromatin structure and the regulation of transcription. *Nature Reviews Molecular Cell Biology*, 16(3), 178–189. <https://doi.org/10.1038/nrm3941>
- Verfaillie, A., Svetlichnyy, D., Imrichova, H., Davie, K., Fiers, M., Kalender Atak, Z., Hulselmans, G., Christiaens, V., & Aerts, S. (2016a). Multiplex enhancer-reporter assays uncover unsophisticated TP53 enhancer logic. *Genome Research*, 26(7), 882–895. <https://doi.org/10.1101/gr.204149.116>

- Verfaillie, A., Svetlichnyy, D., Imrichova, H., Davie, K., Fiers, M., Kalender Atak, Z., Hulselmans, G., Christiaens, V., & Aerts, S. (2016b). Multiplex enhancer-reporter assays uncover unsophisticated TP53 enhancer logic. *Genome Research*, 26(7), 882–895.
<https://doi.org/10.1101/gr.204149.116>
- Vieler, M., & Sanyal, S. (2018). P53 Isoforms and Their Implications in Cancer. *Cancers*, 10(9), 288. <https://doi.org/10.3390/cancers10090288>
- Vierbuchen, T., Ling, E., Cowley, C. J., Couch, C. H., Wang, X., Harmin, D. A., Roberts, C. W. M., & Greenberg, M. E. (2017). AP-1 Transcription Factors and the BAF Complex Mediate Signal-Dependent Enhancer Selection. *Molecular Cell*, 68(6), 1067-1082.e12.
<https://doi.org/10.1016/j.molcel.2017.11.026>
- Vo Ngoc, L., Cassidy, C. J., Huang, C. Y., Duttke, S. H. C., & Kadonaga, J. T. (2017). The human initiator is a distinct and abundant element that is precisely positioned in focused core promoters. *Genes & Development*, 31(1), 6–11.
<https://doi.org/10.1101/gad.293837.116>
- Vousden, K. H., & Lane, D. P. (2007). P53 in health and disease. *Nat Rev Mol Cell Biol*, 8, 275–283. <https://doi.org/10.1038/nrm2147>
- Wang, S.-J., Li, D., Ou, Y., Jiang, L., Chen, Y., Zhao, Y., & Gu, W. (2016). Acetylation Is Crucial for p53-Mediated Ferroptosis and Tumor Suppression. *Cell Reports*, 17(2), 366–373. <https://doi.org/10.1016/j.celrep.2016.09.022>
- Webster, G. A., & Perkins, N. D. (1999). Transcriptional cross talk between NF-kappaB and p53. *Molecular and Cellular Biology*, 19(5), 3485–3495.
- Wei, C.-L., Wu, Q., Vega, V. B., Chiu, K. P., Ng, P., Zhang, T., Shahab, A., Yong, H. C., Fu, Y., Weng, Z., Liu, J., Zhao, X. D., Chew, J.-L., Lee, Y. L., Kuznetsov, V. A., Sung, W.-K.,

- Miller, L. D., Lim, B., Liu, E. T., ... Ruan, Y. (2006). A Global Map of p53 Transcription-Factor Binding Sites in the Human Genome. *Cell*, 124(1), 207–219.
<https://doi.org/10.1016/j.cell.2005.10.043>
- Wei, S. J., Joseph, T., Sim, A. Y. L., Yurlova, L., Zolghadr, K., Lane, D., Verma, C., & Ghadessy, F. (2013). In vitro selection of mutant HDM2 resistant to Nutlin inhibition. *PloS One*, 8(4), e62564. <https://doi.org/10.1371/journal.pone.0062564>
- Yan, C., Lu, D., Hai, T., & Boyd, D. D. (2005). Activating transcription factor 3, a stress sensor, activates p53 by blocking its ubiquitination. *The EMBO Journal*, 24(13), 2425–2435.
<https://doi.org/10.1038/sj.emboj.7600712>
- Yang, A., Schweitzer, R., Sun, D., Kaghad, M., Walker, N., Bronson, R. T., Tabin, C., Sharpe, A., Caput, D., Crum, C., & McKeon, F. (1999). P63 is essential for regenerative proliferation in limb, craniofacial and epithelial development. *Nature*, 398, 714–718.
<https://doi.org/10.1038/19539>
- Yang, Annie, Zhu, Z., Kapranov, P., McKeon, F., Church, G. M., Gingeras, T. R., & Struhl, K. (2006). Relationships between p63 Binding, DNA Sequence, Transcription Activity, and Biological Function in Human Cells. *Molecular Cell*, 24(4), 593–602.
<https://doi.org/10.1016/j.molcel.2006.10.018>
- Yoh, K. E., Regunath, K., Guzman, A., Lee, S.-M., Pfister, N. T., Akanni, O., Kaufman, L. J., Prives, C., & Prywes, R. (2016). Repression of p63 and induction of EMT by mutant Ras in mammary epithelial cells. *Proceedings of the National Academy of Sciences*, 113(41), E6107–E6116. <https://doi.org/10.1073/pnas.1613417113>

- Younger, S. T., Kenzelmann-Broz, D., Jung, H., Attardi, L. D., & Rinn, J. L. (2015a). Integrative genomic analysis reveals widespread enhancer regulation by p53 in response to DNA damage. *Nucleic Acids Research*, 43(9), 4447–4462. <https://doi.org/10.1093/nar/gkv284>
- Younger, S. T., Kenzelmann-Broz, D., Jung, H., Attardi, L. D., & Rinn, J. L. (2015b). Integrative genomic analysis reveals widespread enhancer regulation by p53 in response to DNA damage. *Nucleic Acids Research*, 43(9), 4447–4462. <https://doi.org/10.1093/nar/gkv284>
- Younger, S. T., & Rinn, J. L. (2017a). P53 regulates enhancer accessibility and activity in response to DNA damage. *Nucleic Acids Research*, 45(17), 9889–9900.
<https://doi.org/10.1093/nar/gkx577>
- Younger, S. T., & Rinn, J. L. (2017b). P53 regulates enhancer accessibility and activity in response to DNA damage. *Nucleic Acids Research*, 45(17), 9889–9900.
<https://doi.org/10.1093/nar/gkx577>
- Zaret, K. S., & Carroll, J. S. (2011). Pioneer transcription factors: Establishing competence for gene expression. *Genes Dev*, 25, 2227–2241. <https://doi.org/10.1101/gad.176826.111>
- Zaret, K. S., & Mango, S. E. (2016). Pioneer transcription factors, chromatin dynamics, and cell fate control. *Curr Opin Genet Dev*, 37, 76–81. <https://doi.org/10.1016/j.gde.2015.12.003>
- Zaret, Kenneth S., & Carroll, J. S. (2011). Pioneer transcription factors: Establishing competence for gene expression. *Genes & Development*, 25(21), 2227–2241.
<https://doi.org/10.1101/gad.176826.111>
- Zeron-Medina, J., Wang, X., Repapi, E., Campbell, M. R., Su, D., Castro-Giner, F., Davies, B., Peterse, E. F., Sacilotto, N., Walker, G. J., Terzian, T., Tomlinson, I. P., Box, N. F., Meinshausen, N., De Val, S., Bell, D. A., & Bond, G. L. (2013). A polymorphic p53

- response element in KIT ligand influences cancer risk and has undergone natural selection. *Cell*, 155, 410–422. <https://doi.org/10.1016/j.cell.2013.09.017>
- Zhang, Y., Liu, T., Meyer, C. A., Eeckhoute, J., Johnson, D. S., Bernstein, B. E., Nusbaum, C., Myers, R. M., Brown, M., Li, W., & Liu, X. S. (2008). Model-based analysis of ChIP-Seq (MACS). *Genome Biology*, 9(9), R137. <https://doi.org/10.1186/gb-2008-9-9-r137>
- Zhao, J., Li, X., Guo, M., Yu, J., & Yan, C. (2016). The common stress responsive transcription factor ATF3 binds genomic sites enriched with p300 and H3K27ac for transcriptional regulation. *BMC Genomics*, 17, 335. <https://doi.org/10.1186/s12864-016-2664-8>
- Zhou, D., Zhang, Z., He, L.-M., Du, J., Zhang, F., Sun, C.-K., Zhou, Y., Wang, X.-W., Lin, G., Song, K.-M., Wu, L.-G., & Yang, Q. (2014). Conversion of Fibroblasts to Neural Cells by p53 Depletion. *Cell Reports*, 9(6), 2034–2042.
<https://doi.org/10.1016/j.celrep.2014.11.040>
- Zhu, J., Dou, Z., Sammons, M. A., Levine, A. J., & Berger, S. L. (2016). Lysine methylation represses p53 activity in teratocarcinoma cancer cells. *Proceedings of the National Academy of Sciences of the United States of America*, 113(35), 9822–9827.
<https://doi.org/10.1073/pnas.1610387113>
- Zilfou, J. T., & Lowe, S. W. (2009). Tumor suppressive functions of p53. *Cold Spring Harb Perspect Biol*, 1, a001883. <https://doi.org/10.1101/cshperspect.a001883>